UC Irvine
UC Irvine Electronic Theses and Dissertations

Title
Simultaneously inhibiting multiple nutrient acquisition pathways using synthetic sphingolipid compounds

Permalink
https://escholarship.org/uc/item/9wr99118

Author
Kim, Seong Min

Publication Date
2016

Peer reviewed|Thesis/dissertation

eScholarship.org Powered by the California Digital Library
University of California

UNIVERSITY OF CALIFORNIA,
IRVINE

Simultaneously inhibiting multiple nutrient acquisition pathways using synthetic sphingolipid compounds

DISSERTATION

submitted in partial satisfaction for the requirement

for the degree of

DOCTOR OF PHILOSOPHY

in Biological Sciences

by

Seong Min Kim

Dissertation Committee:
Associate Professor Aimee L. Edinger, Chair
Professor David Fruman
Professor Anand Ganesan
Assistant Professor Susanne Rafelski
Associate Professor Christine Suetterlin

2016

Chapter 1 © 2016 *Journal of Clinical Investigation*

All other materials © Seong Min Kim

TABLE of CONTENTS

LIST OF FIGURES & TABLES

CHAPTER 2

ACKNOWLEDGEMENTS

I would like to thank my committee chair, Dr. Aimee Edinger, for allowing me to pursue such exciting projects. Thank you so much for all your mentorship and encouragements. I have learned so much from you in every way. Through your mentorship, I have gained not only valuable laboratory and analytical skills but also many life lessons that helped me mature in my personhood. I could not have asked for a better role model in being trained to be an independent female scientist. Thank you for believing in me even when I doubted myself. I loved working in your lab and will always remember these past five years with gratitude and happiness.

I would like to thank the members of my committee, Dr. David Fruman, Dr. Anand Ganesan, Dr. Susanne Rafelski and Dr. Christine Suetterlin. I sincerely thank you for all your guidance and advices you have provided in such encouraging ways. It has been so wonderful to have such brilliant and devoted faculties in my committee. I always left my committee meetings feeling encouraged and motivated. Your caring attitudes for graduate students left deep impression on me and they inspire me to be a more considerate mentor to others.

I would like to thank all the members of Edinger lab, past and present. I am so grateful to have had the opportunity to work alongside such wonderful people. Thank you so much for all the help and pep-talks! You all are so hard working and diligent and yet so kind and easy to get along. You have been like second family to me. Thank you for all the laughs and happy memories.

I would like to thank Dr. Stephen Hanessian for making this project possible by generating the sphingolipid compounds. Thank you also for all your inputs throughout our lab's projects. I really appreciated the times you were able to attend my presentations and for the encouraging words at the end of the talks.

I would like to thank all our collaborators who contributed to my projects: Dr. Hanessian's lab, Dr. Weisman's lab, Dr. Sasaki's lab, Dr. Edward's lab, Dr. Tromberg's lab, and Dr. Digman's lab. I really appreciate all your timely input and help.

I would like to thank Dr. Debra Mauzyme-Melitz for the financial support through GAANN (P200A120207). Thank you for helping me gain so much teaching experience under your leadership through GAANN activities. GAANN made such a difference in my graduate training and I will treasure the memories.

I would like to thank the staffs in the department of Developmental & Cell Biology. Thank you for being so supportive throughout my stay in the department and for answering all my questions with smiles and kindness. I could not have come this far without your help!

Lastly, I would like to thank my family for all their support and love. Mom, thank you so much for all your prayers and encouragement. I would not be here today if it were not for you and your unconditional love. To all my siblings, thank you for being there for me through everything. I love you all so much.

CURRICULUM VITAE

Seong M Kim

Education

2011-2016	Ph.D. Biological Sciences, University of California, Irvine [Department of Developmental & Cell Biology]
2011	Masters of Science. Biological Sciences, University of California, Irvine [Master's program in Biotechnology- Department of Molecular Biology and Biochemistry] Cumulative GPA: 4.00
2006-2008	Thomas Haider Biomed Program University of California, Riverside / University of California, Los Angeles
2006	Bachelor of Science. Biological Sciences, University of California, Riverside Cumulative GPA: 4.00
2002-2004	Cerritos College

Publications

Seong M. Kim, Saurabh G. Roy, Bin Chen, Tiffany Nguyen, Ryan J. McMonigle, Alison N. McCracken, Yanling Zhang, Satoshi Kofuji, Jue Hou, Elizabeth Selwan, Tricia Nguyen, Archna Ravi, Brendan T. Finicle, Manuel U. Ramirez, Tim Wiher, Garret G. Guenther, Mari Kono, Atsuo T. Sasaki, Lois S. Weisman, Eric O. Potma, Bruce J. Tromberg, Robert A. Edwards, Stephen Hanessian, and Aimee L. Edinger. (2016) Targeting cancer metabolism by simultaneously disrupting primary and adaptive nutrient access pathways. (*J. Clin. Invest.*, *in press*)

Seong M. Kim*, Archna Ravi*, Tricia T. Nguyen*, Peter Kubiniok, Jue Hou, Brendan Finicle, Leonel Malacrida, Michelle Digman, Bruce J. Tromberg, Pierre Thibault, and Aimee L. Edinger (2016) Prostate cancer cells convert cell corpses into biomass via macropinocytosis. *(in preparation)*

Alison N. McCracken, Rebecca Fransson, Ryan J. McMonigle, Jérémie Tessier, Andrew Keebaugh, Sarah A. Barr, Daniel Fallegger, Elizabeth Selwan, **Seong M. Kim**, Saurabh G. Roy, Ashley Snider, Simon Clare, Markus Müschen, Lina Obeid, Andrea Huwiler, Michael T. Kleinman, Stephen Hanessian, and Aimee L. Edinger. (2016) Phosphorylation increases the anti-leukemic activity of an S1P receptor-inactive constrained azacyclic FTY720 analog. *(Leukemia, in press)*

Michael Perryman, Jeremie Tessier, Timothy Wiher, Heather O'Donoghue, Alison N. McCracken, **Seong M. Kim**, Dean G. Nguyen, Grigor S. Stone, Matheus Viana, Susanne Rafelski, Aimee L. Edinger, and Stephen Hanessian. (2016) Effects of stereochemistry, saturation, and hydrocarbon chain length on the ability of synthetic constrained azacyclic sphingolipids to trigger nutrient transporter down-regulation, vacuolation, and cell death. (*Bioorg. Med. Chem., in press)*

Nadia Jaber, Noor Mohd-Naim, Ziqing Wang, Jennifer DeLeon, **Seong Kim** , Hua Zhong, Namratha Sheshadri, Zhixun Dou, Aimee Edinger, Guangwei Du, Vania Braga, and Wei-Xing Zong. (2016) Class III PI 3-kinase Vps34 regulates Rab7 through recruitment of the GTPase activating protein Armus. (*in preparation*)

Elizabeth M. Selwan, Brendan T. Finicle, **Seong M. Kim**, Aimee L. Edinger. (2016) Attacking the supply wagons to starve cancer cells to death. *FEBS Lett.* 590(7):885-907.

Mina Kalantari, Kathryn Osann, Itzel E. Calleja-Macias, **Seong Kim**, Bing Yan, Sara Jordan, Dana M. Chase, Krishnansu S. Tewari, Hans-Ulrich Bernard. (2014) Methylation of human papillomavirus 16, 18, 31, and 45 L2 and L1 genes and the cellular DAPK gene: Considerations for use as biomarkers of the progression of cervical neoplasia. *Virology* 448:314-21.

Garret G. Guenther*, Gang Liu*, Manuel U. Ramirez, Ryan J. McMonigle, **Seong M. Kim**, Alison N. McCracken, Yoosun Joo, Irina Ushach, Natalie L. Nguyen, and Aimee L. Edinger. (2013) Loss of TSC2 confers resistance to ceramide and nutrient deprivation. *Oncogene* 33(14):1776-87.

Ongoing study for publication to be submitted by end of 2016:
1. Arf6-dependent recycling defect induced by sphingolipid compounds.
2. Allele-specific oligonucleotide uptake in cancer cells via macropinocytosis. (in collaboration with IONIS Pharmaceuticals)

Presentations/ conferences

Oral presentation at Cellular & Molecular Biosciences Recruitment weekend (UC Irvine, 2016)
Oral presentation at GTCBio Cancer Metabolism Conference (San Francisco, 2015)
Poster presentation at Campuswide Symposium on Basic Cancer Research (UC Irvine, 2014-15)
Poster presentation at Developmental & Cell Biology Department Retreat (UC Irvine, 2013-15)
Medi-Workshop presentation (on primary literature reading) at Regional Association for Biology Laboratory Education meeting (UC Irvine, 2015)
Poster at Keystone Symposium on Integrating Metabolism and Tumor Biology conference (Vancouver, Canada, 2015)
Mini-Workshop presentation (on effective presentation skill and feedback) at Association for Biology Laboratory Education conference (University of Oregon, Eugene, 2014)
Poster presentation at Metabolism, Diet and Disease: Cancer and Metabolism conference
(Georgetown University, Washington D.C., 2014)
Poster presentation at Translational Medicine Research Day (UC Irvine, 2014)
Oral presentation at Cancer Biology Training Grant Retreat (UC Irvine, 2013)

Teaching experiences

During the second year of Master's program in Biotechnology in the Department of Molecular Biology and Biochemistry at UCI, I had the opportunity to teach the first-year Master's students as well as the undergraduate courses. I also had **teaching assistant** positions during my rotation for Cellular & Molecular Biosciences. As a Howard Hughes Medical Institute (HHMI) UCI Graduate Teaching Fellow, I have led three discussion sections for Bio 93 for fall quarter 2012 and also served as a head TA for the course for fall 2013. I have gained valuable teaching principles and techniques from these experiences.
The courses that I served as TA so far are:

UC Irvine

Honors section BIO SCI 93 (DNA to Organisms) Fall 2014
BIO SCI 93 (DNA to Organisms) Fall 2012 & Fall 2013 (Head-TA)
BIO SCI M118L (Exp Microbiology Lab) Fall 2011
BIO SCI M143 (Human Parasitology) Fall 2011
BIO SCI 99 (Molecular Biology) Spring 2011
BIO SCI M227L (BIOTECH LAB-Virology & Immunology) Spring 2011
BIO SCI 98 (Biochemistry) Winter 2011
MOL BIO 251L(BIOTECH LAB-Protein) Winter 2011
BIO SCI M116L (Molecular Biology Lab) Fall 2010
MOL BIO 250L (BIOTECH LAB-Nucleic Acid) Fall 2010

I have been **mentoring and supervising undergraduate researchers** since 2012 (7 students total).

Along with other Graduate Assistance in Areas of National Need (GAANN) fellows in the department of Developmental & Cell Biology, I developed and facilitated a **symposium** for science major undergraduate students and graduate students in 2014. Some of the workshops I helped develop and presented were on: how to become a successful undergraduate researcher, how to give effective presentation and feedback, and how to develop a teaching portfolio.

Instructor for STEM-UPP Pre-Biology Course in Moodle (UCI Extension; 2015)
Along with two other graduate students, I have developed an online summer course to help incoming freshman students to review basics of biology to help them succeed in introductory biology course they would be taking in the fall quarter. We designed the course from writing up syllabus to creating hands-on activities and writing quizzes and exams as well as facilitating student participation. This experience allowed me to gain valuable insights to online instruction.

UC Riverside — Biology 5A Course tutor (Learning Center, 2006)

Academic & Professional Honors

Dr. William F. Holcomb Scholarship (Ayala School of Biological Sciences, UC Irvine, June 2016)
Winner in poster contest (Campuswide Symposium on Basic Cancer Research, UC Irvine, May 2015)
Third place in poster contest (Developmental & Cell Biology, UC Irvine, April 2015)
Fine Science Tools Graduate Travel Award (Ayala School of Biological Sciences, UC Irvine, June 2014)
Great Lakes National Scholarship Finalist (Great Lakes Educational Loan Services, 2014)
Head-TA Award (HHMI-UCI Teaching Fellows Program, UC Irvine, 2013-2014)
GAANN Fellowship (Department of Developmental & Cell Biology, UC Irvine, 2013 & 2014)
Graduate Fellow Award (HHMI-UCI Teaching Fellows Program, UC Irvine, 2012-2013)
Francisco J. Ayala Graduate Fellowship Award (Cellular & Molecular Biosciences, UC Irvine, 2011)
Graduate Fellowship Award (Molecular Biology & Biochemistry, UC Irvine, 2010)
B.S. with Highest Honor (UC Riverside, Jun 2006)
Theodore W Mitchell Scholarship (UC Riverside, 2005-2006)
Mabel Wilson Richards Scholarship (UC Riverside, 2005-2006)
Los Angeles Olympic Lions Club Scholarship Award (LA Olympic Lions Club, May 2005)
Korean Heritage Scholarship (Korean Heritage Scholarship Foundation, April 2005)
Royal Cultural Foundation Scholarship (Royal Cultural Foundation, Nov 2004)
Chancellor's Honor List (UC Riverside, 2004-2006)
Dean's List (UC Riverside, 2004- 2006)
Dean's Honor List (Cerritos College, 2002-2004)

Other positions

Internship at Allergan, Inc. in Irvine, CA (summer 2010)
Molecular laboratory work and assistance with rat models in retina research
Summer Externship at Kaiser Permanente (summer 2007)
Rotation through family medicine, internal medicine, psychiatry, pediatrics, and general surgery with OB/GYN

ABSTRACT OF THE DISSERTATION

Simultaneously inhibiting multiple nutrient acquisition pathways using synthetic sphingolipid compounds

By

Seong Min Kim

Doctor of Philosophy in Biological Sciences

University of California, Irvine 2016

Dr. Aimee L. Edinger, Chair

Despite the advances in therapeutics targeting key players that drive cancer metabolism, clinical benefits of these therapies have been limited. As tumors consist of heterogeneous population of cells, targeting a specific oncoprotein may provide selective advantage to cancer cells that are not driven by that oncoprotein. Also, upregulation of anabolic pathways that are not being directly targeted may also contribute to development of resistance to the therapy. Instead of focusing on a specific metabolic protein, our lab is interested in striking cancer metabolism at its apex—cancer cells' dependence on nutrients. To fuel constitutive anabolism and proliferation, cancer cells must have influx of nutrients. When nutrients become limiting, unlike non-transformed cell that can discontinue anabolic processes and become quiescent, cancer cells undergo metabolic chaos as oncogene-driven growth signals continue to force anabolism. Developing a therapy against this cancer-specific phenotype will have efficacy against broad classes of cancers as all cancers need nutrients to survive. In searching for a compound that can inhibit nutrient uptake, our lab has been focusing on sphingolipids, a class of bioactive lipid that plays important roles in cellular functions including membrane biology. In yeast, stress-induced nutrient transporter down-regulation is regulated by sphingolipid phytosphingosine. Sphingolipid ceramide down-regulates nutrient transporters in mammalian cells. A sphingolipid-

derived compound FTY720 is also able to trigger surface amino acid and glucose transporter loss. FTY720, an FDA-approved drug for treatment of multiple sclerosis, has anti-cancer activities in a various cancer models. Unfortunately, FTY720 causes bradycardia at the doses needed for anti-neoplastic effects. However, mechanism by which FTY720 kills cancer cells is completely separate from its effect on heart rate. SH-BC-893 is a constrained analog of FTY720 that lacks its dose-limiting side effect but retains anti-neoplastic activities. SH-BC-893, like ceramide and FTY720, down-regulates surface nutrient transporters. In addition, SH-BC-893 induces cytoplasmic vacuolation secondary to mis-localization of lipid kinase PIKfyve. This blocks lysosomal degradation of autophagosomes and macropinosomes, alternate nutrient acquisition pathways cancer cells can use to adapt to nutrient stress triggered by loss of surface nutrient transporters. LDL receptors are also down-regulated and LDL degradation is blocked by SH-BC-893. Prostate cancers rely heavily on LDL uptake for growth and proliferation and are thereby very sensitive to SH-BC-893. Surprisingly, prostate cancer cells are resistant to amino acid and glucose withdrawal. Our ongoing works have uncovered that this is because PTEN loss in prostate cancers upregulates macropinocytosis. This previously-unappreciated macropinocytosis in prostate cancers requires AMPK activation. Our works demonstrate that prostate cancer cells can use macropinocytosis to consume necrotic debris to build protein biomass and lipid storage to survive and proliferate in low nutrient environment. These findings highlight cancer cells' addiction to nutrients and offer insights into therapeutic opportunities for targeting this Achilles' heels of cancer metabolism. SH-BC-893 prevents cancer cells from using nutrients taken up via macropinocytosis by inhibiting lysosomal degradation of macropinosomes. By simultaneously blocking import and lysosomal degradation of nutrients, this water soluble and orally bioavailable compound effectively starves cancer cells to death. Future investigations will help further fine-tune SH-BC-893 into a safe and effective anti-cancer agent that can overcome the problems of tumor heterogeneity and adaptive resistances seen with current metabolic therapies.

INTRODUCTION

I. Cancer cells are addicted to nutrients.

Cancer cells must have continuous influx of nutrients in order to support macromolecular synthesis needed for oncogene-driven growth and proliferation (1–6). In order to fuel the various anabolic processes, cancer cells undergo an active metabolic reprogramming (7,8). One of the essential metabolic rewiring cancer cells undergo is upregulation of nutrient acquisition pathways. Four major nutrient uptake pathways increased in cancers will be discussed here: nutrient transporters, macropinocytosis, lipid uptake, and autophagy (Figure 1). Chapter 1 of this dissertation will address how sphingolipid-derived therapy can simultaneously target all four of these pathways.

A) Surface nutrient transporter expression is increased in cancers.

Oncogenic mutations that drive proliferation are often the same mutations that enhance cancer cells' ability to increase nutrient uptake. For example, Ras activation, Myc over-expression, and PI 3-kinase pathway activation increase glucose and amino acid transporter expression and uptake (2–4,9–15).

Cancer cells convert the majority of glucose into lactate even when there is plenty of oxygen, and this phenomenon, first described by Otto Warburg, is known as the "Warburg effect" (5). This characteristic increase in glucose uptake and usage observed in many cancer types is the basis of the diagnostic tool (18F)-2-deoxy-2-(18F)fluoro-D-glucose positron emission tomography ((^{18}F)-FDG-PET). Increased glucose uptake in cancers, particularly in breast, NSCLC, thyroid, head and neck, colon, and esophagus cancers, makes (^{18}F)-FDG-PET an effective tool not only for diagnosis and staging but also for monitoring response to therapy (16). In addition to generating ATP, increased glycolysis allows cancer cells generate biosynthetic intermediates needed for building biomass (7,17). Increased levels of glucose

transporter expression are negatively correlated with patient prognosis (6,18). Of the many isoforms of GLUT family of facilitated glucose transporters, GLUT1 and GLUT3 are most often over-expressed in cancers (1,6). GLUT1 over-expression enhances tumor growth and GLUT3 over-expression in 3D culture system converts non-malignant breast cancer epithelial cells to malignant cells (19,20). Reducing GLUT1/3 levels reduces tumor growth and sensitizes cancer cells to chemotherapy (1,6). Other types of glucose transporters such as sodium-coupled glucose transporters (SGLT) are also often up-upregulated in cancer cells (1,6). SGLT transports glucose via the Na+ gradient generated by Na^+/K^+ ATPase. Transport of glycolytic products pyruvate and lactate is also important in cancer progression (1,6). MCT1 and MCT4 are monocarboxylate transporters that couple proton transport with pyruvate, lactate, or acetate transport. Lactate generated in highly glycolytic cells can be exported out by these transporters, while lactate secreted by cancer-associated fibroblasts can also be imported by cancer cells through these same transporters to support growth (21). Both MCT1 and MCT4 require the chaperone protein CD147 (basigin) for cell surface expression (1,6)

In addition to increased glucose uptake, amino acid uptake is also frequently up-regulated in cancers (1,6). Many types of cancers are mainly addicted to glutamine (11,22), but other amino acids can be conditionally essential in certain cancer classes. For example, asparagine is required for acute lymphoblastic leukemia which is treated with the asparagine-degrading enzyme, asparaginase (23). Arginine plays a similar role in a subset of leukemias and solid tumors (24). Serine and glycine are also required by some cancer cells (25–27). Similar to glucose transporters, increased levels of amino acid transporters enhance tumor growth and proliferation (1,6). CD98 (4F2 heavy chain) is a chaperone protein that dimerizes with amino acid exchangers LAT1 and xCT both of which are upregulated in several different types of cancer. CD98 over-expression is correlated with poor prognosis in patients. xCT exports glutamate and imports cystine, while LAT1 import essential amino acids in exchange for non-

essential amino acids glutamine and alanine. LAT1 up-regulation increases amino acid levels to activate mTORC1 and enhances proliferation in lung and renal cancers (28,29). ASCT2 transports neutral amino acids, including glutamine which feeds into the TCA cycle and glutathione synthesis (1). ASCT2 overexpression in non-small cell lung cancer plays a crucial role in driving metastasis (30). Other amino acids transporters such as $ATB^{0,+}$, SNAT1, and SNAT2 also increase net amino acid import and may contribute to tumorigenesis (1,6).

In addition to being regulated at the transcriptional level, nutrient transporters are also post-translationally regulated. Several of nutrient transporters, including CD98, LAT1, GLUT1, and CD147, are internalized through a clathrin-independent endocytic pathway (31). ADP-ribosylation factor 6 (Arf6) regulates internalization and recycling of these cargos. ASCT2, LAT1, MCT1, and MCT4 also associate with cell proliferation factors such as epithelial cell adhesion molecule (EpCAM) and CD147-CD98 complex (32). These findings suggest that multiple nutrient transporters exist on the cell surface as clusters in the same membrane domain, allowing for co-regulation. Ubiquitination, phosphorylation, and glycosylation also regulate nutrient transporter trafficking. CD98, for example, can be ubiquitinated and to be sent to late endosomes instead of being recycled back to surface membrane (33). Other nutrient transporters, including GLUT1, LAT1, and xCT, also have ubiquitylation sites (34). GLUT1, LAT1, and CD98 also have cell-cycle dependent phosphorylation sites, suggesting that nutrient transporter activity may be regulated by growth and cell-cycle (35). GLUT1 trafficking to the cell surface is increased in T cells by increase in glycosylation (36). Regulation of nutrient transporter trafficking and activity by post-translational modification offers exciting therapeutic opportunities to target cancer cells' addiction to nutrients. Sphingolipids that post-translationally regulate multiple nutrient transporters will be discussed under heading II.

B) Macropinocytosis allows cancer cells to engulf extracellular nutrients.

In addition to promoting nutrient acquisition through transporters, cancer cells can acquire extracellular nutrients through a non-specific engulfment process called macropinocytosis (6,37). Normally, macropinocytosis occurs in specific cell types such as macrophages and kidney podocytes (37–39). Upon growth factor or inflammatory stimulation, these cells form actin-mediated ruffles on the plasma membrane which fold back, trapping extracellular materials (39). Actin-reorganization required for membrane ruffling requires activation of the small GTPase, Rac1. Resulting vesicles are not coated with clathrin and are heterogenous in size, some of which can be as large as 5 μm in diameter. These macropinosomes are visualized using fluid phase markers such as fluorescent dextran or Ficoll. Once formed, macropinosomes are trafficked to the lysosomes to be degraded or be recycled back to fuse with the plasma membrane (39). Amino acids derived from macropinocytosis activates mTORC1, which then can prevent fusion between macropinosomes and lysosomes as part of a feedback mechanism (40). Fatty acids that are bound to albumin can also be taken up by macropinocytosis (38).

Oncogenic Ras mutations promote the acquisition of amino acids through macropinocytosis which fuels proliferation in amino acid-depleted conditions (40–42). Currently, only Ras-driven cancers have been shown to use macropinocytosis to survive amino acid deprivation. Although PI 3-kinase inhibition blocksRas-driven macropinocytosis, knocking down PTEN was not sufficient to stimulate macropinocytosis in MEFs in leucine-deficient media (40). The context in which PTEN loss can stimulate macropinocytosis will be discussed in Chapter 2 of this thesis.

In addition to PI 3-kinase inhibition, there are several ways to block macropinocytosis. 5-[N-ethyl-N-isopropyl] amiloride (EIPA) inhibits Na^+/H^+ exchanger 1 (NHE1) and disrupts the pH near plasma membrane, preventing actin re-organization needed for macropinocytosis (43). The allosteric Rac1 inhibitor EHT-1864 and the actin polymerization inhibitor cytochalasin D also block macropinocytosis (39,44). However, these inhibitors target regulatory proteins

upstream of macropinocytosis or cytoskeletal reorganization in general and therefore lack specificity to macropinocytic process. Since macropinocytosis-specific inhibitors are lacking, a deeper molecular understanding of this pathway is a high priority.

C) Lipid metabolism fuels cancer growth and proliferation.

Cancer cells also alter lipid metabolism to fuel growth and proliferation. Cancer cells can increase both *de novo* synthesis of lipids and lipolysis (45,46). Fatty acid biosynthesis plays crucial role in tumorigenesis. For example, ATP-citrate lyase, an enzyme that converts citrate into acetyl-CoA for fatty acid biosynthesis, is required for tumor formation. Fatty-acid synthase (FASN) expression is increased in breast and prostate cancers. Other key enzymes involved in the fatty acid biosynthesis such as acetyl-CoA carboxylase (ACC) and fatty acid elongase are also frequently up-regulated in cancers. Inhibition of fatty acid biosynthesis pathways disrupts cancer growth and proliferation.

Cholesterol synthesis is another important lipid biosynthetic process up-regulated in cancers (47). Cholesterol is an essential component of the plasma membrane, regulating the fluidity of the lipid bilayer and forming lipid rafts that can serve as a platform for signaling pathways and membrane trafficking (48). Intermediates derived from the cholesterol biosynthetic processes also serve as precursors for isoprenylation of small GTPases like Ras and Rho. Isoprenylation anchors these proteins to the plasma membrane for proper signaling. Statins, inhibitors of HMG-CoA reductase (HMGCR), a rate-limiting enzyme in cholesterol synthesis that converts 3-hydroxy-3-methylglutaryl (HMG)-CoA into mevalonate, has anti-neoplastic activity and sensitizes cancer cells to chemotherapy (49).

Uptake of extracellular lipid also plays an important role for tumor growth. In particular, prostate cancer cells depend on exogenous low-density lipoprotein (LDL) for growth and survival (50). Loss of tumor suppressor PTEN activates PI 3-kinase pathways that results in activation of

sterol regulatory element-binding protein (SREBP) and low-density lipoprotein receptor (LDLr). Receptor-bound LDL is endocytosed via clathrin-dependent endocytosis and LDL is degraded in lysosomes to produce free cholesterol and fatty acids (51). Blocking LDL uptake or depleting cholesteryl ester stores reduces prostate cancer cell proliferation (50).

In addition to lipogenesis, fatty acid oxidation also contributes to malignancy in multiple cancer types (47). Mitochondrial beta oxidation is up-regulated in prostate cancers and inhibiting fatty acid oxidation results in apoptosis in leukemia cells and glioblastoma cells. Exploiting the alterations in lipid metabolism in cancer cells, is thus another important approach to targeting cancer metabolism.

D) Autophagy is a source of intracellular nutrients when cancer cells are under nutrient stress.

When extracellular nutrients become limiting, cells can derive nutrients from intracellular proteins and organelles via a catabolic process called autophagy, or “self-digestion” (52). Autophagy is tightly regulated and plays an important role in maintaining metabolic homeostasis. During the initiation step of autophagy, small cup-shaped double-membrane sacs called phagophores emerge. This step is mediated by UNC51-like kinase (ULK) complex that consists of ULK1/ULK2, autophagy-related protein 13 (ATG13), FAK family kinase interacting protein of 200 kDa (FIP200) and ATG101. Elongation of phagophores is mediated by vacuolar protein sorting 34 (VPS34), which is a class III PI 3-kinase, as well as ATG14L, VPS15, and beclin 1. Old proteins and organelles are sequestered as the isolation membranes are elongated. Then ATG5-ATG12 conjugates form a complex with ATG16L and LC3-I (microtubule-associated protein 1 light chain 3) is lipidated with phosphatidylethanolamine (PE) to form LC3-II. WD-repeat PI3P effector protein 2 (WIPI2) is required for recruiting the ATG12-

5-16L complex and for LC3 lipidation (53). This expands the autophagosome membranes to completion and the resulting autophagosomes are trafficked to multivesicular bodies (MVB) and lysosomes for degradation.

Autophagy is regulated both at the initiation/elongation step and at the degradation step (54,55). When there are plenty of nutrients or growth signals, mTORC1 inhibits the initiation of autophagy by suppressing ULK1 kinase activity. AMPK opposes this inhibition by activating the TSC complex, which is a negative regulator of mTORC1, by phosphorylating the mTORC1 binding partner raptor, or by directly activating ULK1 (56–58). Once autophagy is initiated, the resulting autophagosomes mature and fuse with components of the late endocytic pathway. Thus, disruptions in late endocytic trafficking can limit autophagic flux (59,60). If autophagosomes are not properly trafficked to lysosomes, they cannot be degraded to derive nutrients. Autophagosome fusion with lysosomes requires the small GTPase Rab7, components of the homotypic fusion and protein sorting (HOPS) complex, and SNARE proteins (61).

Phosphatidylinositol 3,5-bisphosphate ($PI(3,5)P_2$) generated by the phosphotidylinositide 5-kinase, PIKfyve, also regulates autophagosome-lysosome fusion events (Figure 2) (62,63). $PI(3,5)P_2$ binds and activates the calcium channel TRPML1 (transient receptor potential cation channel, mucolipin subfamily, member 1) that is primarily localized to late endosomal and lysosomal membranes. TRPML1 activity is dramatically increased upon nutrient starvation, and juxtaorganellar Ca^{2+} release from TRPML1 triggers lysosomal fusion and fission, allowing autophagosomes to be effectively degraded in lysosomes (64,65). Reducing $PI(3,5)P_2$ levels results in the accumulation of autophagy proteins LC3-II and p62, indication of a block in autophagosome degradation. Interestingly, $PI(3,5)P_2$ may also regulate autophagosome formation. *In vivo*, $PI(3,5)P_2$ is the major precursor for PI(5)P which is required for autophagosome biogenesis under glucose-limiting conditions (66,67). $PI(3,5)P_2$ may also

stimulate autophagy by increasing TRPML1-mediated Ca^{2+} release that will activate the Ca^{2+}-activated kinase CAMKKβ, which directly activates AMPK (68). TRPML3, another member of mucolipin family, is also recruited to autophagosomes and may play a similar role as TRPML1 in regulating autophagy (69).

Autophagy plays a dual role in cancer (54). Because autophagy serves as a quality control mechanism that degrades old proteins and organelles such as defective mitochondria that generate reactive oxygen species (ROS), lack of autophagy leads to an increased DNA mutation rate and subsequent tumorigenesis (70,71). For example, Beclin1, an essential protein for autophagosome formation, is frequently monoallelically lost in human breast, ovarian, and prostate cancers (72,73). On the other hand, once the tumor is established, autophagy-derived nutrients can fuel cancer cells to proliferate (54,74,75). Reducing autophagy is detrimental to tumor cells, particularly those with mutations that activate Ras (74,75). Interestingly, oncogenic signaling pathways generally suppress autophagy. For example, activation of mTORC1 downstream of PI 3-kinase signaling inhibits autophagy, although metabolic stress can overcome this inhibition (76–80). Over-expression of the anti-apoptotic protein Bcl-2 in cancer can also suppress autophagy, as can loss of p53 (81–83). Thus, cancer cells would be expected to have a reduced autophagic reserve capacity relative to normal cells. Consistent with this hypothesis, autophagy inhibitors can increase the therapeutic index of both cytotoxic and targeted chemotherapeutic agents (54,84–88). Although new agents blocking autophagosome formation are under development (89–91), currently available inhibitors are non-selective blockers of lysosomal degradation (87). For example, blocking lysosomal degradation of autophagosomes with chloroquine decrease tumor growth when combined with alkylating agents or HDAC inhibitor SAHA (74). However, as there are emerging evidences that these effects of chloroquine may be independent of autophagy, other methods of blocking autophagy are in need of development (92).

II. Sphingolipid-based therapies target cancer metabolism.

Current therapeutic efforts targeting the nutrient addiction of cancer cells focus on developing small molecule inhibitors of the enzymes required for flux through the relevant anabolic pathways (93). The pre-clinical studies examining the consequences of silencing these anabolic enzymes and clinical success with enzymatic depletion of amino acids suggest that nutrient limitation could be an effective and selective therapeutic approach in many cancers.

A) Sphingolipids regulate surface nutrient transporters.

Cancer cells' addiction to nutrients is a vulnerability that could be exploited for therapeutic purposes. Targeting key metabolic enzymes, however, has proven difficult as cancers frequently develop drug resistance. Cancer cells can adapt and up-regulate compensatory metabolic pathways and thus become resistant to the original inhibitor. In addition, tumors consist of heterogeneous populations of cells, and enzymatic inhibitors may provide selective pressure that enriches for the cancer cells that have a different driver oncogene mutation and thus different metabolic liabilities.

Preventing cancer cells from accessing nutrients targets a cancer phenotype—their addiction to nutrients—rather than a specific oncogenic mutation. As all cancer cells must take up nutrients to survive and fuel proliferation regardless of which specific driver mutations they carry, preventing nutrient uptake may be an effective therapeutic approach for broad classes of cancers. Competitive inhibitors of glucose and amino acid transporters are of limited utility because they must be present at millimolar concentrations to be effective (93,94). This is therapeutically difficult to achieve in patients and these inhibitors do not block the other nutrient acquisition uptake pathways mentioned above.

Sphingolipids are bioactive lipids that have a variety of cellular functions, including regulation of the actin cytoskeleton, endocytosis, the cell cycle, apoptosis, the stress response, senescence, and survival (95). Sphingolipid synthesis and signaling pathways are complex and interconnected. Of interest to targeting cancer cells' addiction to nutrients, sphingolipids regulate the endocytosis and recycling of nutrient transporters. Budding yeast under heat stress generate the sphingolipid phytosphingosine to trigger amino acid permease down-regulation and arrest growth (96–98). While mammalian cells do not synthesize phytosphingosine, the related sphingolipid ceramide induces a similar down-regulation of glucose and amino acid transporters in multiple mammalian cell types (99). Ceramide activates protein phosphatase 2A (PP2A) and this step is required for down-regulation of nutrient transporters (99). PP2A is a ubiquitously expressed serine threonine phosphatase and is composed of catalytic (C), scaffold (A) and regulatory (B) subunits (100). PP2A inhibition by chemical inhibitors or by expression of small t, which binds to the scaffolding A subunit of PP2A and blocks PP2A complex formation, prevents sphingolipid-induced glucose and amino acid transporter loss from the cell surface (99,101).

B) Synthetic sphingolipid FTY720 and its analogs have anti-neoplastic activities.

Because ceramide is extremely hydrophobic and readily metabolized into other sphingoids, its therapeutic potential is limited. Interestingly, the FDA-approved and water-soluble sphingolipid drug FTY720 also activates PP2A and down-regulates nutrient transporters, inducing a starvation response in both mammalian cells and yeast (97,101,102). FTY720 became the first oral therapy for multiple sclerosis based on its actions at sphingosine-1-phosphate receptors. Once phosphorylated by sphingosine kinase 2, FTY720 acts as a functional antagonist of S1P receptor 1 ($S1P_1$), thereby trapping lymphocytes in secondary lymphoid organs (103). At higher doses than needed for immunosuppression, FTY720 has profound anti-neoplastic activity in a

variety of model systems (101,104–115). Despite these promising results in animal models, FTY720 cannot be tested in human cancer patients due to dose-limiting bradycardia secondary to activation of $S1P_1$ and/or $S1P_3$ (103,116–118). Fortunately, the anti-cancer activities of FTY720 are unrelated to its S1P receptor effects. A conformationally constrained analog of FTY720, SH-BC-893, down-regulates nutrient transporters and retains the broad anti-neoplastic effects of the parent compound but lacks the S1P receptor activity that is responsible for FTY720's dose-limiting toxicity (119).

Having developed a synthetic sphingolipid with favorable drug properties and demonstrated that it kills a variety of cancer cells (119), its mechanism of action and selectivity for transformed cells were further evaluated in more in-depth biological assays. As will be discussed in the first part of this dissertation, SH-BC-893, in addition to triggering nutrient transporter loss, produces profound cytoplasmic vacuolation secondary to the mislocalization of PIKfyve. Altered PIKfyve trafficking was determined to be independent of the trafficking defects responsible for transporter down-regulation. PIKfyve mislocalization contributed to the anti-neoplastic activity of SH-BC-893 *in vitro* and *in vivo* by blocking autophagosome, LDL, and macropinosome degradation, thereby intensifying the nutrient stress caused by amino acid and glucose transporter down-regulation.

SH-BC-893 was especially effective against prostate cancers. As SH-BC-893 killed cancer cells by simultaneously inhibiting multiple nutrient uptake pathways, we hypothesized that prostate cancers would be very sensitive to depletion of amino acids and glucose deprivation from the medium. Surprisingly, they were resistant to amino acid and glucose withdrawal. The second part of this dissertation will highlight these PTEN-deficient prostate cancer cells' ability to survive in low nutrients by relying on macropinocytosis. PTEN-deficient cells required AMPK activation in order to exhibit macropinocytosis and this provided an explanation as to why macropinocytosis was not observed in amino acid-depleted media in MEFs expressing PTEN

shRNA (40). Prostate cancers used macropinocytosis to consume necrotic cell debris to build biomass and proliferate. These findings have profound implications in understanding and targeting macropinocytosis as an important nutrient uptake pathway in many cancer types.

REFERENCES

1. McCracken AN, Edinger AL: Nutrient transporters: the Achilles' heel of anabolism. *Trends Endocrinol Metab* 2013, 24:200–8.

2. Garcia-Cao I, Song MS, Hobbs RM, Laurent G, Giorgi C, De Boer VCJ, Anastasiou D, Ito K, Sasaki AT, Rameh L, Carracedo A, Vander Heiden MG, Cantley LC, Pinton P, Haigis MC, Pandolfi PP: Systemic elevation of PTEN induces a tumor-suppressive metabolic state. *Cell* 2012, 149:49–62.

3. Shroff EH, Eberlin LS, Dang VM, Gouw AM, Gabay M, Adam SJ, Bellovin DI, Tran PT, Philbrick WM, Garcia-Ocana A, Casey SC, Li Y, Dang C V., Zare RN, Felsher DW: MYC oncogene overexpression drives renal cell carcinoma in a mouse model through glutamine metabolism. *Proc Natl Acad Sci* 2015, 112:6539–6544.

4. Ying H, Kimmelman AC, Lyssiotis C a., Hua S, Chu GC, Fletcher-Sananikone E, Locasale JW, Son J, Zhang H, Coloff JL, Yan H, Wang W, Chen S, Viale A, Zheng H, Paik JH, Lim C, Guimaraes AR, Martin ES, Chang J, Hezel AF, Perry SR, Hu J, Gan B, Xiao Y, Asara JM, Weissleder R, Wang YA, Chin L, Cantley LC, et al.: Oncogenic kras maintains pancreatic tumors through regulation of anabolic glucose metabolism. *Cell* 2012, 149:656–670.

5. Ward PS, Thompson CB: Metabolic Reprogramming: A Cancer Hallmark Even Warburg Did Not Anticipate. *Cancer Cell* 2012, 21:297–308.

6. Selwan EM, Finicle BT, Kim SM, Edinger AL: Attacking the supply wagons to starve cancer cells to death. *FEBS Lett* 2016, 590:885–907.

7. Schulze A, Harris AL: How cancer metabolism is tuned for proliferation and vulnerable to disruption. *Nature* 2012, 491:364–73.

8. Tennant D a, Durán R V, Gottlieb E: Targeting metabolic transformation for cancer therapy. *Nat Rev Cancer* 2010, 10:267–77.

9. Wise DR, DeBerardinis RJ, Mancuso A, Sayed N, Zhang X-Y, Pfeiffer HK, Nissim I, Daikhin E, Yudkoff M, McMahon SB, Thompson CB: Myc regulates a transcriptional program that stimulates mitochondrial glutaminolysis and leads to glutamine addiction. *Proc Natl Acad Sci U S A* 2008, 105:18782–18787.

10. Osthus RC, Shim H, Kim S, Li Q, Reddy R, Mukherjee M, Xu Y, Wonsey D, Lee L a., Dang C V.: Deregulation of glucose transporter 1 and glycolytic gene expression by c-Myc. *J Biol Chem* 2000, 275:21797–21800.

11. Bhutia YD, Babu E, Ramachandran S, Ganapathy V: Amino Acid Transporters in Cancer and Their Relevance to "Glutamine Addiction": Novel Targets for the Design of a New Class of Anticancer Drugs. *Cancer Res* 2015, 75:1782–1789.

12. Jitschin R, Braun M, Qorraj M, Saul D, Blanc K Le, Zenz T: Stromal cell – mediated glycolytic switch in CLL cells involves. *Blood* 2015, 125:3432–3437.

13. Son J, Lyssiotis C a, Ying H, Wang X, Hua S, Ligorio M, Perera RM, Ferrone CR, Mullarky E, Shyh-Chang N, Kang Y, Fleming JB, Bardeesy N, Asara JM, Haigis MC, DePinho R a, Cantley LC, Kimmelman AC: Glutamine supports pancreatic cancer growth through a KRAS-regulated metabolic pathway. *Nature* 2013, 496:101–5.

14. Saqcena M, Mukhopadhyay S, Hosny C, Alhamed a, Chatterjee a, Foster D a: Blocking

anaplerotic entry of glutamine into the TCA cycle sensitizes K-Ras mutant cancer cells to cytotoxic drugs. *Oncogene* 2014, 34(May):1–9.

15. Wang Y, Li G, Mao F, Li X, Liu Q, Chen L, Lv L, Wang X, Wu J, Dai W, Wang G, Zhao E, Tang K-F, Sun ZS: Ras-induced Epigenetic Inactivation of the RRAD (Ras-related Associated with Diabetes) Gene Promotes Glucose Uptake in a Human Ovarian Cancer Model. *J Biol Chem* 2014, 289:14225–14238.

16. Kelloff GJ, Hoffman JM, Johnson B, Scher HI, Siegel B, Cheng EY, Cheson BD, Shaughnessy JO, Guyton KZ, Mankoff DA, Shankar L, Larson SM, Sigman CC, Schilsky RL, Sullivan DC: Progress and Promise of FDG-PET Imaging for Cancer Patient Management and Oncologic Drug Development. 2005, 11:2785–2808.

17. Hsu PP, Sabatini DM: Cancer cell metabolism: Warburg and beyond. *Cell* 2008, 134:703–7.

18. Rathan A, Weiser KR, Pritsker A, Itzkowitz SH, Bodian C, Slater G, Weiss A, Burstein DE: GLUT1 Glucose Transporter Expression in Colorectal Carcinoma A Marker for Poor Prognosis. *Am Cancer Soc* 1998:34–40.

19. Young CD, Lewis AS, Rudolph MC, Ruehle MD, Jackman MR, Yun UJ, Ilkun O, Pereira R, Abel ED, Anderson SM: Modulation of Glucose Transporter 1 (GLUT1) Expression Levels Alters Mouse Mammary Tumor Cell Growth In Vitro and In Vivo. *PLoS One* 2011, 6:e23205.

20. Onodera Y, Nam J, Bissell MJ: Increased sugar uptake promotes oncogenesis via EPAC / RAP1 and O-GlcNAc pathways. *J Clin Invest* 2014, 124:367–384.

21. Doherty JR, Cleveland JL: Targeting lactate metabolism for cancer therapeutics. *J Clin Invest* 2013, 123:3685–3692.

22. DeBerardinis RJ, Cheng T: Q's next: the diverse functions of glutamine in metabolism, cell biology and cancer. *Oncogene* 2010, 29:313–324.

23. Pieters R, Hunger SP, Boos J, Rizzari C, Silverman L, Baruchel A, Goekbuget N, Schrappe M, Pui CH: L-asparaginase treatment in acute lymphoblastic leukemia. *Cancer* 2011, 117:238–249.

24. Rodríguez PC, Ochoa AC: Arginine regulation by myeloid derived suppressor cells and tolerance in cancer: Mechanisms and therapeutic perspectives. *Immunol Rev* 2008, 222:180–191.

25. Jain M, Nilsson R, Sharma S, Madhusudhan N, Kitami T, Souza AL, Kafri R, Kirschner MW, Clish CB, Mootha VK: Metabolite Profiling Identifies a Key Role for Glycine in Rapid Cancer Cell Proliferation. *Science (80-)* 2012, 336(May):1040–1044.

26. Maddocks ODK, Berkers CR, Mason SM, Zheng L, Blyth K, Gottlieb E, Vousden KH: Serine starvation induces stress and p53-dependent metabolic remodelling in cancer cells. *Nature* 2013, 493:542–6.

27. Labuschagne CF, van den Broek NJF, Mackay GM, Vousden KH, Maddocks ODK: Serine, but not glycine, supports one-carbon metabolism and proliferation of cancer cells. *Cell Rep* 2014, 7:1248–1258.

28. Rodrı V, Marsboom G, Elorza A, Vara-vega A, Salinas A, Sa R, Martı R, Gime JM, Malumbres M, Landa MO, Sa F: HIF2 a Acts as an mTORC1 Activator through the Amino Acid Carrier SLC7A5. *Mol Cancer Ther* 2012, 48:681–691.

29. Nicklin P, Bergman P, Zhang B, Triantafellow E, Wang H, Nyfeler B, Yang H, Hild M, Kung C, Wilson C, Myer VE, Mackeigan JP, Porter JA, Wang YK, Cantley LC, Finan PM, Murphy LO: Bidirectional Transport of Amino Acids Regulates mTOR and Autophagy. *Cell* 2009, 136:521–534.

30. Shimizu K, Kaira K, Tomizawa Y, Sunaga N, Kawashima O, Oriuchi N, Tominaga H, Nagamori S: ASC amino-acid transporter 2 (ASCT2) as a novel prognostic marker in non-small cell lung cancer. *Br J Cancer* 2014, 110:2030–2039.

31. Eyster C a, Higginson JD, Huebner R, Porat-Shliom N, Weigert R, Wu WW, Shen R-F, Donaldson JG: Discovery of new cargo proteins that enter cells through clathrin-independent endocytosis. *Traffic* 2009, 10:590–9.

32. Palac M: The role of amino acid transporters in inherited and acquired diseases. *Biochem J* 2011, 211:193–211.

33. Eyster CA, Cole NB, Petersen S, Viswanathan K, Früh K, Gruenberg JE: MARCH ubiquitin ligases alter the itinerary of clathrin-independent cargo from recycling to degradation. *Mol Biol Cell* 2011, 22:3218–3230.

34. Kim J, Guan K: Amino Acid Signaling in TOR Activation. *Annu Rev Biochem* 2011, 80:1001–1032.

35. Olsen J V, Vermeulen M, Santamaria A, Kumar C, Miller ML, Jensen LJ, Gnad F, Cox J, Jensen TS, Nigg EA, Brunak S, Mann M: Quantitative Phosphoproteomics Reveals Widespread Full Phosphorylation Site Occupancy During Mitosis. *Sci Signal* 2010, 3:1–16.

36. Jacobs SR, Herman CE, Maciver NJ, Wofford JA, Wieman HL, Hammen JJ, Rathmell JC, Jacobs SR, Herman CE, Maciver NJ, Wofford JA, Wieman HL, Hammen JJ, Rathmell JC: Glucose Uptake Is Limiting in T Cell Activation and Requires CD28-Mediated Akt-Dependent and Independent Pathways. *J Imunol* 2016, 180:4476–4486.

37. Bloomfield G, Kay RR: Uses and abuses of macropinocytosis. *J Cell Sci* 2016, 0:1–9.

38. Chung J, Huber TB, Gödel M: Albumin-associated free fatty acids induce macropinocytosis in podocytes. *J Clin Invest* 2015, 125:2037–2316.

39. Lim JP, Gleeson PA: Macropinocytosis : an endocytic pathway for internalising large gulps. *Immunol Cell Biol* 2011, 89:836–843.

40. Palm W, Park Y, Wright K, Pavlova NN, Tuveson DA, Thompson CB: The Utilization of Extracellular Proteins as Nutrients Is Suppressed by mTORC1. *Cell* 2015, 162:1–12.

41. Kamphorst JJ, Nofal M, Commisso C, Hackett SR, Lu W, Grabocka E, Vander Heiden MG, Miller G, Drebin J a., Bar-Sagi D, Thompson CB, Rabinowitz JD: Human Pancreatic Cancer Tumors Are Nutrient Poor and Tumor Cells Actively Scavenge Extracellular Protein. *Cancer Res* 2015, 75:544–553.

42. Overmeyer JH, Kaul A, Johnson EE, Maltese W a: Active ras triggers death in glioblastoma cells through hyperstimulation of macropinocytosis. *Mol Cancer Res* 2008, 6:965–977.

43. Koivusalo M, Welch C, Hayashi H, Scott CC, Kim M, Alexander T, Touret N, Hahn KM, Grinstein S, Koivusalo M, Welch C, Hayashi H, Scott CC, Kim M, Alexander T, Touret N, Hahn KM, Grinstein S: JCB: Correction. 2010.

44. Bhanot H, Young AM, Overmeyer JH, Maltese WA: Induction of Nonapoptotic Cell Death by

Activated Ras Requires Inverse Regulation of Rac1 and Arf6. *Mol cancer Res* 2010, 8:1358–1374.

45. Santos CR, Schulze A: Lipid metabolism in cancer. *FEBS J* 2012, 279:2610–2623.

46. Nomura DK, Long JZ, Niessen S, Hoover HS, Ng S, Cravatt BF: Monoacylglycerol Lipase Regulates a Fatty Acid Network that Promotes Cancer Pathogenesis. *Cell* 2010, 140:49–61.

47. Wu X, Daniels G, Lee P, Monaco ME: Lipid metabolism in prostate cancer. *Am J Clin Exp Urol* 2014, 2:111–20.

48. Simons K, Ikonen E: How cells handle cholesterol. *Science (80-)* 2000, 290(December):1721–1727.

49. Hindler K: The Role of Statins in Cancer Therapy. *Oncologist* 2006, 11:306–315.

50. Yue S, Li J, Lee SY, Lee HJ, Shao T, Song B, Cheng L, Masterson T a., Liu X, Ratliff TL, Cheng JX: Cholesteryl ester accumulation induced by PTEN loss and PI3K/AKT activation underlies human prostate cancer aggressiveness. *Cell Metab* 2014, 19:393–406.

51. Goldstein JL, Brown MS, Anderson RGW, Russell DW, Schneider WJ: RECEPTOR-MEDIATED ENDOCYTOSIS: Concepts Emerging from the LDL Receptor System. *Ann Rev Cell Bioi* 1985, 1:1–39.

52. Kaur J, Debnath J: Autophagy at the crossroads of catabolism and anabolism. *Nat Rev Mol Cell Biol* 2015, 16:461–472.

53. Dooley HC, Razi M, Polson HEJ, Girardin SE, Wilson MI, Tooze S a.: WIPI2 Links LC3 Conjugation with PI3P, Autophagosome Formation, and Pathogen Clearance by Recruiting Atg12-5-16L1. *Mol Cell* 2014, 55:238–252.

54. White E: Deconvoluting the context-dependent role for autophagy in cancer. *Nat Rev Cancer* 2012, 12:401–10.

55. Boya P, Reggiori F, Codogno P: Emerging regulation and functions of autophagy. *Nat Cell Biol* 2013, 15:713–20.

56. Russell RC, Yuan H-X, Guan K-L: Autophagy regulation by nutrient signaling. *Cell Res* 2014, 24:42–57.

57. Mizushima N: Autophagy : process and function. *Genes Dev* 2007, 15:2861–2873.

58. Gwinn DM, Shackelford DB, Egan DF, Mihaylova MM, Vasquez DS, Turk BE, Shaw RJ: AMPK phosphorylation of raptor mediates a metabolic checkpoint. *Mol Cell* 2008, 30:214–226.

59. Huotari J, Helenius A: Endosome maturation. *EMBO J* 2011, 30:3481–500.

60. Rink J, Ghigo E, Kalaidzidis Y, Zerial M: Rab conversion as a mechanism of progression from early to late endosomes. *Cell* 2005, 122:735–749.

61. He C, Klionsky DJ: Regulation Mechanisms and Signalling Pathways of Autophagy. *Annu Rev Genet* 2009, 43:67.

62. Zeevi D a, Lev S, Frumkin A, Minke B, Bach G: Heteromultimeric TRPML channel assemblies play a crucial role in the regulation of cell viability models and starvation-induced autophagy. *J Cell Sci* 2010, 123(Pt 18):3112–24.

63. Cheng X, Shen D, Samie M, Xu H: Mucolipins: Intracellular TRPML1-3 channels. *FEBS Lett*

2010, 584:2013–21.

64. Wang W, Gao Q, Yang M, Zhang X, Yu L, Lawas M, Li X, Bryant-Genevier M, Southall NT, Marugan J, Ferrer M, Xu H: Up-regulation of lysosomal TRPML1 channels is essential for lysosomal adaptation to nutrient starvation. *Proc Natl Acad Sci* 2015, 112:E1373–81.

65. Dong X, Shen D, Wang X, Dawson T, Li X, Zhang Q, Cheng X, Zhang Y, Weisman LS, Delling M, Xu H: PI(3,5)P(2) controls membrane trafficking by direct activation of mucolipin Ca(2+) release channels in the endolysosome. *Nat Commun* 2010, 1:38.

66. Zolov SN, Bridges D, Zhang Y, Lee W-W, Riehle E, Verma R, Lenk GM, Converso-Baran K, Weide T, Albin RL, Saltiel a. R, Meisler MH, Russell MW, Weisman LS: In vivo, Pikfyve generates PI(3,5)P2, which serves as both a signaling lipid and the major precursor for PI5P. *Proc Natl Acad Sci* 2012, 109:17472–17477.

67. Vicinanza M, Korolchuk VI, Ashkenazi A, Puri C, Menzies FM, Clarke JH, Rubinsztein DC: PI(5)P Regulates Autophagosome Biogenesis. *Mol Cell* 2015, 57:219–234.

68. Ghislat G, Patron M, Rizzuto R, Knecht E: Withdrawal of essential amino acids increases autophagy by a pathway involving Ca2+/calmodulin-dependent kinase kinase-β (CaMKK-β). *J Biol Chem* 2012, 287:38625–36.

69. Kim HJ, Soyombo AA, Tjon-Kon-Sang S, So I, Muallem S: The Ca2+ channel TRPML3 regulates membrane trafficking and autophagy. *Traffic* 2009, 10:1157–1167.

70. Mathew R, Karantza-wadsworth V, White E: Role of autophagy in cancer. 2007, 7(december):961–967.

71. Mathew R, White E: Autophagy in tumorigenesis and energy metabolism: Friend by day, foe by night. *Curr Opin Genet Dev* 2011, 21:113–119.

72. Yue Z, Jin S, Yang C, Levine AJ, Heintz N: Beclin 1, an autophagy gene essential for early embryonic development, is a haploinsufficient tumor suppressor. *Proc Natl Acad Sci U S A* 2003, 100:15077–15082.

73. Galluzzi L, Pietrocola F, Pedro JMB, Ravi K, Maiuri MC, Martin SJ, Penninger J, Piacentini M: Autophagy in malignant transformation and cancer progression. *EMBO J* 2015, 34:856–880.

74. White E: Exploiting the bad eating habits of Ras-driven cancers. *Genes Dev* 2013, 27:2065–2071.

75. Guo JY, Chen HY, Mathew R, Fan J, Strohecker AM, Karsli-Uzunbas G, Kamphorst JJ, Chen G, Lemons JMS, Karantza V, Coller H a., DiPaola RS, Gelinas C, Rabinowitz JD, White E: Activated Ras requires autophagy to maintain oxidative metabolism and tumorigenesis. *Genes Dev* 2011, 25:460–470.

76. Jung CH, Ro SH, Cao J, Otto NM, Kim Do-Hyung DH: MTOR regulation of autophagy. *FEBS Lett* 2010, 584:1287–1295.

77. Kim J, Kundu M, Viollet B, Guan K-L: AMPK and mTOR regulate autophagy through direct phosphorylation of Ulk1. *Nat Cell Biol* 2011, 13:132–141.

78. Alers S, Löffler AS, Wesselborg S, Stork B: Role of AMPK-mTOR-Ulk1/2 in the regulation of autophagy: cross talk, shortcuts, and feedbacks. *Mol Cell Biol* 2012, 32:2–11.

79. Høyer-Hansen M, Jäättelä M: Connecting endoplasmic reticulum stress to autophagy by unfolded protein response and calcium. *Cell Death Differ* 2007, 14:1576–1582.

80. Malpica R, Malpica R, Pe GR, Pe GR, Rodr C, Rodr C, Franco B, Franco B, Georgellis D, Georgellis D: Oxidative Stress and Autophagy. *Antioxid Redox Signal* 2006, 8:152–162.

81. Pattingre S, Tassa A, Qu X, Garuti R, Xiao HL, Mizushima N, Packer M, Schneider MD, Levine B: Bcl-2 antiapoptotic proteins inhibit Beclin 1-dependent autophagy. *Cell* 2005, 122:927–939.

82. Crighton D, Wilkinson S, O'Prey J, Syed N, Smith P, Harrison PR, Gasco M, Garrone O, Crook T, Ryan KM: DRAM, a p53-Induced Modulator of Autophagy, Is Critical for Apoptosis. *Cell* 2006, 126:121–134.

83. Kenzelmann Broz D, Mello SS, Bieging KT, Jiang D, Dusek RL, Brady C a., Sidow A, Attardi LD: Global genomic profiling reveals an extensive p53-regulated autophagy program contributing to key p53 responses. *Genes Dev* 2013, 27:1016–1031.

84. Rubinsztein DC, Codogno P, Levine B: Autophagy modulation as a potential therapeutic target for diverse diseases. *Nat Rev Drug Discov* 2012, 11:709–30.

85. Cheong H, Lu C, Lindsten T, Thompson CB: Therapeutic targets in cancer cell metabolism and autophagy. *Nat Biotechnol* 2012, 30:671–678.

86. Amaravadi RK, Lippincott-Schwartz J, Yin XM, Weiss W a., Takebe N, Timmer W, DiPaola RS, Lotze MT, White E: Principles and current strategies for targeting autophagy for cancer treatment. *Clin Cancer Res* 2011, 17:654–666.

87. Yang Y, Hu L, Zheng H, Mao C, Hu W, Xiong K, Wang F, Liu C: Application and interpretation of current autophagy inhibitors and activators. *Acta Pharmacol Sin* 2013, 34:625–35.

88. Yang ZJ, Chee CE, Huang S, Sinicrope F a: The role of autophagy in cancer: therapeutic implications. *Mol Cancer Ther* 2011, 10:1533–1541.

89. Dowdle WE, Nyfeler B, Nagel J, Elling R a., Liu S, Triantafellow E, Menon S, Wang Z, Honda A, Pardee G, Cantwell J, Luu C, Cornella-Taracido I, Harrington E, Fekkes P, Lei H, Fang Q, Digan ME, Burdick D, Powers AF, Helliwell SB, D'Aquin S, Bastien J, Wang H, Wiederschain D, Kuerth J, Bergman P, Schwalb D, Thomas J, Ugwonali S, et al.: Selective VPS34 inhibitor blocks autophagy and uncovers a role for NCOA4 in ferritin degradation and iron homeostasis in vivo. *Nat Cell Biol* 2014, 16.

90. Ronan B, Flamand O, Vescovi L, Dureuil C, Durand L, Fassy F, Bachelot M, Lamberton A, Mathieu M, Bertrand T, Marquette J, El-ahmad Y, Filoche-romme B, Schio L, Garcia-echeverria C, Goulaouic H, Pasquier B: A highly potent and selective Vps34 inhibitor alters vesicle trafficking and autophagy. *Nat Chem Biol* 2014, 10(October):1013–1019.

91. Egan DF, Chun MGH, Vamos M, Zou H, Rong J, Miller CJ, Lou HJ, Raveendra-Panickar D, Yang C-C, Sheffler DJ, Teriete P, Asara JM, Turk BE, Cosford NDP, Shaw RJ: Small Molecule Inhibition of the Autophagy Kinase ULK1 and Identification of ULK1 Substrates. *Mol Cell* 2015, 59:1–13.

92. Eng CH, Wang Z, Tkach D, Toral-barza L, Ugwonali S, Liu S, Fitzgerald SL, George E, Frias E, Cochran N, Jesus R De, Mcallister G, Hoffman GR, Bray K, Lemon L, Lucas J, Fantin VR, Abraham RT: Macroautophagy is dispensable for growth of KRAS mutant tumors and chloroquine efficacy. *Proc Natl Acad Sci U S A* 2016, 113:3–8.

93. Galluzzi L, Kepp O, Vander Heiden MG, Kroemer G: Metabolic targets for cancer therapy. *Nat Rev Drug Discov* 2013, 12:829–46.

94. Karunakaran S, Ramachandran S, Coothankandaswamy V, Elangovan S, Babu E, Periyasamy-Thandavan S, Gurav A, Gnanaprakasam JP, Singh N, Schoenlein P V., Prasad PD, Thangaraju M, Ganapathy V: SLC6A14 (ATB 0,+) protein, a highly concentrative and broad specific amino acid transporter, is a novel and effective drug target for treatment of estrogen receptor-positive breast cancer. *J Biol Chem* 2011, 286:31830–31838.

95. Hannun YA, Obeid LM: Principles of bioactive lipid signalling: lessons from sphingolipids. *Nat Rev Mol Cell Biol* 2008, 9:139–150.

96. Skrzypek MS, Nagiec MM, Lester RL, Dickson RC: Inhibition of amino acid transport by sphingoid long chain bases in Saccharomyces cerevisiae. *J Biol Chem* 1998, 273:2829–2834.

97. Welsch C a., Roth LW a, Goetschy JF, Movva NR: Genetic, biochemical, and transcriptional responses of Saccharomyces cerevisiae to the novel immunomodulator FTY720 largely mimic those of the natural sphingolipid phytosphingosine. *J Biol Chem* 2004, 279:36720–36731.

98. Chung N, Mao C, Heitman J, Hannun Y a, Obeid LM: Phytosphingosine as a specific inhibitor of growth and nutrient import in Saccharomyces cerevisiae. *J Biol Chem* 2001, 276:35614–21.

99. Guenther GG, Peralta ER, Rosales KR, Wong SY, Siskind LJ, Edinger AL: Ceramide starves cells to death by downregulating nutrient transporter proteins. *Proc Natl Acad Sci U S A* 2008, 105:17402–7.

100. Mumby M: PP2A: Unveiling a Reluctant Tumor Suppressor. *Cell* 2007, 130:21–24.

101. Romero Rosales K, Singh G, Wu K, Chen J, Janes MR, Lilly MB, Peralta ER, Siskind LJ, Bennett MJ, Fruman D a, Edinger AL: Sphingolipid-based drugs selectively kill cancer cells by down-regulating nutrient transporter proteins. *Biochem J* 2011, 439:299–311.

102. Welsch C a., Hagiwara S, Goetschy JF, Movva NR: Ubiquitin pathway proteins influence the mechanism of action of the novel immunosuppressive drug FTY720 in Saccharomyces cerevisiae. *J Biol Chem* 2003, 278:26976–26982.

103. Brinkmann V: FTY720 (fingolimod) in Multiple Sclerosis: Therapeutic effects in the immune and the central nervous system. *Br J Pharmacol* 2009, 158:1173–1182.

104. Azuma H, Takahara S, Ichimaru N, Agent I, Breast M: Marked Prevention of Tumor Growth and Metastasis by a Novel Immunosuppressive Agent, FTY720, in Mouse Breast Cancer Models Marked Prevention of Tumor Growth and Metastasis by a Novel. *Cancer Res* 2002, 62:1410–1419.

105. Azuma H, Takahara S, Horie S, Muto S, Otsuki Y, Katsuoka Y: Induction of apoptosis in human bladder cancer cells in vitro and in vivo caused by FTY720 treatment. *J Urol* 2003, 169:2372–7.

106. Chua CW, Chiu YT, Yuen HF, Chan KW, Man K, Wang X, Ling MT, Wong YC: Suppression of androgen-independent prostate cancer cell aggressiveness by FTY720: Validating Runx2 as a potential antimetastatic drug screening platform. *Clin Cancer Res* 2009, 15:4322–4335.

107. Chua C-W, Lee DT-W, Ling M-T, Zhou C, Man K, Ho J, Chan FL, Wang X, Wong Y-C: FTY720, a fungus metabolite, inhibits in vivo growth of androgen-independent prostate cancer. *Int J Cancer* 2005, 117:1039–48.

108. Estrada-bernal A, Palanichamy K, Chaudhury AR, Brocklyn JR Van: Induction of brain

tumor stem cell apoptosis by FTY720 : a potential therapeutic agent for glioblastoma. *Neuro Oncol* 2012, 14:405–415.

109. Lee TK, Man K, Ho JW, Wang XH, Poon RTP, Xu Y, Ng KT, Chu AC, Sun CK, Ng IO, Sun HC, Tang ZY, Xu R, Fan ST: FTY720: a promising agent for treatment of metastatic hepatocellular carcinoma. *Clin Cancer Res* 2005, 11:8458–66.

110. Neviani P, Santhanam R, Oaks JJ, Eiring AM, Notari M, Blaser BW, Liu S, Trotta R, Muthusamy N, Gambacorti-passerini C, Druker BJ, Cortes J, Marcucci G, Chen C, Verrills NM, Roy DC, Caligiuri MA, Bloomfield CD, Byrd JC, Perrotti D: FTY720 , a new alternative for treating blast crisis chronic myelogenous leukemia and Philadelphia chromosome – positive acute lymphocytic leukemia. *J Clin Invest* 2007, 117:2408–2421.

111. Neviani P, Harb JG, Oaks JJ, Santhanam R, Walker CJ, Ellis JJ, Ferenchak G, Dorrance AM, Paisie CA, Eiring AM, Ma Y, Mao HC, Zhang B, Wunderlich M, May PC, Sun C, Saddoughi SA, Bielawski J, Blum W, Klisovic RB, Solt JA, Byrd JC, Volinia S, Cortes J, Huettner CS, Koschmieder S, Holyoake TL, Devine S, Caligiuri MA, Croce CM, et al.: PP2A-activating drugs selectively eradicate TKI-resistant chronic myeloid leukemic stem cells. *J Clin Invest* 2013, 123.

112. Oaks JJ, Santhanam R, Walker CJ, Roof S, Harb JG, Ferenchak G, Eisfeld AK, Van Brocklyn JR, Briesewitz R, Saddoughi S a., Nagata K, Bittman R, Caligiuri M a., Abdel-Wahab O, Levine R, Arlinghaus RB, Quintas-Cardama A, Goldman JM, Apperley J, Reid A, Milojkovic D, Ziolo MT, Marcucci G, Ogretmen B, Neviani P, Perrotti D: Antagonistic activities of the immunomodulator and PP2A-activating drug FTY720 (Fingolimod, Gilenya) in Jak2-driven hematologic malignancies. *Blood* 2013, 122:1923–1934.

113. Omar H a., Chou CC, Berman-Booty LD, Ma Y, Hung JH, Wang D, Kogure T, Patel T, Terracciano L, Muthusamy N, Byrd JC, Kulp SK, Chen CS: Antitumor effects of OSU-2S, a nonimmunosuppressive analogue of FTY720, in hepatocellular carcinoma. *Hepatology* 2011, 53:1943–1958.

114. Pchejetski D, Bohler T, Brizuela L, Sauer L, Doumerc N, Golzio M, Salunkhe V, Teissié J, Malavaud B, Waxman J, Cuvillier O: FTY720 (fingolimod) sensitizes prostate cancer cells to radiotherapy by inhibition of sphingosine kinase-1. *Cancer Res* 2010, 70:8651–8661.

115. Saddoughi S a., Gencer S, Peterson YK, Ward KE, Mukhopadhyay A, Oaks J, Bielawski J, Szulc ZM, Thomas RJ, Selvam SP, Senkal CE, Garrett-Mayer E, De Palma RM, Fedarovich D, Liu A, Habib A a., Stahelin R V., Perrotti D, Ogretmen B: Sphingosine analogue drug FTY720 targets I2PP2A/SET and mediates lung tumour suppression via activation of PP2A-RIPK1-dependent necroptosis. *EMBO Mol Med* 2013, 5:105–121.

116. Sanna MG, Liao J, Jo E, Alfonso C, Ahn MY, Peterson MS, Webb B, Lefebvre S, Chun J, Gray N, Rosen H: Sphingosine 1-Phosphate (S1P) Receptor Subtypes S1P1 and S1P3, Respectively, Regulate Lymphocyte Recirculation and Heart Rate. *J Biol Chem* 2004, 279:13839–13848.

117. Koyrakh L, Roman MI, Brinkmann V, Wickman K: The heart rate decrease caused by acute FTY720 administration is mediated by the G protein-gated potassium channel I. *Am J Transplant* 2005, 5:529–36.

118. Budde K, Schmouder RL, Brunkhorst R, Nashan B, Lücker PW, Mayer T, Choudhury S, Skerjanec A, Kraus G, Neumayer HH: First human trial of FTY720, a novel immunomodulator, in stable renal transplant patients. *J Am Soc Nephrol* 2002, 13:1073–1083.

119. Chen B, Roy SG, McMonigle RJ, Keebaugh A, McCracken AN, Selwan E, Fransson R,

Fallegger D, Huwiler A, Kleinman MT, Edinger AL, Hanessian S: Azacyclic FTY720 Analogues That Limit Nutrient Transporter Expression but Lack S1P Receptor Activity and Negative Chronotropic Effects Offer a Novel and Effective Strategy to Kill Cancer Cells in Vivo. *ACS Chem Biol* 2016, 11:409–14.

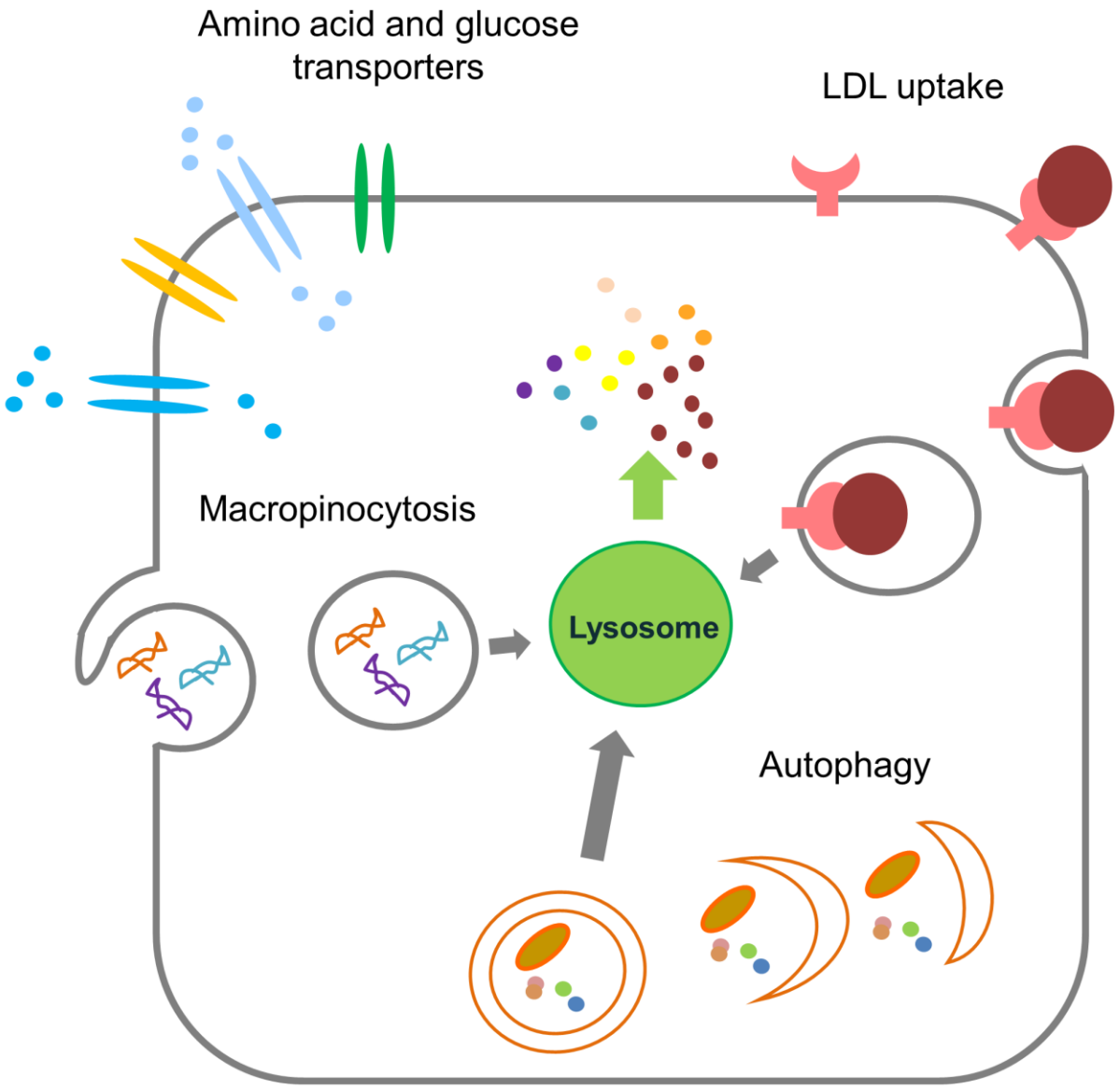

Figure 1: Cancer cells are addicted to nutrients. Oncogene-driven anabolic processes require cancer cells to have continuous influx of nutrients. Cancer cells can increase amino acid and glucose uptake by increasing expression of surface nutrient transporters. Macropinocytosis allows cancer cells to engulf extracellular proteins and lipids. Uptake of lipoprotein via receptor mediated endocytosis also provides nutrients. Recycling of intracellular organelles and proteins via autophagy helps cancer cells adapt to nutrient stress. Nutrient acquisition through macropinocytosis, LDL uptake, and autophagy all require lysosomal degradation.

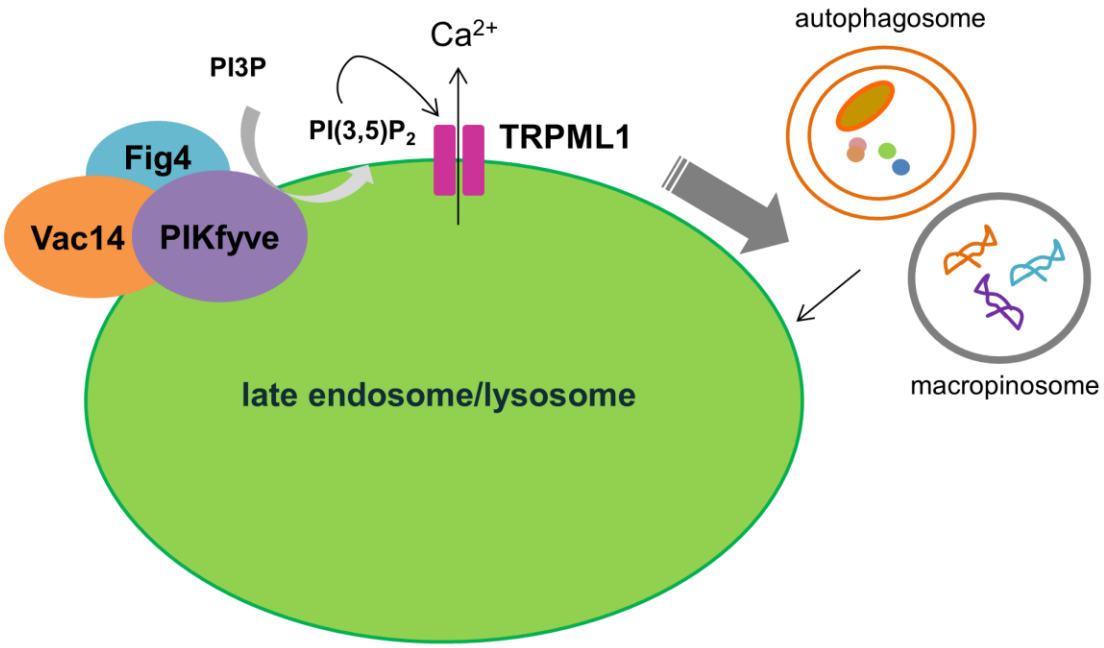

Figure 2: Lysosomal fusion reactions require PIKfyve activity. Phosphoinositide 5-kinase, PIKfyve, forms a complex with its scaffold protein Vac14 and phosphatase Fig4 and generates $(PI3,5)P_2$. The calcium channel TRPML1 on late endosomes or lysosomes is activated by $(PI3,5)P_2$ and promotes fusion of autophagosomes or macropinosomes to lysosomes.

CHAPTER 1

Targeting cancer metabolism by simultaneously disrupting parallel nutrient access pathways

Seong M. Kim[1], Saurabh G. Roy[1], Bin Chen[2], Tiffany Nguyen[1], Ryan J. McMonigle[1], Alison N. McCracken[1], Yanling Zhang[3], Satoshi Kofuji[4], Jue Hou[5], Elizabeth Selwan[1], Brendan T. Finicle[1], Tricia Nguyen[1], Archna Ravi[1], Manuel U. Ramirez[1], Tim Wiher[1], Garret G. Guenther[1], Mari Kono[6], Atsuo T. Sasaki[4], Lois S. Weisman[3], Eric O. Potma[5], Bruce J. Tromberg[5], Robert A. Edwards[7], Stephen Hanessian[2,8], and Aimee L. Edinger[1,*]

[1]Department of Developmental and Cell Biology, University of California Irvine, Irvine CA 92697

[2]Department of Chemistry, Université de Montréal, Quebec, Canada H3C 3J7

[3]Department of Cell and Developmental Biology, University of Michigan, Ann Arbor, MI 48109

[4]Departments of Internal Medicine, Neurosurgery, and Cancer Biology, University of Cincinnati College of Medicine, Cincinnati, OH 45267

[5]Department of Biomedical Engineering, University of California Irvine, Irvine CA 92697

[6]National Institute of Diabetes and Digestive and Kidney Diseases, Bethesda, MD 20892

[7]Department of Pathology, University of California Irvine School of Medicine, Irvine CA 92697

[8]Department of Pharmaceutical Sciences, University of California Irvine, Irvine CA 92697

ABSTRACT: Oncogenic mutations drive anabolism creating a dependency on nutrient influx through transporters, receptors, and macropinocytosis. Sphingolipids suppress tumor growth by down-regulating nutrient transporters, but macropinocytosis and autophagy still provide cancer cells with fuel. Therapeutics that simultaneously disrupt these parallel nutrient access pathways would be more powerful starvation agents. Here we describe a water-soluble, orally bioavailable synthetic sphingolipid, SH-BC-893, that triggers nutrient transporter internalization but also blocks lysosome-dependent nutrient generation pathways. SH-BC-893 activated protein phosphatase 2A (PP2A) leading to mislocalization of the lipid kinase PIKfyve. The concomitant mislocalization of the PIKfyve product, $PI(3,5)P_2$, triggered cytosolic vacuolation and blocked lysosomal fusion reactions essential for LDL, autophagosome, and macropinosome degradation. By simultaneously limiting access to both extracellular and intracellular nutrients, SH-BC-893 selectively killed cells expressing activated Ras, a potently anabolic oncogene, both in vitro and in vivo. However, slower growing, autochthonous PTEN-deficient prostate tumors that do not exhibit a classic “Warburg” phenotype were equally sensitive. Remarkably, normal proliferative tissues were unaffected by doses of SH-BC-893 that profoundly inhibited tumor growth. These studies demonstrate that simultaneously blocking parallel nutrient access pathways with sphingolipid-based drugs is broadly effective and cancer selective, suggesting a novel strategy to overcome resistance conferred by tumor heterogeneity.

INTRODUCTION

To meet the anabolic demands of cell division, oncogenic mutations drive glucose and glutamine transporter gene expression (1–4). The LDL receptor is similarly up-regulated in cancer cells to provide exogenous cholesterol and fatty acids that fuel cell growth (5,6). Oncogenic signaling pathways also promote nutrient uptake post-transcriptionally by preventing the lysosomal degradation of these nutrient transport proteins (7). Tumors with activated Ras acquire additional extracellular nutrients via macropinocytosis, an endocytic process that produces amino acids when engulfed proteins are degraded in the lysosome (8,9). Cancer cells are “addicted” to these nutrient influx pathways because oncogenic mutations create a continuous, high demand for fuel and limit metabolic flexibility. A classic example of how this addiction can be exploited therapeutically is the use of L-asparaginase to kill acute lymphoblastic leukemia cells that cannot synthesize sufficient quantities of the non-essential amino acid asparagine to meet their metabolic demand (10). Pre-clinical studies show that a subset of human cancers likewise require imported LDL, arginine, serine, or glycine for growth and survival (5,11–13). These studies demonstrate that limiting nutrient uptake can selectively eliminate transformed cells, but also highlight that the specific nutrient addictions of different cancer classes diverge depending on the molecular defects present.

An increasingly sophisticated understanding of how individual oncogenes and tumor suppressors alter flux through key metabolic pathways and the expanding ability to catalog the mutations present in tumors will facilitate the use of targeted metabolic therapies. However, tumor heterogeneity limits the effectiveness of these agents. Pre-existing tumor cells that rely on a distinct set of anabolic enzymes would be enriched during treatment with small molecule metabolic inhibitors contributing to the development of resistance (14,15). Selective pressures may also promote rewiring of metabolic pathways in tumor cells that are crippled but not killed by targeted metabolic therapies akin to what has been observed with cytostatic agents targeting

oncogenic signal transduction pathways (16). One means to circumvent these hurdles would be to target the apex of the anabolic pyramid, nutrient uptake. No matter which biosynthetic pathways are essential in a given tumor cell, exogenous nutrients will be required to build biomass. If access to multiple nutrients could be restricted simultaneously, many different tumor classes would be sensitive and potential resistance pathways suppressed.

Identifying compounds with good pharmacological properties that restrict access to multiple nutrients presents a significant challenge (17). Sphingolipids offer a promising alternative to competitive inhibitors of individual nutrient uptake pathways. Natural and synthetic sphingolipids limit glucose and amino acid transporter surface expression through evolutionarily conserved effects on membrane trafficking (18–20). Unfortunately, most sphingolipids have significant pharmacological liabilities that prevent their use in cancer patients despite their activity in vitro and in animal models (21,22). Even if sphingolipids with acceptable drug properties were developed, lysosomal nutrient generation from macropinosome and/or autophagosome degradation could afford resistance, particularly in tumors with activated Ras where these pathways are up-regulated (9,23). Here we report that SH-BC-893, a pharmacologically viable synthetic sphingolipid, is an apical inhibitor of cancer metabolism that blocks nutrient access through multiple, parallel pathways by altering membrane trafficking.

RESULTS

SH-BC-893 starves cancer cells to death. At higher doses than required for immunosuppression, the FDA-approved multiple sclerosis therapy FTY720 selectively kills cancer cells in vitro and in vivo in part by triggering the internalization of glucose and amino acid transporters (20,24–26). Unfortunately, FTY720 cannot be re-purposed for use in cancer patients because it dramatically slows heart rate at the anti-neoplastic dose by activating sphingosine-1-phosphate (S1P) receptor 1 in the heart (22,27,28). The conformationally constrained FTY720 analog SH-BC-893, in contrast, could be used therapeutically as it does not activate $S1P_1$ in reporter cells (Figure 1, A and B). Moreover, neither SH-BC-893 nor its phosphate trigger lymphocyte sequestration, an $S1P_1$-dependent effect (27). Importantly, SH-BC-893 still triggers the selective internalization of amino acid (4F2hc (SLC3A2) or ASCT2 (SLC1A5)) and glucose (GLUT1 (SLC2A1)) transporters (17,27) (Figure 1,C and D). Other surface proteins, such as CD147, a chaperone protein with similar functions to 4F2hc, are not affected. As expected if cells are nutrient-limited, blocking apoptosis via Bcl-X_L over-expression did not prevent SH-BC-893-induced cell death (Figure 1E and Supplemental Figure 1, A and B). In contrast, the transporter-independent, membrane-permeant nutrients methyl pyruvate and dimethyl-α-ketoglutarate rescued SH-BC-893-treated cells (Figure 1E). These results confirm that, like FTY720 (20), SH-BC-893 kills cells by limiting nutrient access.

Cells adapt to nutrient limitation by increasing oxidative phosphorylation (29). The relative rate of glycolysis and oxidative phosphorylation can be monitored by measuring the fluorescence lifetime of the reduced form of nicotinamide adenine dinucleotide (NADH) (30). A higher ratio of protein-bound to free NADH (increased lifetime) correlates with increased oxidative phosphorylation in multiple cell types both in vitro and in vivo (31–36). As expected, cells treated with oligomycin or rotenone/antimycin A compensated for the loss of oxidative phosphorylation by increasing glycolysis, reducing the bound NADH fraction (Figure 1F).

Conversely, the glycolysis inhibitor 2-deoxy-glucose (2-DG) or glucose and amino acid deprivation increased oxidative phosphorylation and the bound to free NADH ratio. As predicted, SH-BC-893 mimicked the effect of amino acid and glucose starvation, increasing the bound NADH fraction and cellular oxygen consumption (Figure 1, F and G). Cells responded similarly to the parent compound, FTY720. Thus, the metabolic changes triggered by SH-BC-893 parallel those seen in cells with restricted access to key metabolic substrates.

If SH-BC-893 kills cells by limiting nutrient access, cells with a higher anabolic rate should be more sensitive. The anabolic rate of murine FL5.12 cells can be titrated by modulating the levels of their required growth factor, IL-3 (37); comparing FL5.12 cells grown in high and low IL-3 allows the impact of elevated growth factor signaling and anabolism to be evaluated in a constant genetic background. High concentrations of IL-3 drive aerobic glycolysis and a rapid doubling time (12 h). Reducing IL-3 levels slows proliferation and increases oxidative phosphorylation without compromising cell viability (Figure 2, A and B) (37). As predicted, maintenance in low IL-3 medium reduced the need for metabolic adaptation (Figure 2B) and protected cells from SH-BC-893-induced death (Figure 2A) suggesting that elevated growth factor signaling and anabolism in transformed cells will confer hypersensitivity to SH-BC-893. Indeed, non-transformed murine OP9 bone marrow stromal cells and primary murine embryonic fibroblasts (MEFs) were less sensitive to SH-BC-893 than human cancer cell lines (Figure 2C). Many of these cancer cell lines carry activating mutations in Ras. In fact, K-Ras activation following Cre expression in Lox-STOP-Lox-KRasG12D MEFs (38) was sufficient to limit metabolic flexibility and sensitize cells to SH-BC-893 (Figure 2, D and E). Loss of the tumor suppressor PTEN produced similar effects (Supplemental Figure 2, A and B). Importantly, oncogenic mutations did not affect surface nutrient transporter down-regulation in K-Ras G12D-expressing or PTEN-deficient MEFs (Supplemental Figure 2C). These results indicate that both normal and transformed cells express the SH-BC-893 target and differential sensitivity to the

compound stems from the lack of metabolic adaptation in cancer cells. Consistent with these results in MEFs, normal human peripheral blood mononuclear cells (PBMC) were also resistant to SH-BC-893 relative to SW620 colon cancer cells (Figure 2F) in colony formation assays. Taken together, these data suggest that constitutive anabolism sensitizes cancer cells to SH-BC-893 and could generate an acceptable therapeutic index.

To determine whether SH-BC-893 inhibited tumor growth in vivo, luciferase-expressing SW620 xenografts were generated. Bioluminescence imaging (BLI), caliper measurements, and tumor mass at sacrifice were reduced to a similar degree by SH-BC-893 and FTY720 (Figure 2, G-I and Supplemental Figure 2D). Consistent with these effects, SH-BC-893 was present at low micromolar concentrations in both tumors and plasma at sacrifice (Supplemental Figure 2E). Mild weight loss occurred in treated mice as expected given that nutrient access would be restricted in both normal and transformed cells (Supplemental Figure 2F). These results suggest that SH-BC-893 could provide a safe and effective means to target Ras-driven cancer anabolism in vivo.

SH-BC-893 interferes with late endocytic trafficking. SH-BC-893 was surprisingly effective given that Ras activation increases macropinocytosis and autophagy (9,23), processes that should provide resistance to surface nutrient transporter loss. We therefore hypothesized that SH-BC-893 might affect additional trafficking pathways. Interestingly, SH-BC-893 induced equally striking cytosolic vacuolation in both non-transformed and cancer cells (Figure 3A and Supplemental Figure 3, A, B, and C). These vacuoles contained intraluminal vesicles (ILVs) as well as amorphous, partially degraded material suggesting that they originate from multivesicular bodies (MVBs) or another late endocytic compartment (Figure 3B). Vacuoles were positive for the late endosomal markers Lamp1 and Rab7 (Figure 3C) and negative for the early endosomal markers EEA1 and Rab5 and the lipid stain Nile Red (Supplemental Figure

3D). Acidified puncta, likely lysosomes, were observed within or proximal to vacuoles along with material marked as autophagosomes by GFP-LC3 (Figure 3,C and D and Supplemental Figure 3E). Taken together, these results suggest that SH-BC-893 enlarges MVBs.

$PI(3,5)P_2$, the product of the PI3P 5-kinase PIKfyve, regulates membrane fusion and ILV formation in MVBs (39). Reducing PIKfyve activity with the inhibitor YM201636 produced PI3P-positive, $PI(3,5)P_2$-negative vacuoles phenotypically similar to those generated by SH-BC-893 and FTY720 (Figure 3, A and E and Supplemental Figure 3, A and F) (40–42). The Ca^{2+} channel TRPML1 (transient receptor potential cation channel, mucolipin subfamily, member 1) is found in MVB membranes where it is activated by $PI(3,5)P_2$ generated by PIKfyve (43). TRPML1 accumulated in vacuolar membranes in FTY720- and YM201636-treated cells (Figure 3E). Over-expression of PIKfyve, its scaffolding protein Vac14, or its effector protein TRMPL1 rescued from either FTY720- or YM201636-induced vacuolation while a Vac14 mutant that does not associate with PIKfyve was ineffective (Figure 3F). Together, these data suggest that SH-BC-893 and FTY720 enlarge MVBs by reducing PIKfyve activity similar to YM201636.

Unexpectedly, FTY720 did not inhibit PIKfyve kinase activity or reduce $PI(3,5)P_2$ levels at concentrations that profoundly vacuolate cells (Figure 4, A and B). Rather, FTY720 disrupted PIKfyve localization. While mCitrine-tagged PIKfyve localized to the limiting membrane of YM201636-induced vacuoles as expected, PIKfyve was present in clumps between vacuoles in FTY720-treated cells (Figure 4C and Supplemental Figure 3F). Validated antibodies recognizing endogenous PIKfyve and Vac14 confirmed this result (Figure 4C and Supplemental Figure 4, A and B). Consistent with their disparate mechanisms of action, YM201636 abolished membrane association of the $PI(3,5)P_2$ probe mCherry-ML1N*2 (44), while in FTY720 or SH-BC-893 treated cells, mCherry-ML1N*2 co-localized with PIKfyve to puncta between the vacuoles (Supplemental Figure 3F). Moreover, neither PIKfyve (Figure 4D) nor mCherry-

ML1N*2 (Supplemental Figure 4D) co-localized with the PI(3,5)P_2 effector protein TRPML1 on vacuoles in FTY720- or SH-BC-893-treated cells. As TRPML1 was present on both YM201636- and SH-BC-893-induced vacuoles (Figure 3E and Supplemental Figure 4D), PIKfyve and not TRPML1 was mislocalized by FTY720 and SH-BC-893. FTY720 and SH-BC-893 also eliminated PIKfyve from the TRPML1-positive vacuoles in YM201636-treated cells (Figure 4D). Consistent with its lack of vacuolating activity (Figure 3A), ceramide did not disrupt PIKfyve-TRMPL1 co-localization in the presence or absence of YM201636 (Figure 4D). These results indicate that FTY720 and SH-BC-893 induce vacuolation by mislocalizing PIKfyve leading to generation of the membrane anchored lipid, PI(3,5)P_2, in separate compartment from its transmembrane effector protein, TRPML1.

Ceramide, FTY720, and SH-BC-893 trigger nutrient transporter loss by activating PP2A (Figure 5, A and B) (18,20,27,45,46). Activation of PP2A by sphingolipids is specific as dihydroceramide, which differs from ceramide by a single saturated bond, fails to activate PP2A, does not kill cells, and does not trigger transporter loss or vacuolation (Figure 5A and Supplemental Figure 5A) (46,47). FTY720 or SH-BC-893 also caused vacuolation by activating PP2A as the selective PP2A inhibitor calyculin A and the protein inhibitor of PP2A, SV40 small t antigen, both blocked this effect (Figure 5C); YM201636-induced vacuolation was unaffected by PP2A inhibition (Supplemental Figure 5B). PP2A activation triggered PIKfyve mislocalization as inhibiting PP2A restored PIKfyve to YM201636-induced vacuoles in FTY720- or SH-BC-893-treated cells (Figure 4D). As ceramide triggers transporter loss by activating PP2A (18) but does not vacuolate cells (Figure 3A) or induce PIKfyve mislocalization (Figure 4D), different PP2A heterotrimers or distinct pools of PP2A promote nutrient transporter down-regulation and vacuolation. Consistent with a model where FTY720 and SH-BC-893 disrupt two distinct trafficking pathways downstream of different PP2A complexes, amino acid and glucose transporters internalized by FTY720 and SH-BC-893 did not co-localize with the PIKfyve

complex (Supplemental Figure 5C). Moreover, triggering vacuolation with YM201636 did not decrease surface nutrient transporter levels, and preventing vacuolation by over-expressing Vac14 did not interfere with nutrient transporter down-regulation by FTY720 (Supplemental Figure 5, D and E). Taken together, these data indicate that FTY720 and SH-BC-893 disrupt PIKfyve localization and nutrient transporter trafficking in both normal and transformed cells through two distinct PP2A-dependent mechanisms.

PIKfyve mislocalization blocks lysosomal nutrient production. Cells adapt to nutrient stress by increasing autophagic flux (17). However, autophagosome-lysosome fusion reactions depend upon Ca^{2+} released through TRPML1 channels that are activated by $PI(3,5)P_2$ (43,48). The loss of PIKfyve and $PI(3,5)P_2$ co-localization with TRPML1 (Figure 4D and Supplemental Figure 4D) suggested that SH-BC-893 might limit autophagic flux. In cells where autophagolysosomes were stabilized by chloroquine (CQ), addition of FTY720, SH-BC-893, or YM201636 reduced fusion of LC3-positive autophagosomes with LAMP1-positive lysosomes (Figure 6, A and B). Interestingly, vacuolating sphingolipids also decreased the total number of LC3 puncta per cell, suggesting that autophagosome formation was reduced (Figure 6C). PI5P is essential for autophagosome biogenesis upon glucose depletion (49). As PI5P is produced by dephosphorylating $PI(3,5)P_2$ (50), PI5P might also be mislocalized in SH-BC-893-treated cells, thereby disrupting autophagosome formation. Indeed, FTY720 and SH-BC-893 reduced the number of WIPI2-positive nascent autophagosomes detected in low-nutrient media without affecting PI5P levels (Figure 6, D and E and Supplemental Figure 6A). Thus, SH-BC-893 inhibited both autophagosome formation and degradation. Vac14 over-expression limits vacuolation (Figure 3F and 6F, Supplemental Figure 6B) and should rescue autophagic flux in SH-BC-893-treated cells. Vac14 over-expression restored both autophagosome formation and lysosomal fusion in FTY720- and SH-BC-893-treated cells (Figure 6, A,B,D, and E). Together, these data indicate that SH-BC-893 blocks autophagic flux at multiple levels through effects on

PIKfyve, likely enhancing the bioenergetic stress induced by transporter down-regulation (Figure 1).

In cells with activated Ras, macropinocytosis might also confer resistance to nutrient transporter down-regulation (9). However, $PI(3,5)P_2$ is also required for macropinosome degradation (51). While K-RasG12D expressing cells efficiently macropinocytosed dextran in an 5-(N-ethyl-N-isopropyl) amiloride (EIPA) sensitive manner, both YM201636 and SH-BC-893 dramatically reduced macropinosome fusion with lysosomes (Figure 6, G and H). Macropinosomes that fail to fuse with lysosomes would not supply amino acids (8). Thus, by disrupting PIKfyve localization, SH-BC-893 limits access to lysosomally-derived nutrients (Figure 6) at the same time it down-regulates transporters for amino acids and glucose (Figure 1,C and D).

Vacuolation increases the anti-neoplastic activity of SH-BC-893. To assess the relative contribution of vacuolation to SH-BC-893's anti-neoplastic activity, cells were treated with YM201636 (vacuolation only) and ceramide (transporter loss without vacuolation) alone and in combination. YM201636 was minimally cytotoxic as a single agent but significantly enhanced ceramide-induced death in multiple cancer cell lines without increasing nutrient transporter loss (Figure 7, A and B and Supplemental Figures 5D and 7A). Moreover, Vac14 over-expressing cells that did not vacuolate (Figures 3F and 6F) were resistant to SH-BC-893- and FTY720-induced death but were not protected from death induced by the non-vacuolating sphingolipid ceramide (Figure 7, C and D and Supplemental Figure 7B). Taken together, these data suggest that vacuolation contributes to the ability of SH-BC-893 to kill cancer cells. To assess whether vacuolation enhances the anti-neoplastic activity of SH-BC-893 in vivo, mice bearing SW480 xenografts expressing empty vector or Vac14 were treated with vehicle or SH-BC-893 by gavage. Tumors were harvested while still small in order to limit tumor necrosis that might confound microscopic analysis of SH-BC-893-induced vacuolation. As seen in vitro, Vac14

over-expression conferred resistance to both vacuolation and growth inhibition by SH-BC-893 (Figure 7, E and F). These results demonstrate that vacuolation contributes to the anti-neoplastic effects of SH-BC-893 both in vitro and in vivo.

The multifaceted actions of SH-BC-893 confer activity in slower growing, autochthonous prostate tumors. Because the activity of SH-BC-893 was linked to metabolic rate (Figure 2, A and B), it was not clear whether slower-growing tumors that do not exhibit the classic Warburg phenotype would be also be sensitive. To test this, SH-BC-893 was evaluated in a validated genetically-engineered mouse model for invasive castration-resistant prostate cancer that lacks p53 and PTEN expression exclusively in the prostate (pDKO) (52–54). Cells derived from tumors in these mice (mouse prostate cancer epithelial cells, mPCEs) exhibited reduced glycolysis and were not dependent on extracellular glucose and amino acids for survival (Figure 8, A and B). However, SH-BC-893 still produced a phenotype consistent with starvation as the bound NADH fraction increased and cell permeant nutrients protected mPCE cells from death (Figure 8, A and C). Prostate cancer cells depend on exogenous LDL for growth and survival (5). Interestingly, SH-BC-893 not only vacuolated mPCE cells and down-regulated 4F2hc, but also dramatically decreased surface levels of the LDL receptor (LDLr), LDL uptake, and lipid droplet accumulation (Figure 8D-H and Supplemental Figures 3B and 8, A and B). Ceramide and YM201636 both reduced surface LDLr levels but LDLr accumulated in different intracellular compartments (Supplemental Figure 8A). Consistent with their ability to block lysosomal fusion (Figure 6), both YM201636 and SH-BC-893 reduced LDL co-localization with Lysotracker Blue (Figure 8, F and G). In keeping with the inhibition of LDL degradation in lysosomes, cellular lipid droplet content was inversely correlated with the extent of vacuolation (Supplemental Figure 8B). In summary, SH-BC-893 starves prostate cancer cells for essential nutrients both by down-regulating transporters and by blocking lysosomal nutrient generation.

The effect of SH-BC-893 on prostate tumor growth in vivo was next evaluated. In C57BL/6 mice bearing mPCE subcutaneous isografts, 60 mg/kg SH-BC-893 given daily by gavage slowed tumor growth by 60% similar to results with SW620 xenografts dosed with 20 mg/kg i.p. (Figure 2G-I and 8I). At 120 mg/kg, SH-BC-893 inhibited prostate tumor growth by more than 90% (Figure 8I). Similarly, SH-BC-893 decreased autochthonous tumor growth in pDKO mice by 62% (60 mg/kg) or 82% (120 mg/kg) (Figure 8J). Histologically, SH-BC-893 slowed prostate tumor progression, eliminating invasive disease and dramatically reducing cellular pleomorphism, hyperchromasia, and nuclear atypia; SH-BC-893-treated mice exclusively exhibited prostatic intraepithelial neoplasia while adenocarcinoma was present in all vehicle-treated animals (Supplemental Figure 9). As expected if amino acid transporters are down-regulated (Figure 8D), TORC1-dependent ribosomal protein S6 phosphorylation was reduced in SH-BC-893-treated tumors (Supplemental Figure 8C). Akt activity was slightly elevated by SH-BC-893 consistent with loss of TORC1-mediated negative feedback. Thus, SH-BC-893 is effective against tumors with distinct molecular defects and metabolic characteristics.

SH-BC-893 produces equivalent transporter loss and vacuolation in normal and transformed cells and therefore limits the access of normal cells to nutrients (Figures 1, C and E, and Supplemental Figure 3, B and C). Consistent with this, SH-BC-893-treated pDKO mice gained less weight than controls (Supplemental Figure 8D). However, even mice treated with the highest dose of SH-BC-893 gained weight, and all treated mice exhibited normal behavior and activity levels. Blood chemistry analysis at sacrifice indicated that SH-BC-893 was not toxic to the liver or kidneys at the anti-neoplastic dose (Supplemental Table 1). The slight elevation in serum creatine phosphokinase in animals treated with 120 mg/kg SH-BC-893 is suggestive of mild muscle catabolism in response to nutrient restriction. Importantly, proliferating normal tissues were minimally affected by SH-BC-893 as evidenced by normal complete blood counts and histopathology of intestinal crypts in mice treated with 120 mg/kg SH-BC-893 for 11 weeks

(Supplemental Table 2 and Supplemental Figure 8E). The lack of toxicity to normal tissues is consistent with our finding that non-transformed cells can adapt to nutrient stress that triggers a bioenergetic crisis in less metabolically flexible tumor cells (Figure 2, D and E). In conclusion, blocking parallel nutrient access pathways by disrupting membrane trafficking is a safe and effective means to target constitutive anabolism in cancer cells with divergent metabolic programs.

DISCUSSION

These studies demonstrate that synthetic sphingolipids with vacuolating properties starve multiple classes of cancer cells to death while sparing normal tissues. SH-BC-893 was effective against tumors with distinct metabolic signatures and growth characteristics most likely because it inhibits both primary and adaptive nutrient acquisition pathways, down-regulating cell surface transporters/receptors while simultaneously blocking the lysosomal degradation of autophagosomes, macropinosomes, and LDL particles (Figure 9) (17). The target of SH-BC-893, PP2A, is activated in both non-transformed and cancer cells leading to nutrient transporter loss and profound vacuolation (Figures 1, C and D and Supplemental Figure 2C and 3A-C). However, non-transformed cells survive SH-BC-893 induced nutrient stress due to their ability to make appropriate metabolic adaptations; oncogenic mutations lock cancer cells into a pro-growth metabolic program that sensitizes them to nutrient stress (Figure 2A-F and Supplemental Figure 2, A and B). By blocking multiple nutrient access pathways, SH-BC-893 acts as a cellular starvation mimetic; tumor cells are also hypersensitive to dietary restriction and intermittent fasting (55). However, as dietary restriction is ineffective against PTEN-deficient tumors (56) and SH-BC-893 profoundly inhibited the growth of PTEN-null prostate tumors (Figure 8, I and J), cellular and organismal nutrient limitation likely limit tumor growth through distinct mechanisms. While SH-BC-893 was not toxic to normal proliferative tissues at the anti-neoplastic dose (Figure 2F, Supplemental Figure 8E, and Supplemental Tables 1 and 2), a consideration with any cancer therapy that limits nutrient access is how it would affect cachexic patients. Cancer cachexia has a complex etiology and is not simply a consequence of reduced food intake (57). It is possible that compounds that limit tumor lactate production might actually benefit cachexic patients if they reduce the futile Cori cycle through which the liver converts tumor lactate into glucose. How SH-BC-893 administration affects whole body metabolism and cytokine levels merits further investigation.

As a single agent, SH-BC-893 acts like a combination therapy by targeting the multiple nutrient acquisition pathways that fuel cancer anabolism (17). It will be important to test whether pairing SH-BC-893 with drugs that target oncogenic signal transduction pathways will increase efficacy. Our results provide a strong rationale for combining SH-BC-893 with PI3 kinase inhibitors (58). Akt activity increased in SH-BC-893-treated prostate tumors (Supplemental Figure 8C) most likely due to the loss of TORC1-dependent negative feedback in cells where SH-BC-893 restricted access to amino acids. Suppressing Akt activity while administering SH-BC-893 might increase tumor growth inhibition or even cause tumor regression. Combination with androgen signaling inhibitors might also be valuable; the studies shown in Figure 8I and J were performed in intact male mice. Importantly, there are currently no other agents that can reconstitute the multifaceted effects of SH-BC-893. While PIKfyve kinase inhibitors such as apilimod (59) might induce vacuolation, PIKfyve inhibition alone does not reduce surface transporter levels (Supplemental Figure 5D). While Akt activates PIKfyve (60), Akt inhibitors do not induce vacuolation or transporter loss (data not shown and (17)). Indeed, no agents other than sphingolipids coordinately down-regulate transporters for multiple nutrients. Thus SH-BC-893 is a unique, apical inhibitor of cancer metabolism that works by blocking parallel, partially redundant nutrient access pathways (17).

The development of resistance limits the effectiveness of targeted therapies. Because sensitivity to SH-BC-893 is linked to an intrinsic property of cancer cells, constitutive anabolism, rather than a particular genetic lesion, it may be more difficult for cancer cells to become resistant to the metabolic effects of SH-BC-893. Indeed, individual oncogenic mutations were sufficient to limit the metabolic flexibility of nutrient-stressed cells and sensitize them to SH-BC-893-induced death (Figure 2, D and E and Supplemental Figure 2, A and B). The ability of SH-BC-893 to simultaneously block four key pathways for nutrient acquisition (glucose and amino acid transporters, LDL receptors, macropinocytosis, and autophagy) also limits the options for

acquired resistance. These multifaceted actions should also reduce the ability of tumor heterogeneity to confer drug resistance as tumor cells with very different metabolic profiles are equally sensitive (Figures 2 and 8). Although metabolic reprogramming may be unlikely to afford resistance, cancer cells could become insensitive to SH-BC-893 due to mutations in the target or downstream pathways. Eliminating global PP2A activity is cell lethal and therefore not a viable resistance strategy. However, cancer cells may acquire resistance by reducing the activity of the specific PP2A complexes activated by SH-BC-893. Genetic alterations that limit vacuolation may also reduce sensitivity to SH-BC-893. A cBioportal search revealed that Vac14, a protein that confers partial resistance to SH-BC-893 (Figure 7C-F), is amplified in 27% of breast cancer xenografts in one dataset, but amplification was not detected in primary patient breast tumors. On the other hand, Vac14 is deleted in 3-6% of prostate tumors, which might conversely sensitize these cancers to SH-BC-893. It is interesting that we were able to generate SW480, but not SW620, cells that stably over-expressed Vac14. SW620 and SW480 were isolated from the same patient, but SW480 cells were derived from the primary tumor site and SW620 from a lymph node metastasis. It is possible that Vac14 over-expression is poorly compatible with mutations that confer tumor aggressiveness and metastatic potential. Identifying biomarkers that correlate with sensitivity and resistance to SH-BC-893 will help to clarify this issue.

In conclusion, water-soluble and orally bioavailable vacuolating sphingolipid drugs like SH-BC-893 could provide a cell biology- rather than biochemistry-based approach to targeting “cancer metabolism.” Although optimization of pharmacological properties, formulation, dose, and schedule of administration is warranted, the water solubility, oral activity, micromolar trough levels, and accumulation in tumors suggest that SH-BC-893 has good drug-like properties and is worthy of further pre-clinical evaluation.

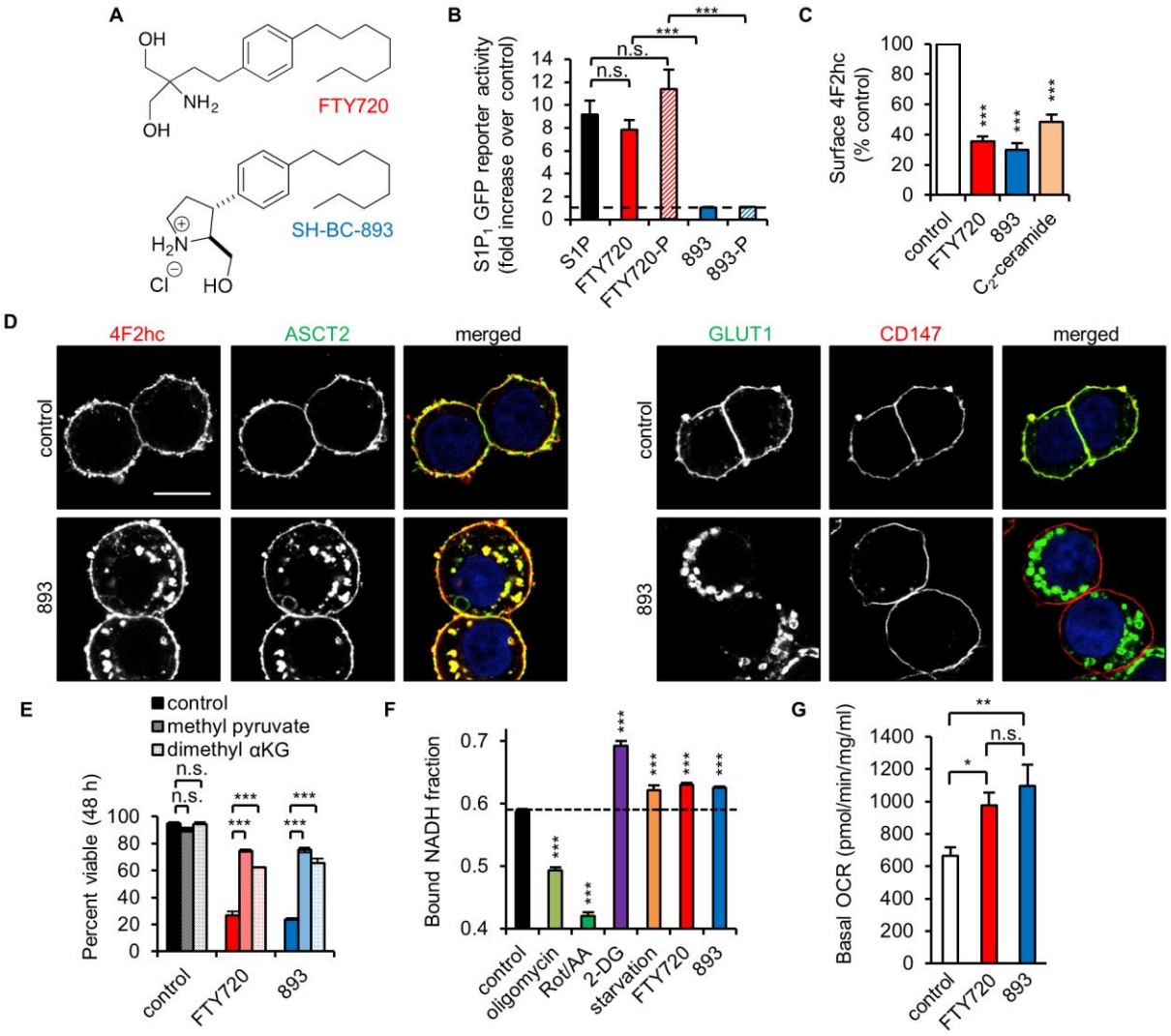

Figure 1: SH-BC-893 triggers nutrient transporter internalization mimicking starvation. (**A**) Structures of FTY720 and SH-BC-893. (**B**) $S1P_1$ receptor-driven GFP expression measured by flow cytometry in reporter MEFs after a 24 h incubation with indicated compounds at 2.5 µM. (**C**) Surface 4F2hc measured by flow cytometry in FL5.12 cells treated with 5 µM FTY720 or SH-BC-893 (893) or 10 µM C_2-ceramide. (**D**) SH-BC-893-treated SW620 cells stained as indicated. Scale bar, 10 µm. (**E**) Viability of Bcl-X_L over-expressing FL5.12 cells treated as indicated +/- 5.5 mM methyl pyruvate or 2 mM dimethyl α-ketoglutarate (α-KG). (**F**) Bound NADH fraction in MEFs treated with mitochondrial inhibitors (1 µM oligomycin or 1 µM rotenone and antimycin A), 1 mM 2-deoxyglucose (2-DG), 5 µM FTY720, or 7.5 µM SH-BC-893 for 16 h. For starvation, growth media was replaced with DMEM lacking glucose and amino acids supplemented with 10% dialyzed FCS. Statistics comparing to respective control. (**G**) Oxygen consumption rate (OCR) in MEFs treated with FTY720 or SH-BC-893 for 16 h measured by XF24 Extracellular Flux Analyzer. Means +/- SEM. Using Student's unpaired, two-tailed t-test, *, P <0.05; **, P <0.01; ***, P <0.001; n.s., not significant (P >0.05). P-value was determined using Tukey's method when correcting for multiple comparisons. Data are representative of at least 3 independent experiments.

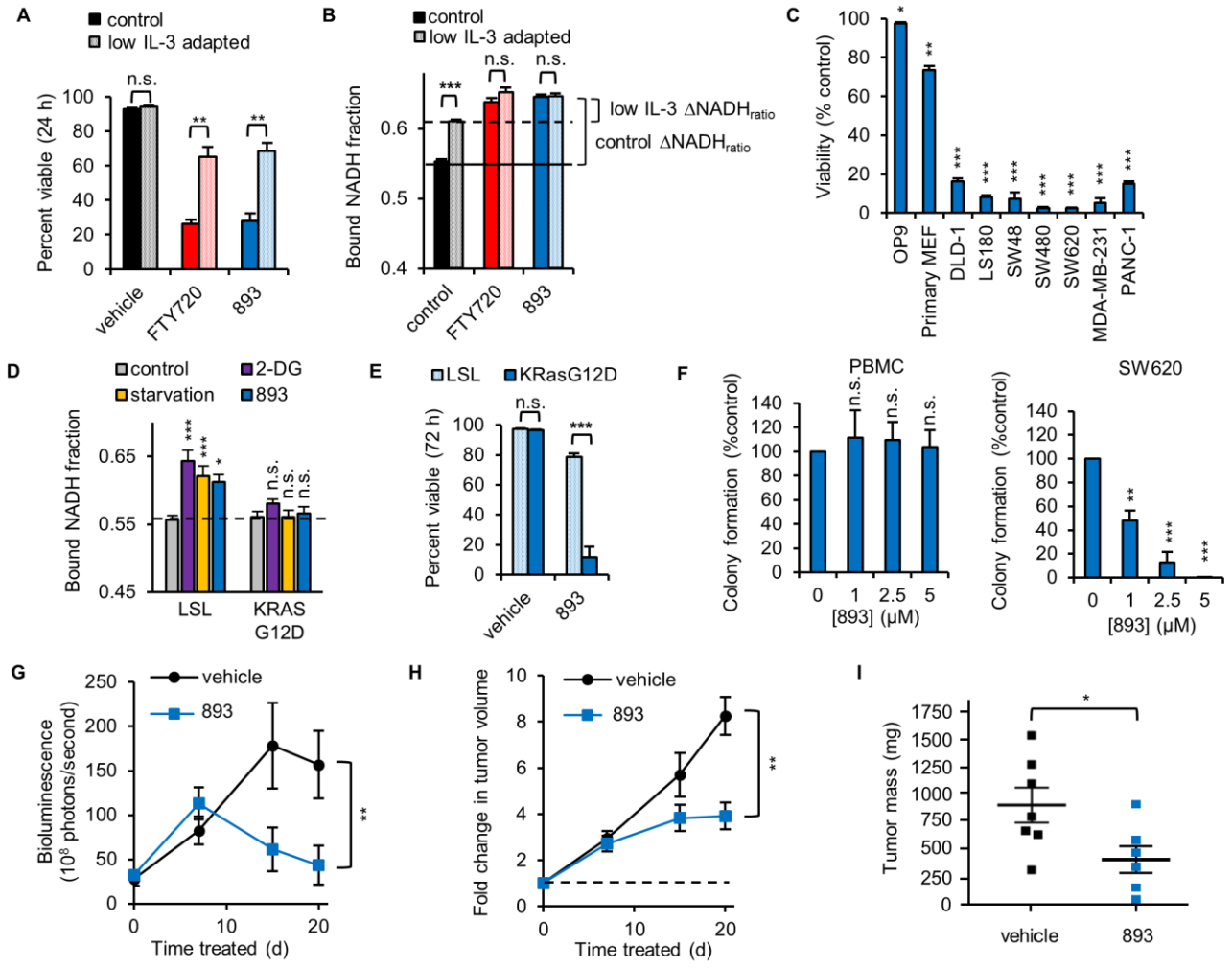

Figure 2: SH-BC-893 selectively kills cancer cells. (**A**) Viability of FL5.12 cells cultured in control medium (500 pg/ml IL-3) or adapted to low IL-3 (25 pg/ml) treated with 5 μM FTY720 or SH-BC-893. (**B**) Bound NADH fraction in FL5.12 cells cultured as in (**A**) and treated with FTY720 or SH-BC-893. (**C**) Viability of the indicated cells treated with 5 μM SH-BC-893 for 72 h. Statistics comparing to vehicle. OP9 (murine bone marrow stromal cells) and primary MEF are non-transformed cells. DLD-1, LS180, SW480, SW480, and SW620 are colon cancer cell lines. MDA-MB-231 and PANC-1 are breast cancer and pancreatic cancer cell lines, respectively. (**D**) Bound NADH fraction in control or K-RasG12D expressing MEFs treated with 1 mM 2-deoxyglucose (2-DG), starvation media (glucose and amino acids supplemented with 10% dialyzed FCS), or 7.5 μM SH-BC-893 for 16 h. Statistics comparing to respective control. (**E**) Viability of $p53^{-/-}$ MEFs that do or do not express K-RasG12D treated with 6 μM SH-BC-893. (**F**) Colony formation by normal human PBMCs or SW620 CRC cells +/- SH-BC-893 at indicated doses. Means +/- SEM. (**G-I**) Subcutaneous SW620 tumor growth as measured by bioluminescence imaging (**G**), calipers (**H**), or tumor weight at sacrifice (**I**). Because FTY720 and SH-BC-893 were similarly potent in vitro (Figure 1C,E) (26), SH-BC-893 was given intraperitoneally at 10 mg/kg for 7 d. Based on BLI (**G**), the dose was increased to 20 mg/kg on day 8. Means +/- S.D., n = 7 mice per group. Using Student's unpaired, two-tailed t-test, *, P <0.05; **, P <0.01; ***, P <0.001; n.s., not significant (P >0.05). P-value was determined using Tukey's method when correcting for multiple comparisons. In vitro data are representative of at least 3 independent experiments.

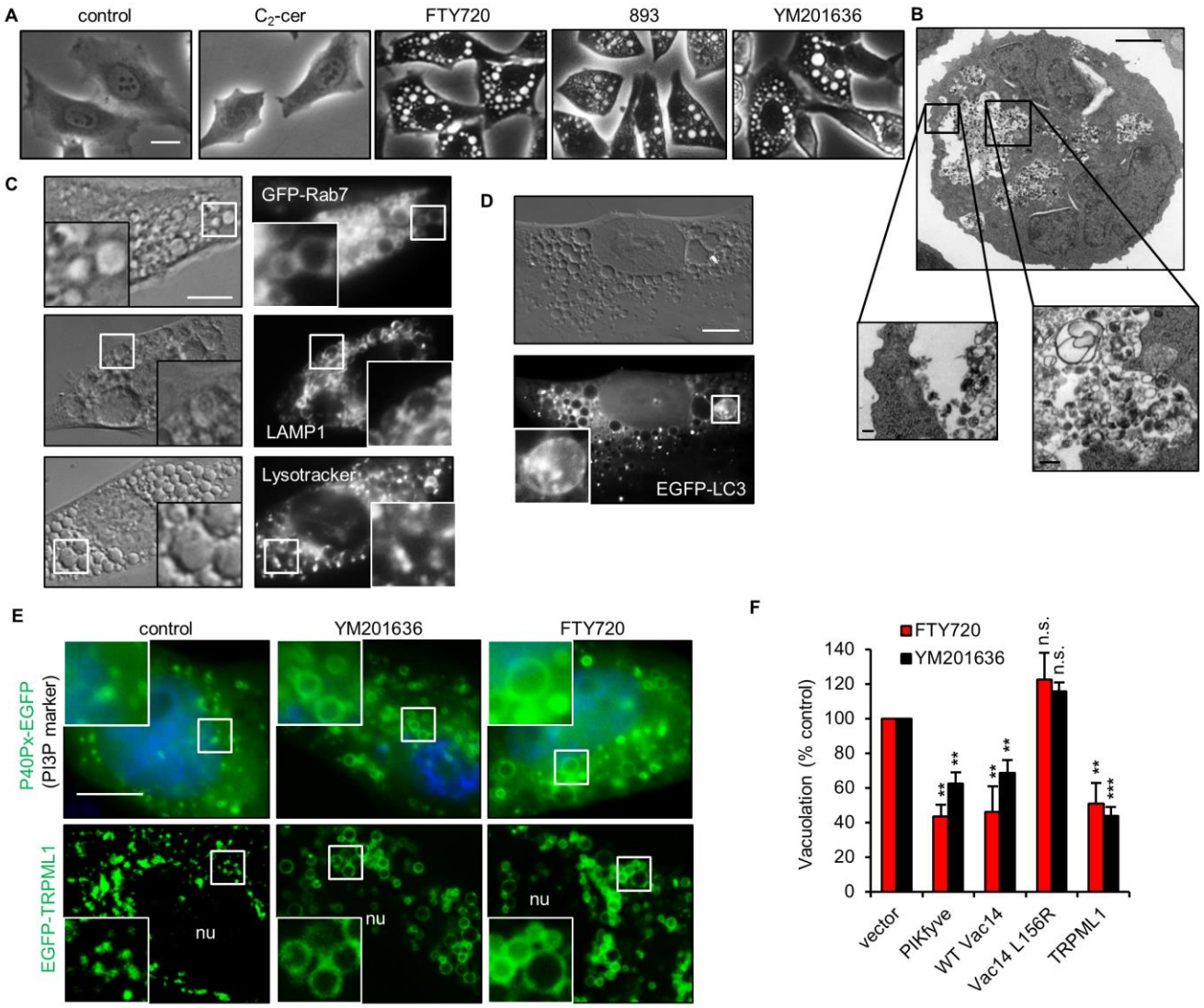

Figure 3: Sphingolipid-induced vacuolation resembles PIKfyve inhibition. (**A**) HeLa cells treated as indicated with 25 µM C_2-ceramide, 5 µM FTY720 or SH-BC-893, or 800 nM YM201636 for 6 h. (**B**) Electron micrograph of an FL5.12 cell treated with FTY720 for 24 h. Scale bar, 2 µm or 0.2 µm in zoom. (**C**) GFP-Rab7 expressing HeLa cells (top) or MEFs treated with FTY720 and stained as indicated. Images of three separate cells are shown. (**D**) EGFP-LC3-expressing MEFs treated with FTY720. (**E**) P40Px-EGFP- or EFGP-TRPML1-expressing HeLa cells treated with YM201636 or FTY720 for 6 h. (**F**) HeLa cells over-expressing PIKfyve, WT Vac14, mutant (L156R) Vac14 or TRPML1 treated with YM201636 or FTY720. Means +/- SEM, n ≥ 3 independent experiments; ≥ 30 cells per condition were analyzed per experiment. Statistics comparing to respective control. Using Student's unpaired, two-tailed t-test, **, *P* <0.01; ***, *P* <0.001; n.s., not significant (*P* >0.05). *P*-value was determined using Tukey's method to correct for multiple comparisons. Scale bar, 10 µm except (**B**).

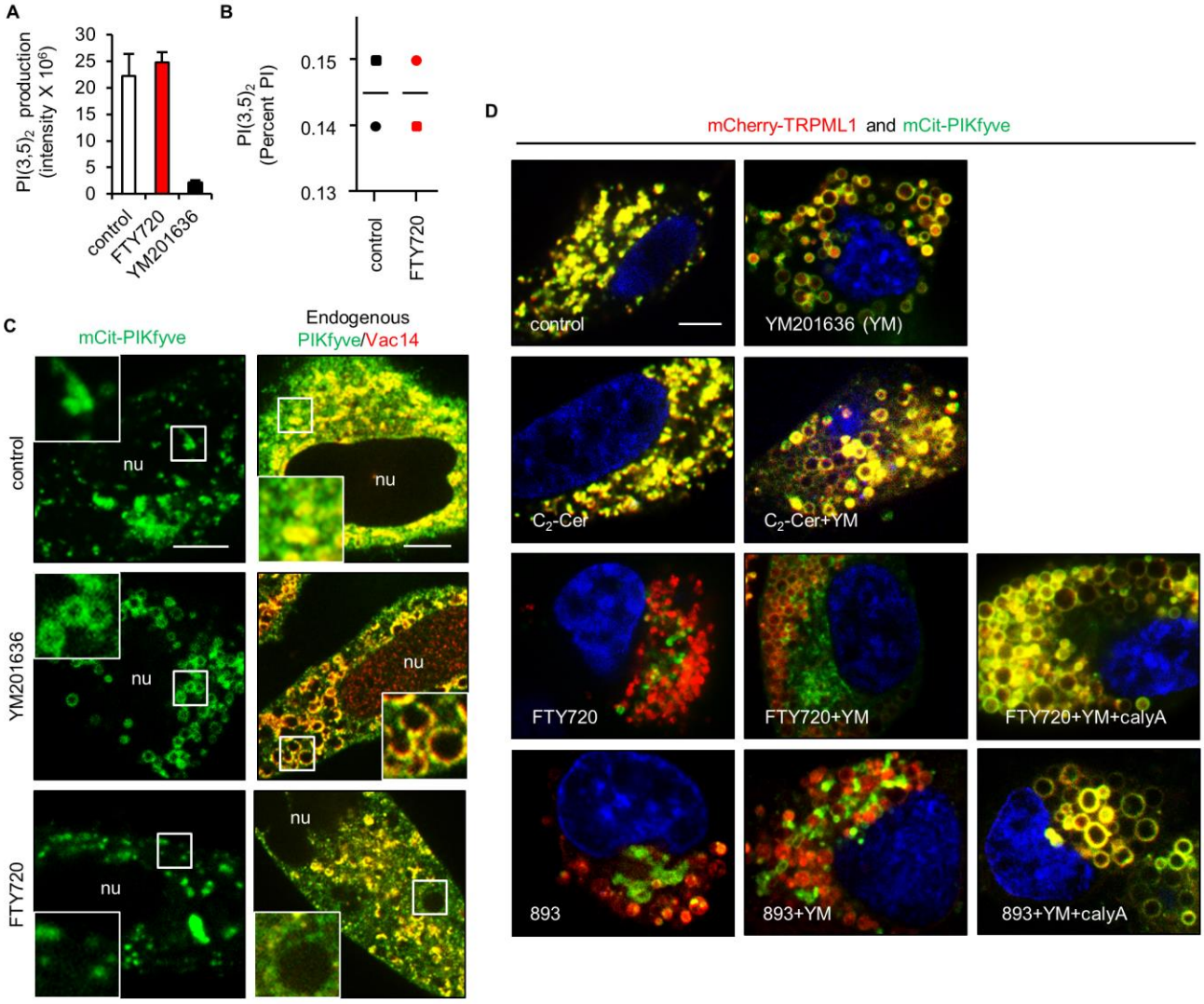

Figure 4: SH-BC-893 and FTY720 disrupt PIKfyve localization but not its activity. (**A**) In vitro kinase assay with purified FLAG-PIKfyve +/- 5 µM FTY720 or 800 nM YM201636. Means +/- S.D. from 3 technical replicates. (**B**) PI(3,5)P_2 levels in HeLa cells treated with FTY720 expressed as a percentage of total phosphatidylinositol. Bar, average from two independent experiments. (**C**) mCitrine-PIKfyve or endogenous PIKfyve/Vac14 in HeLa cells treated with 800 nM YM201636 or 5 µM FTY720 for 6 h. (**D**) HeLa cells expressing low levels of mCitrine-PIKfyve and mCherry-TRPML1 treated as indicated (800 nM YM201636, 5 µM FTY720 or SH-BC-893, 25 µM C_2-ceramide (C_2-Cer), or 5 nM calyculinA (calyA)). Scale bar, 10 µm.

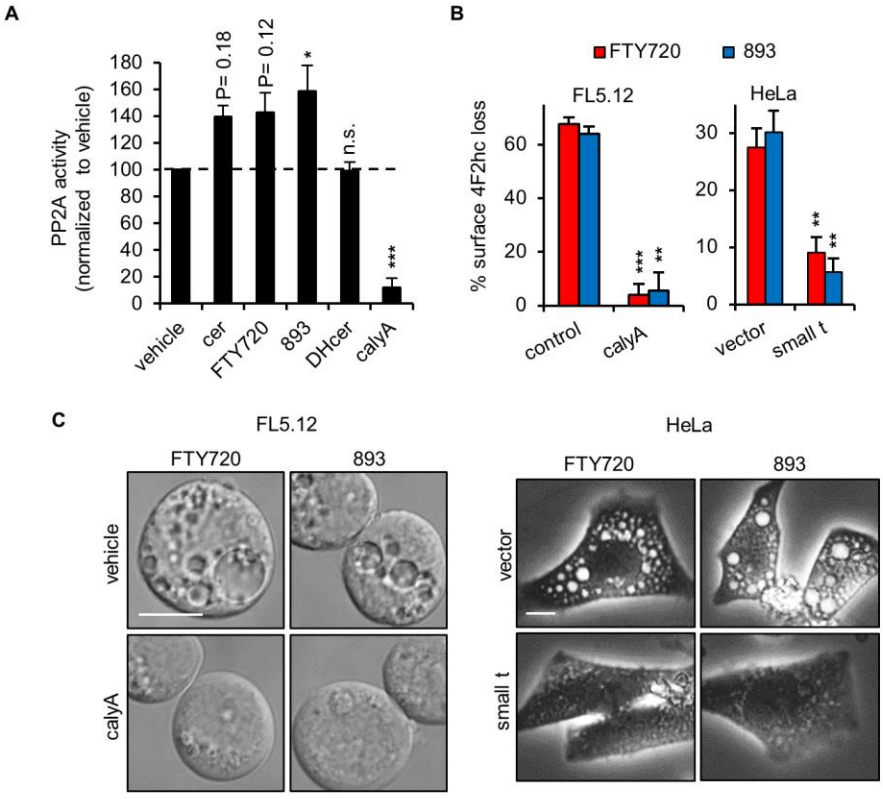

Figure 5: SH-BC-893 and FTY720 activate PP2A to induce vacuolation. (**A**) PP2A phosphatase activity was measured in FL5.12 cell lysates in the presence or absence of 50 µM C_2-ceramide (cer) or dihydro-C_2-ceramide (DHcer), 5 µM FTY720 or SH-BC-893 (893), or 5 nM calyculinA (calyA). (**B-C**) Surface 4F2hc (**B**) or vacuolation (**C**) in FL5.12 cells pre-treated with vehicle or 5 nM calyA or HeLa cells expressing vector or SV40 small t antigen treated as indicated. Means +/- SEM. Using Student's unpaired, two-tailed t-test, *, *P* <0.05; **, *P* <0.01; ***, *P* <0.001; n.s., not significant (*P* >0.05). *P*-value was determined using Tukey's method when correcting for multiple comparisons. Data are representative of at least 3 independent experiments. Scale bar, 10 µm.

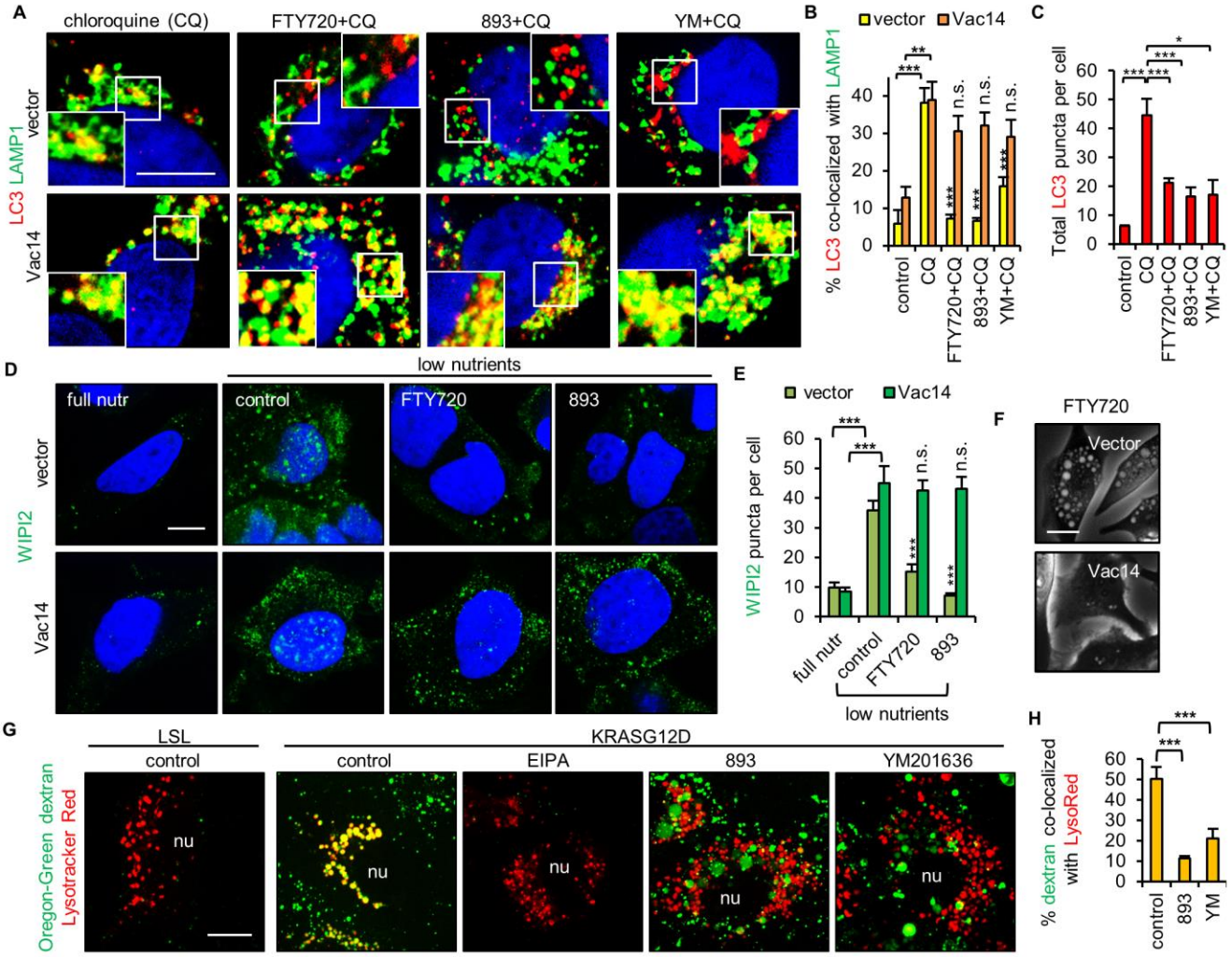

Figure 6: SH-BC-893 reduces autophagic flux and macropinosome degradation. (**A**) Control or Vac14 over-expressing HeLa cells treated with 25 µM chloroquine (CQ) +/- 5 µM FTY720, stained for LC3 and LAMP1, and evaluated by confocal microscopy. (**B-C**) Quantification of LC3/LAMP1 co-localization (**B**) and total LC3 puncta (**C**) in cells treated with CQ +/- FTY720, SH-BC-893, or 800 nM YM201636 for 6 h. Means +/- SEM, n ≥ 35 cells evaluated per condition. (**D**) Vector or Vac14 over-expressing HeLa cells were nutrient-stressed in DMEM lacking amino acids and glucose in the presence or absence of 5 µM FTY720 or SH-BC-893 and stained for WIPI2. (**E**) Quantification of WIPI2 puncta. Means +/- SEM, n ≥ 50 cells evaluated per condition. Statistics comparing to respective low nutrient control where not indicated. (**F**) HeLa cells over-expressing Vac14 treated with 5 µM FTY720 for 6 h. (**G-H**) Dextran uptake in *p53*$^{-/-}$*;LSL-K-RasG12D* MEFs before (LSL) or after (KRasG12D) introduction of Cre +/- the macropinocytosis inhibitor EIPA, SH-BC-893, or YM201636 (**G**). Co-localization of dextran and Lysotracker Red (**H**) was determined using ImageJ. Means +/- SEM shown, n ≥ 15 cells evaluated per condition. Using Student's unpaired, two-tailed t-test, *, *P* <0.05; **, *P* <0.01; ***, *P* <0.001; n.s., not significant (P >0.05). *P*-value was determined using Tukey's method when correcting for multiple comparisons. Scale bar, 20 µm.

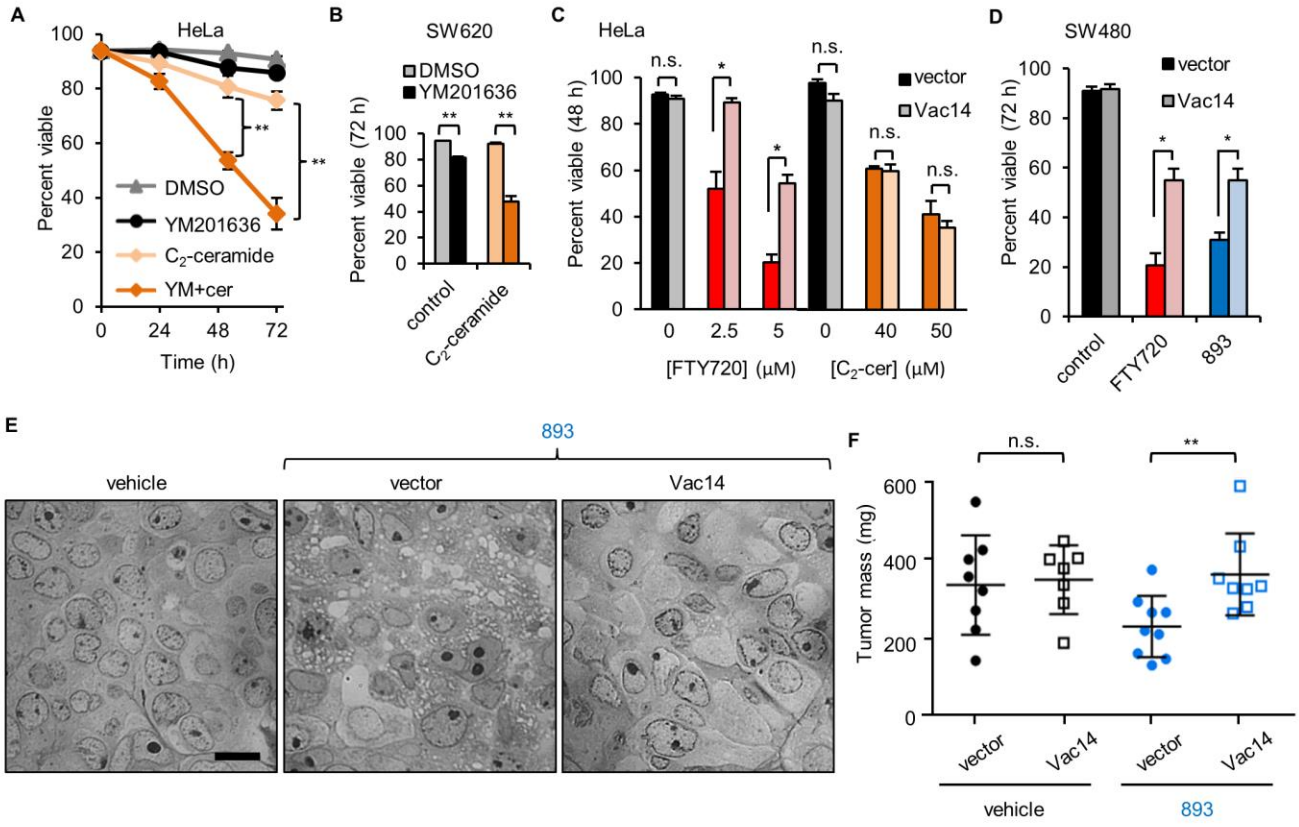

Figure 7: Vacuolation enhances the anti-neoplastic effects of SH-BC-893 in vitro and in vivo. (**A-B**) Viability of HeLa (**A**), or SW620 (**B**) cells treated with DMSO, 800 nM YM201636, 25 μM C_2-ceramide, or with YM201636 + C_2-ceramide. (**C-D**) Viability of control or Vac14 over-expressing cells treated with FTY720 or C_2-ceramide. Means +/- SEM. (**E**) Vacuolation evaluated by brightfield microscopy in SW480 tumors from mice treated with vehicle (water) or 60 mg/kg SH-BC-893 by gavage daily for 18 d. Scale bar, 10 μm. (**F**) Tumor weight at sacrifice. *P* = 0.06 between vehicle and SH-BC-893-treated vector groups. Means +/- S.D., n ≥ 7 mice per group. Using Student's unpaired, two-tailed t-test, *, *P* <0.05; **, *P* <0.01; ***, *P* <0.001; n.s., not significant (*P* >0.05). In vitro data are representative of at least 3 independent experiments.

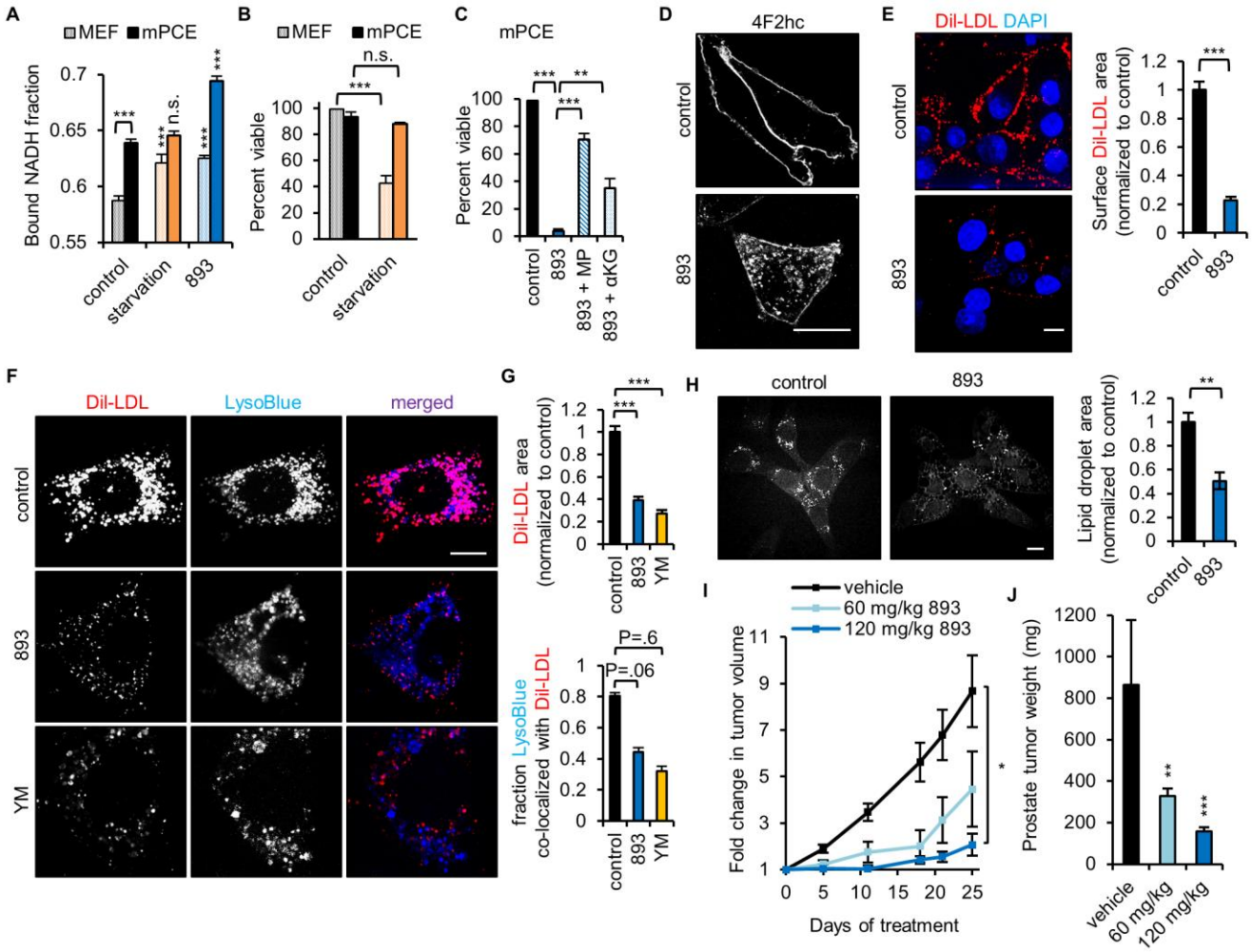

Figure 8: SH-BC-893 starves PTEN$^{-/-}$ prostate cancer cells. (**A**) Bound NADH fraction in MEF or mPCE. Means +/- SEM, n ≥ 50 cells evaluated per condition. (**B**) Viability of MEF or mPCE in starvation media (DMEM lacking glucose and amino acids supplemented with 10% FBS). (**C**) Viability of mPCE treated with 5 µM SH-BC-893 +/- 11 mM methyl pyruvate or 7 mM dimethyl α-ketoglutarate (α-KG). Means +/- SEM. (**D**) mPCE cells treated with 5 µM SH-BC-893 stained for 4F2hc. (**E**) Dil-LDL bound to surface LDL receptors of mPCE cells maintained at 4°C. Means +/- SEM from n ≥ 80 cells per condition. (**F-G**) Dil-LDL uptake and lysosomes in mPCE treated with SH-BC-893 or YM201636. Quantification of total Dil-LDL area (**F**) and co-localization between Dil-LDL and LysoBlue (**G**). Means +/- SEM from n ≥ 30 cells per condition. (**H**) mPCE cells treated with SH-BC-893 for 3 h imaged using coherent anti-Stokes Raman Spectroscopy (CARS) to detect lipid droplets. Means +/- SEM from n = 5 fields. (**I**) Growth of mPCE subcutaneous isografts measured by calipers. n = 7 per group. (**J**) Mean weight of autochthonous prostate tumors at sacrifice. n = 9 for vehicle and 60 mg/kg SH-BC-893 group; n = 8 for 120 mg/kg group. Mann-Whitney U test was used to compare treated mice with controls. Scale bar, 20 µm. Student's unpaired, two-tailed t-test was used in all panels except (**J**). Statistics comparing to respective controls where not indicated. *, *P* <0.05; **, *P* <0.01; ***, *P* <0.001; n.s., not significant (*P* >0.05). *P*-value was determined using Tukey's method when correcting for multiple comparisons.

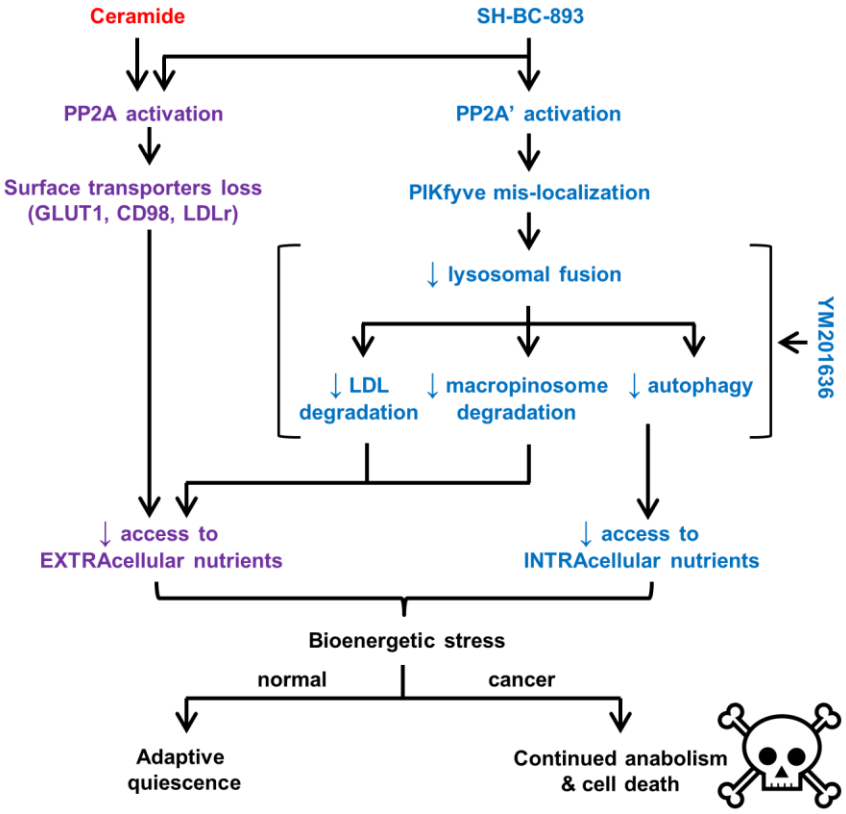

Figure 9: Vacuolating sphingolipid SH-BC-893 targets primary and adaptive pathways for nutrient acquisition. Like ceramide, the synthetic sphingolipid SH-BC-893 activates protein phosphatase 2A (PP2A) to down-regulate nutrient transporters. In addition, SH-BC-893 activates a second PP2A complex, PP2A' that is not affected by ceramide. Activation of PP2A' leads to mis-localization of PIKfyve and $PI(3,5)P_2$, reducing lysosomal fusion reactions. Because $PI(3,5)P_2$ is membrane-anchored and cannot diffuse to its target, loss of $PI(3,5)P_2$ (YM201636 treatment) and $PI(3,5)P_2$ mis-localization (SH-BC-893 treatment) produce similar phenotypes. While ceramide limits access to extracellular nutrients, SH-BC-893 blocks access to both extracellular and intracellular nutrients. Substrate limitation in the context of oncogene-driven anabolism is lethal while non-transformed cells can make adaptive metabolic changes that allow them to survive nutrient stress.

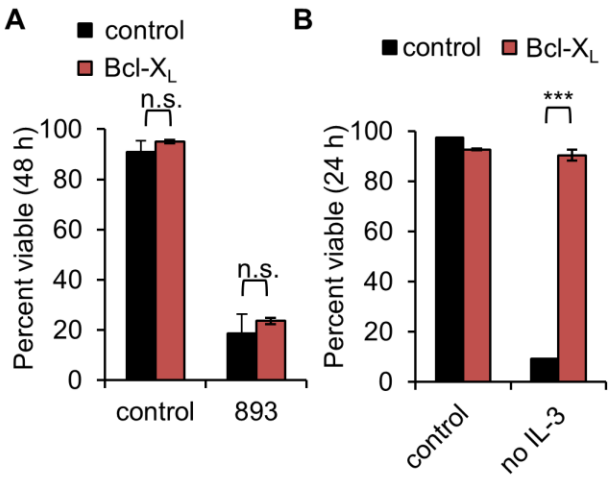

Supplemental Figure 1: Blocking apoptosis does not prevent SH-BC-893-induced cell death. (**A-B**) Viability of control or Bcl-X_L over-expressing FL5.12 cells 24 h after SH-BC-893 (893) treatment (**A**) or IL-3 withdrawal (**B**). Means +/- SEM, n ≥ 3. Using Student's unpaired, two-tailed t-test, ***, P <0.001; n.s., not significant (P >0.05).

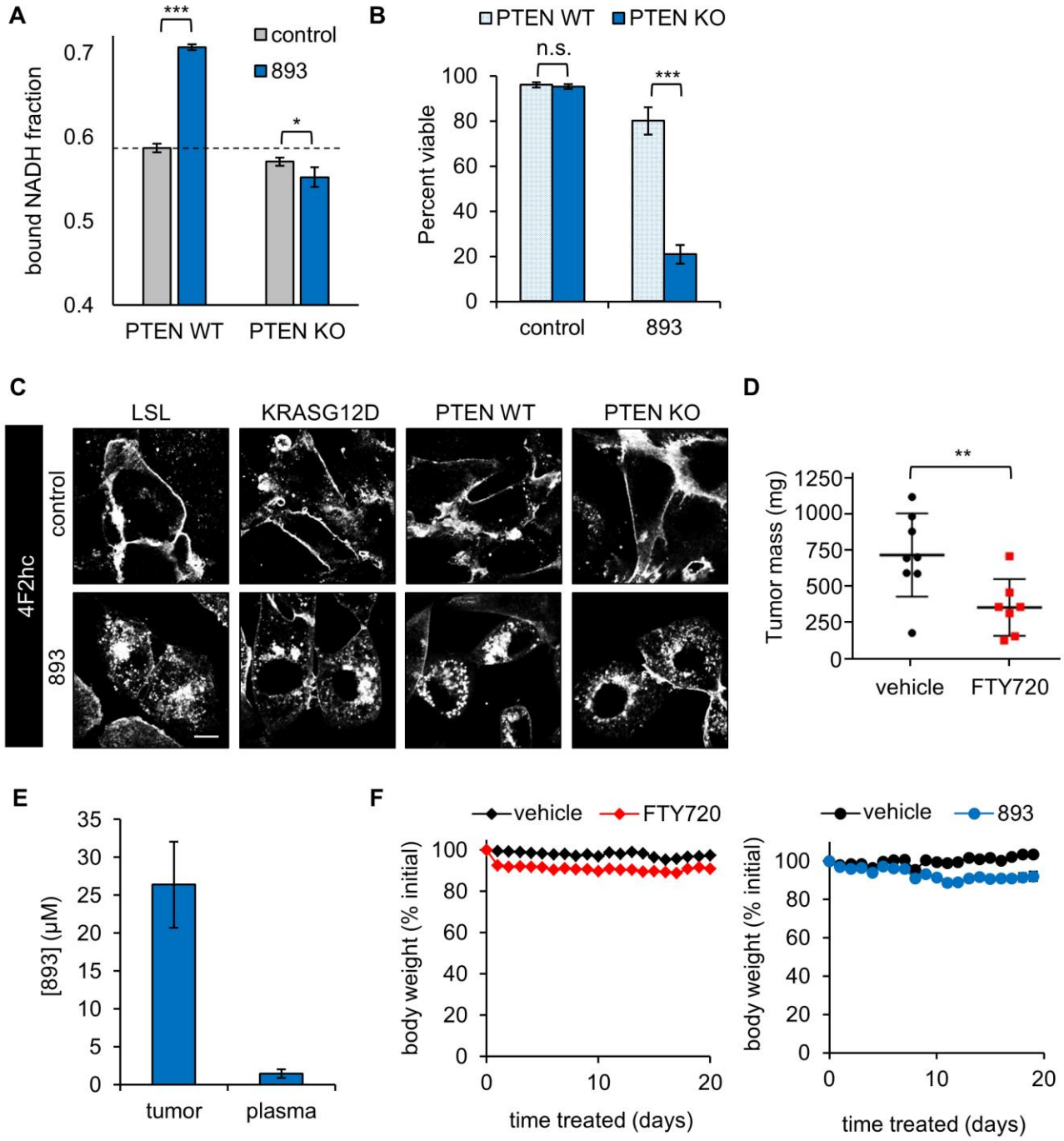

Supplemental Figure 2: FTY720 and SH-BC-893 inhibit tumor growth in vivo. (**A**) Bound NADH fraction in PTEN WT or PTEN KO MEFs treated with 7.5 μM SH-BC-893. (**B**) Viability of $p53^{-/-}$ MEFs that are wildtype (WT) or knocked-out (KO) for PTEN. (**C**) SH-BC-893-treated control (LSL), K-RasG12D-expressing, PTEN WT, or PTEN KO MEFs stained for 4F2hc. Scale bar, 20 μm. (**D**) SW620 tumor weight upon excision in mice treated with 10 mg/kg FTY720. Means +/- S.D., n ≥ 7. (**E**) SH-BC-893 concentration in SW620 tumors and blood plasma 24 h after 11 d of 20 mg/kg i.p. treatment. Means +/- SEM except for (**D**), n ≥ 3. Using Student's unpaired, two-tailed t-test, *, P <0.05; **, P <0.01; ***, P <0.001; n.s., not significant (P >0.05). (**F**) Percent change in body weight of NSG mice from SW620 xenograft study shown in Figure 2G-I or (**D**).

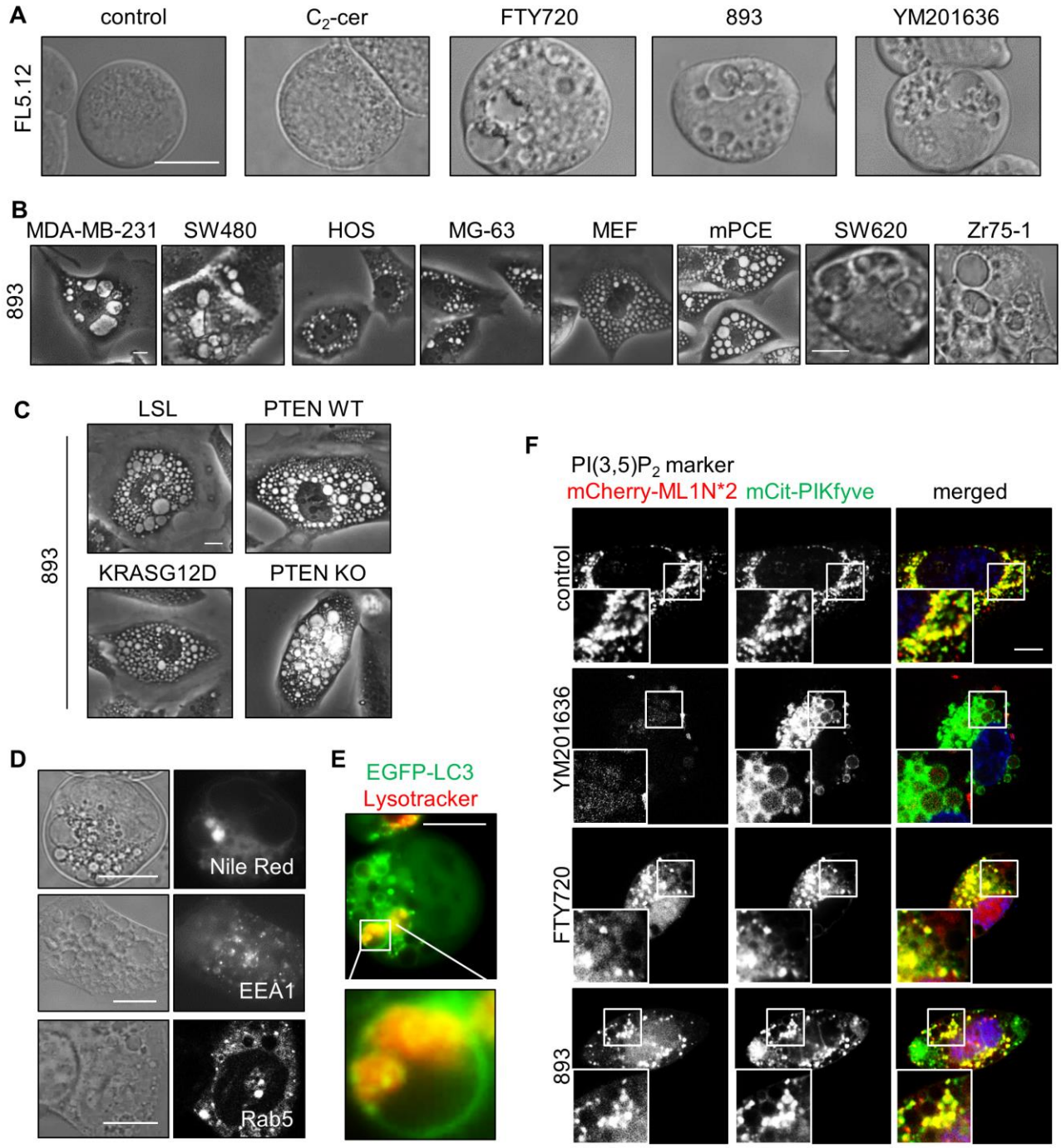

Supplemental Figure 3: Characterization of FTY720- and SH-BC-893-induced vacuolation. (**A,B**) FL5.12 cells (**A**) or the indicated cell lines (**B**) were treated with drugs for 2 h or 6 h, respectively (50 μM C_2-ceramide, 5 μM FTY720, 5 μM SH-BC-893, 800 nM YM201636). (**C**) Control (LSL), K-RasG12D-expressing, PTEN WT, or PTEN KO MEFs treated with SH-BC-893 for 6 h. (**D**) FL5.12, HeLa, or MEFs treated with FTY720 and stained with Nile Red, probed with EEA1 antibodies, or expressing GFP-Rab5, respectively. (**E**) GFP-LC3-expressing FL5.12 treated with 2.5 μM FTY720 for 2 h and stained with Lysotracker Red. (**F**) HeLa cells expressing the PI(3,5)P_2 marker mCherry-ML1N*2 and mCit-PIKfyve were treated with 800 nM YM201636, 5 μM FTY720, or 5 μM SH-BC-893 for 6 h. Scale bar, 10 μm.

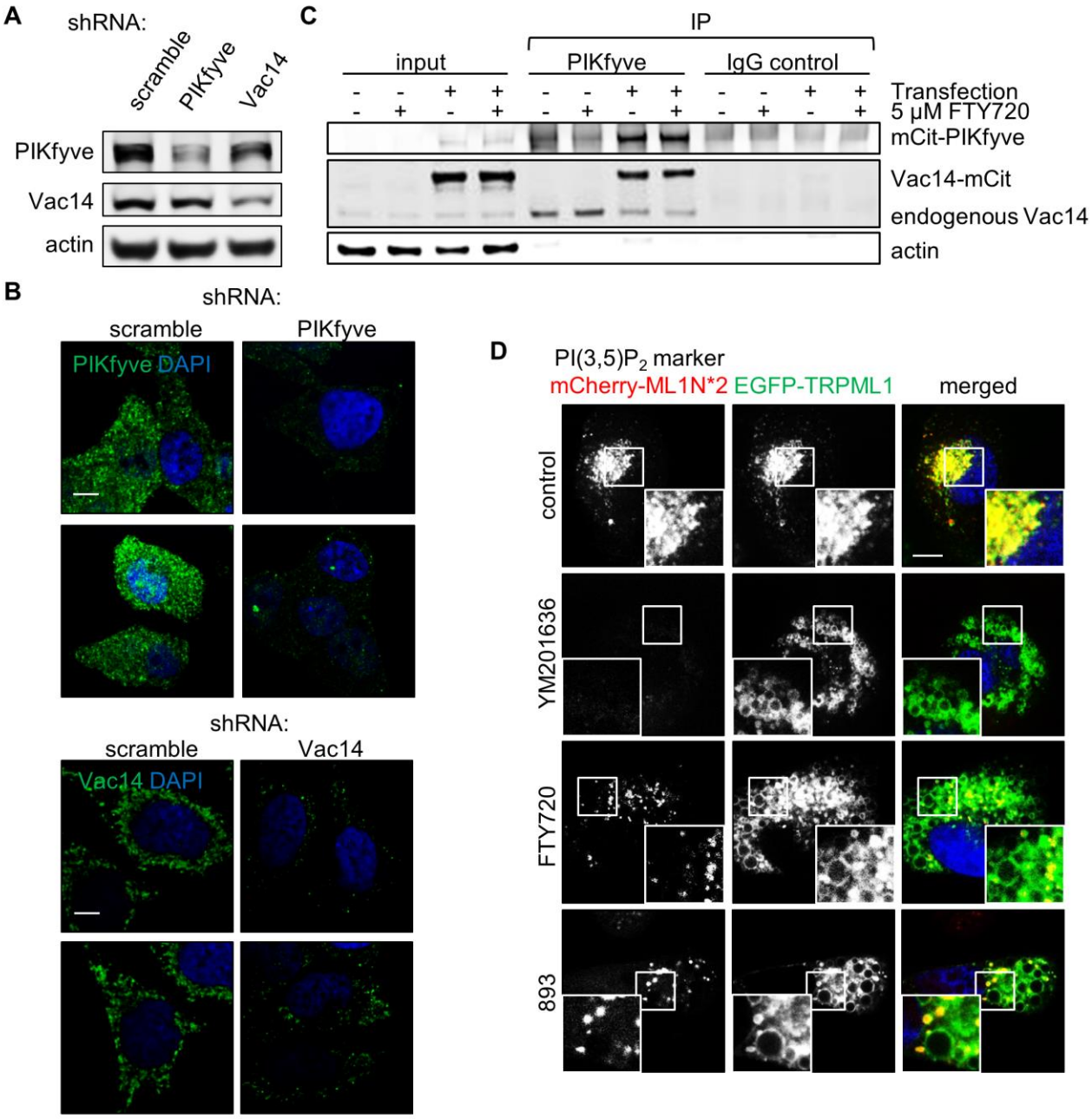

Supplemental Figure 4: FTY720 and SH-BC-893 mislocalizes PIKfyve. (**A,B**) HeLa cells transfected with shRNA scramble, PIKfyve, or Vac14 were evaluated by western blotting (**A**) or by confocal immunofluorescence microscopy (**B**). (**C**) PIKfyve immunoprecipitation from mCitrine-PIKfyve- and Vac14-mCitrine-expressing HeLa cells treated with FTY720. (**D**) HeLa cells expressing PI(3,5)P_2 marker mCherry-ML1N*2 and EGFP-TRPML1 were treated with 800 nM YM201636, 5 μM FTY720, or 5 μM SH-BC-893 for 6 h. Scale bar, 10 μm.

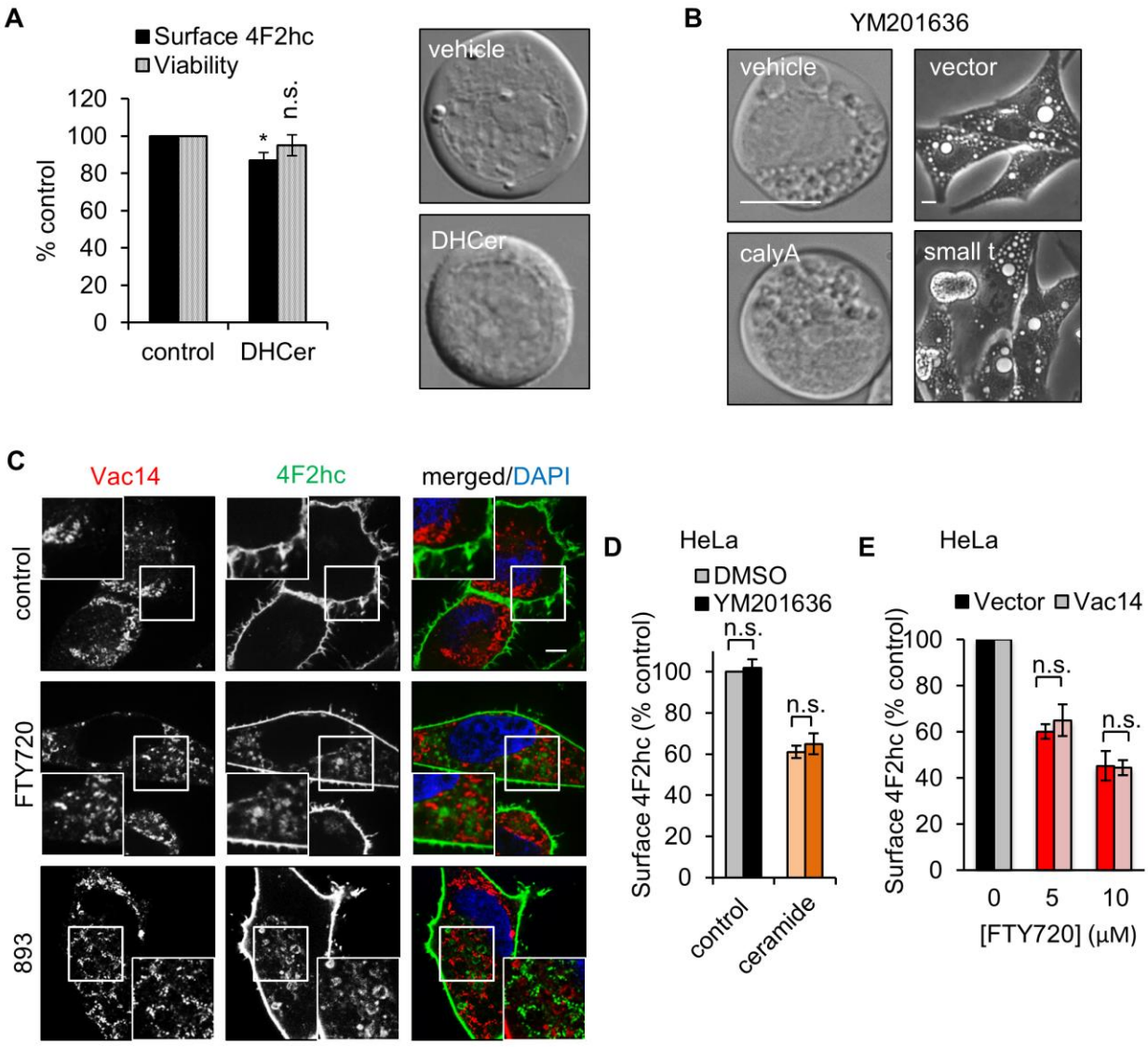

Supplemental Figure 5: FTY720 and SH-BC-893 induce surface nutrient transporter loss and vacuolation via two distinct PP2A-dependent mechanisms. (**A**) Surface 4F2hc levels and viability (left) and vacuolation (right) of FL5.12 cells treated with 50 μM dihydro-C_2-ceramide (DHCer). Statistics comparing to respective controls. (**B**) FL5.12 cells (left) treated with 800 nM YM201636 +/- 5 nM calyculinA (calyA) or HeLa cells (right) expressing SV40 small t antigen treated with YM201636. (**C**) HeLa cells were treated with 5 μM FTY720 or SH-BC-893, stained as indicated, and evaluated by confocal microscopy. (**D**) Surface 4F2hc levels in HeLa cells treated with DMSO, 800 nM YM201636, 25 μM C_2-ceramide, or with YM201636 + C_2-ceramide. (**E**) Surface 4F2hc levels in vector or Vac14 over-expressing HeLa cells treated with FTY720 for 6 h. Scale bar, 10 μm. Means +/- SEM n ≥ 3. Using Student's unpaired, two-tailed t-test, *, P <0.05; n.s., not significant (P >0.05).

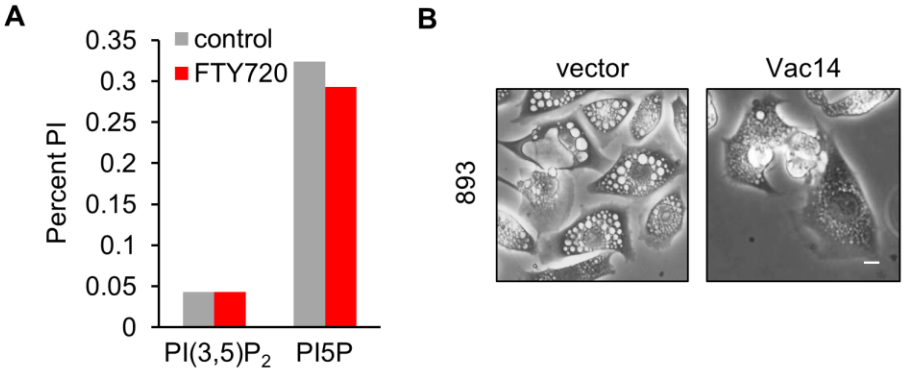

Supplemental Figure 6: SH-BC-893 blocks autophagic flux. (**A**) $PI(3,5)P_2$ and PI5P levels in MEF cells treated with FTY720 expressed as a percentage of total phosphatidylinositol. Average from two independent experiments. (**B**) Mouse prostate cancer epithelial cells expressing vector or Vac14 treated with 5 μM SH-BC-893. Scale bar, 10 μm.

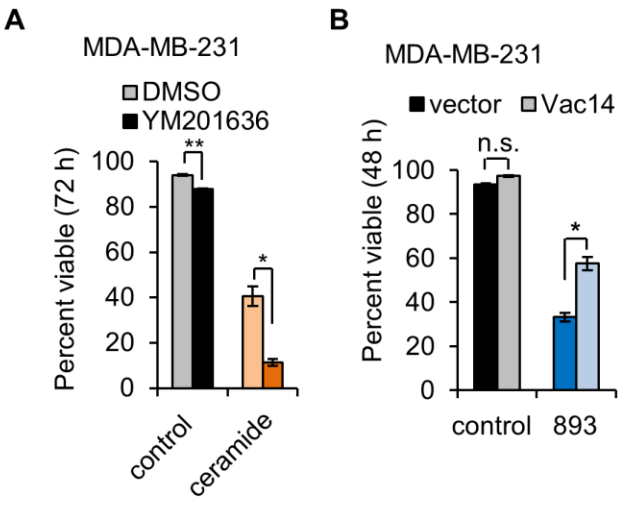

Supplemental Figure 7: Vacuolation enhances cell death. (**A**) Viability of MDA-MB-231 cells treated with DMSO, 800 nM YM201636, 25 μM C_2-ceramide, or with YM201636 + C_2-ceramide. (**B**) Viability of vector or Vac14 over-expressing MDA-MB-231 cells treated with SH-BC-893. Means +/- SEM, n ≥ 3. Using Student's unpaired, two-tailed t-test, *, $P < 0.05$; **, $P < 0.01$; n.s., not significant ($P > 0.05$).

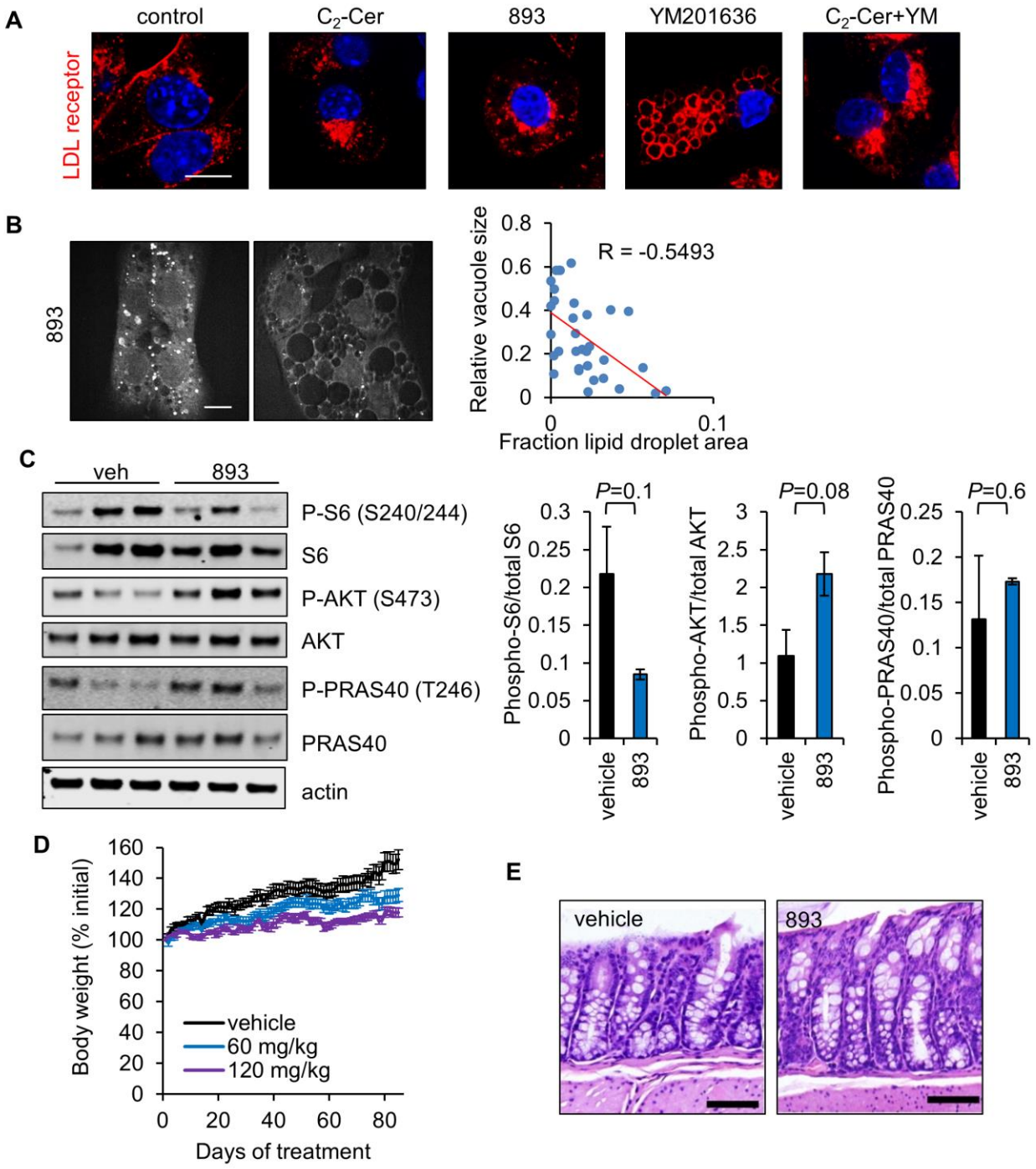

Supplemental Figure 8: SH-BC-893 is selectively toxic to cancer cells. (**A**) mPCE cells treated with indicated compounds and stained for the LDL receptor. Scale bar, 20 μm. (**B**) CARS images of lipid droplets in mPCE cells treated with SH-BC-893. Linear regression plot representing correlation between vacuole size and lipid droplet amount in mPCE cells treated with SH-BC-893. R, Pearson Coefficient. Scale bar, 20 μm. (**C**) Western blotting of tumors from vehicle or SH-BC-893 treated mice in Fig. 8J. On the right, ratio of phosphorylated over total S6, AKT, and PRAS40 from tumors excised from pDKO mice treated with vehicle or 120 mg/kg SH-BC-893. Means +/- SEM, n ≥ 3, *P*-values using Student's unpaired, two-tailed t-test. (**D**) Percent change in body weight of pDKO mice treated with vehicle, 60 mg/kg, or 120 mg/kg SH-BC-893. (**E**) Histology of intestinal crypts in mice treated with 120 mg/kg SH-BC-893 for 11 weeks. Scale bar, 100 μm.

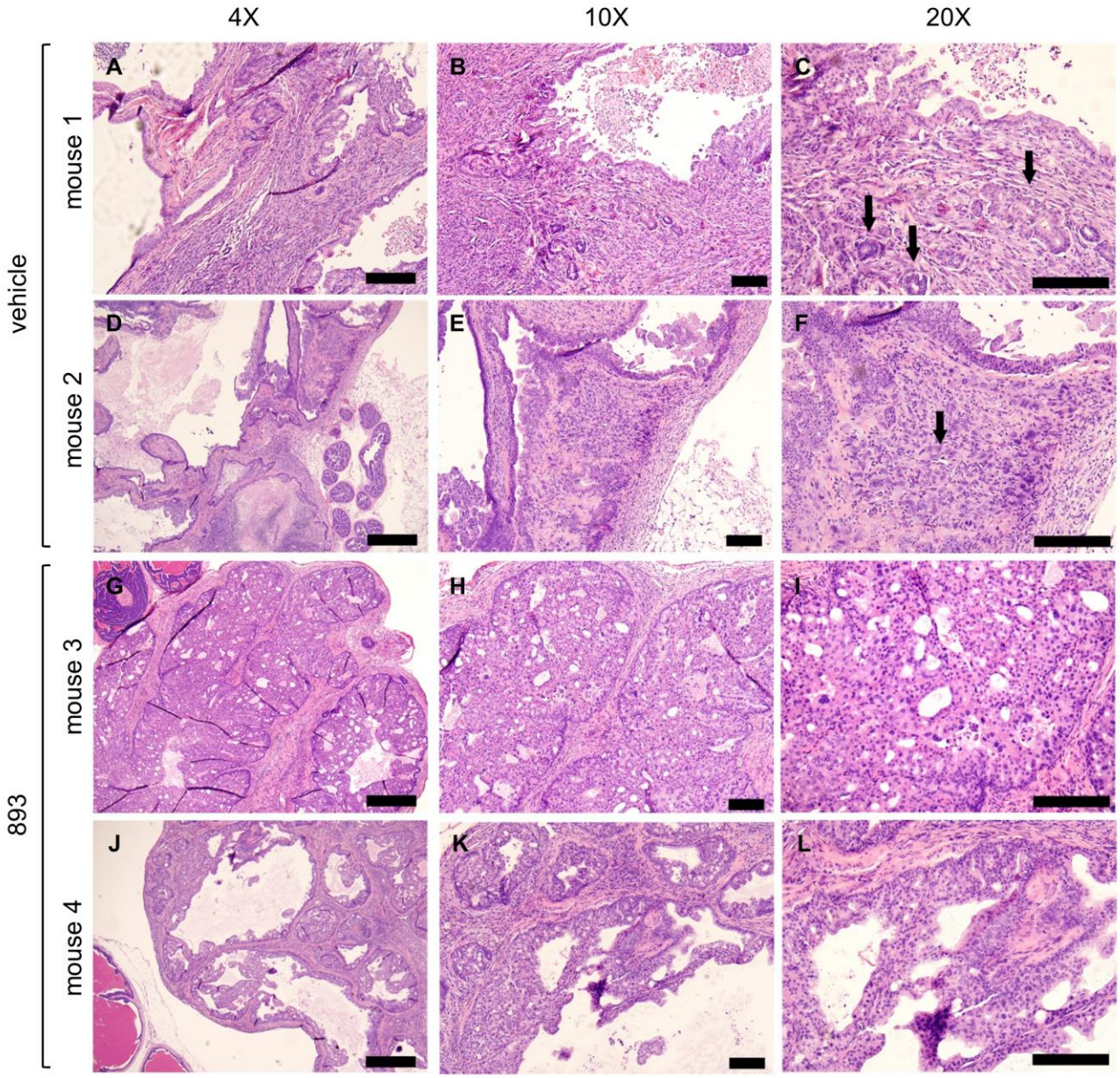

Supplemental Figure 9: SH-BC-893 inhibits prostate cancer progression. (**A**-**L**) H&E staining of $p53^{-/-}$ $PTEN^{-/-}$ prostates excised from mice treated with vehicle (**A**-**F**) or 120 mg/kg SH-BC-893 (**G**-**L**) for 11 weeks. At high power, arrows indicate invasive glandular structures in a reactive stroma (**C,F**). Prostates in SH-BC-893-treated mice exhibited exclusively prostatic intraepithelial neoplasia (**G**-**L**) rather than the locally invasive adenocarcinomas seen in vehicle controls (**A**-**F**) indicating that SH-BC-893 slowed disease progression. Although prostates of treated mice still developed prostatic intraepithelial neoplasia, no invasive component was identified in SH-BC-893-treated pDKO mice. The intraepithelial proliferation present in treated mice showed much lower degrees of cellular pleomorphism, hyperchromasia, and nuclear atypia. Scale bars = 500 mm (4X), 100 mm (10X & 20X).

Supplemental Table 1: Blood chemistry of vehicle or SH-BC-893-treated pDKO mice at sacrifice. Means +/- SEM are shown, n=4. AP: alkaline phosphatase; SGPT (ALT): serum glutamic-pyruvic transaminase (alanine aminotransferase); SGOT (AST): serum glutamic oxaloacetic transaminase (aspartate aminotransferase); CPK: creatine phosphokinase; BUN: blood urea nitrogen; CR: creatinine; CHOL: cholesterol; Ca^{2+}: Calcium; P: phosphorus; $HCO3^{-}$: bicarbonate.

Blood Chemistry Panel

	AP	SGPT (ALT)	SGOT (AST)	CPK	ALBUMIN	TOTAL PROTEIN	GLOBULIN
vehicle	93 ± 5.4	65 ± 10.4	809 ± 200	5,017 ± 1199	3 ± 0.2	6 ± 0.3	3 ± 0.13
60 mg/kg 893	77 ± 7.8	78 ± 25	640 ± 136	5,340 ± 2366	3 ± 0.2	5 ± 0.4	2 ± 0.18
120 mg/kg 893	83 ± 6.2	91 ± 17.2	907 ± 171	10,441 ± 3014	3 ± 0.1	6 ± 0.2	2 ± 0.03

	TOTAL BILIRUBIN	BUN	CR	CHOL	GLUCOSE	Ca^{2+}	P	$HCO3^{-}$
vehicle	0.2 ± 0.03	29 ± 3.1	<0.2	187 ± 8.8	264 ± 43	11 ± 0.8	13 ± 0.6	19 ± 5.8
60 mg/kg 893	0.1 ± 0	19 ± 1.1	<0.2	134 ± 15.8	282 ± 24	10 ± 0.7	11 ± 1.0	20 ± 3.2
120 mg/kg 893	0.2 ± 0.03	23 ± 1.5	<0.2	107 ± 7.5	307 ± 28	10 ± 0.1	13 ± 0.1	17 ± 2.8

Supplemental Table 2: Complete blood count of vehicle or SH-BC-893-treated pDKO mice at sacrifice. Means +/- SEM are shown, n=4. WBC: white blood cells; RBC: red blood cells; HCT: hematocrit

Complete Blood Count

	WBC [10^3 cells/µL]	% neutrophil	% lymphocyte	RBC [M/µL]	HCT
vehicle	5 ± 1	16 ± 5	76 ± 7	9 ± 0	38 ± 3
60 mg/kg 893	5 ± 1	14 ± 3	77 ± 4	8 ± 1	32 ± 5
120 mg/kg 893	8 ± 1	19 ± 5	73 ± 5	9 ± 1	41 ± 3

MATERIALS AND METHODS

Cell culture and reagents. OP9, DLD-1, SW48, SW620, MDA-MB-231, PANC-1, HOS, MG-63, and Zr75-1 cells were obtained from the ATCC. SW480 cells were provided by Marian Waterman (UCI, Irvine CA), HeLa cells by Christine Sütterlin (UCI, Irvine CA), LS180 cells by Bruce Blumberg (UCI, Irvine CA) and FL5.12 cells by Craig Thompson (Memorial Sloan Kettering Cancer Center, New York, NY). *p53$^{-/-}$;LSL-KRasG12D* MEFs with and without Cre-mediated deletion of the STOP cassette were kindly provided by Dr. David Tuveson (Cold Spring Harbor Laboratory, Cold Spring Harbor NY). Primary *p53$^{+/+}$;PTEN$^{+/+}$*, *p53$^{-/-}$;PTEN$^{+/+}$*, and *p53$^{-/-}$;PTEN$^{-/-}$* MEFs were generated in-house from embryos from C57BL/6 mice using standard techniques. mPCE cells generated from p53$^{-/-}$ PTEN$^{-/-}$ mouse prostate tissue were maintained in DMEM with 10% FBS, 25 µg/ml bovine pituitary extract, 5 µg/ml bovine insulin and 6 ng/ml recombinant human epidermal growth factor. FL5.12 cells were maintained in RPMI 1640 medium supplemented with 10% fetal calf serum (FCS), 10 mM HEPES, 55 µM 2-mercaptoethanol, antibiotics, 2 mM L-glutamine, and 500 pg/ml rIL-3. FL5.12 cells were adapted to grow in 25 pg/ml IL-3 by gradually reducing the IL-3 concentration over 2 wk of culture. DLD-1 and Zr75-1 cells were cultured in the same media as FL5.12 but without IL-3. HeLa, OP9, MG-63, and MEF cells were cultured in DMEM with 4.5 g/L glucose and L-glutamine supplemented with 10% FCS and antibiotics. Starvation medium was produced by making DMEM lacking amino acids and glucose from chemical components and supplementing with 10% dialyzed FCS. LS180, SW48, PANC-1, MDA-MB-231, SW480, and SW620 cells were cultured in DMEM supplemented with 10% FCS, antibiotics, and 1 mM sodium pyruvate. Cell viability was measured by vital dye exclusion using either propidium iodide or DAPI at 1 µg/ml. Analysis of cell surface 4F2hc levels with PE-conjugated anti-CD98 was restricted to viable cells as determined by DAPI exclusion. Anchorage-independent growth of SW620 cells was measured in DMEM-10 containing 0.35% low melt agarose with a 0.5% agarose bottom layer. PBMCs were obtained from the normal blood donor program run by the CTSA-supported

Institute for Clinical and Translational Science at UCI under IRB protocols 2015-1883 (Edinger) and 2001-2058 (ICTS). P40Px-EGFP plasmid was provided by Seth Field (UCSD, San Diego), mCherry-Vac14WT and mCherry-Vac14L156R plasmids by Thomas Weide (University Hospital of Muenster, Germany), mCherry-TRPML1, EGFP-TRPML1, and mCherry-ML1N*2 plasmids by Haoxing Xu (University of Michigan, Ann Arbor), and PIKfyve and Vac14 shRNA by Anand Ganesan (UCI, Irvine).

Light Microscopy. Brightfield and epifluorescence microscopy were conducted using a Nikon TE2000-S fluorescence microscope; confocal microscopy was performed on a Zeiss LSM780 confocal microscope or Nikon Eclipse Ti spinning disk confocal microscope. Antibodies were obtained from: Murine 4F2hc (cat# 128208) and Lamp1 (cat# 53-1079-42) from eBioscience; human 4F2hc (cat# 556077) from BD Biosciences; human GLUT1 (cat# NB300-666) from Novus Biologicals; LC3 (cat# 4108) from Cell Signaling Technology; PIKfyve (cat# 4082) from Tocris; Vac14 (cat# SAB4200074) from Sigma-Aldrich; WIPI2 (cat# LS-C154557-100) from Lifespan Biosciences. Co-localization was determined using JACoP plugin in ImageJ software. Macropinocytosis was measured after 16 h incubation in serum-free DMEM. *p53$^{-/-}$;LSL-K-RasG12D* MEFs before (LSL) or after (KRasG12D) introduction of Cre were serum starved for 16 h and then treated with macropinocytosis inhibitor 5-(N-ethyl-N-isopropyl) amiloride (EIPA, 75 μM) for 1 h or SH-BC-893 for 6 h. Oregon Green dextran (Life Technologies, cat# D7173) (1 mg/mL) and Lysotracker Red (Life Technologies, cat# L-7525) (1:2,000 dilution) were added for 30 min and live cells were evaluated on the spinning disc confocal microscope. For Dil-LDL uptake, mPCE were incubated in media with 10% charcoal-stripped serum for 24 h then incubated with 20 μg/ml Dil-LDL (Life Technologies, cat# L3482) +/- SH-BC-893 for 6 h and Lysotracker Blue (Life Technologies, cat# L-7525), for 30 min. To detect surface LDL receptors, Dil-LDL was added at 4°C to mPCE cells treated with SH-BC-893 for 3 h or cells were stained with LDL receptor antibody (R&D Systems, cat#AF2255). SW480 tumors were excised and

fixed in 2.5% glutaraldehyde in 0.1 M phosphate buffer, pH 7.4 and stored in the dark at 4°C until embedding. Tumor samples were processed by the Pathology Research Services Core Facility at UC Irvine.

Electron microscopy. FL5.12 cells treated with FTY720 were fixed with 2.5% glutaraldehyde/2.5% formaldehyde in 0.1 M sodium cacodylate buffer and stored at 4°C until embedding. Cells were post-fixed with 1% osmium tetroxide, serially dehydrated, embedded in eponat12 resin, ultra-thin sections cut, mounted on grids, and stained with uranyl acetate and lead citrate. Samples were analyzed on a Philips CM10 transmission electron microscope. Representative images are shown from two independent experiments.

In vivo studies. Experiments conducted in mice were performed in accordance with the Institutional Animal Care and Use Committee of University of California, Irvine following a power analysis conducted in consultation with the Biostatistics Shared Resource of Chao Family Comprehensive Cancer Center at UCI. Xenografts were produced by injecting 5 million cells subcutaneously in the flank of 10-16 week-old male or female NSG mice. Prostate isografts were produced in the same manner but in male 6-8 wk old C57BL/6 mice. Once tumors reached 100 mm^3, SH-BC-893 was administered by intraperitoneal (i.p.) injection or oral gavage as indicated. Tumor volume was calculated using the formula, volume (mm^3) = length [mm] x (width [mm])^2 x 0.52; BLI was measured using an IVIS imaging system (Xenogen). To generate pDKO mice on the C57BL6 background, *Pten*^{flox} mice (stock No. 0045597) and *p53*^{flox} mice (stock No. 008462) were obtained from the Jackson Laboratory and *PB-Cre4* mice (strain #01XF5) were obtained from the NCI-Frederick Mouse Repository. Age-matched cohorts of pDKO males were generated by in vitro fertilization executed with the assistance of the Transgenic Mouse Facility at UC Irvine. Treatment was begun at 6-7 wks of age. Tumor weight was determined by isolating the complete genitourinary (GU) tract of pDKO mice and

subtracting the average weight of a normal GU tract from age-matched mice (n=3) after it was determined that SH-BC-893 treatment of normal mice did not alter GU tract weight (n=3). Tumor samples were processed and imaged by the Pathology Research Services Core Facility at UC Irvine. Blood chemistry was analyzed by IDEXX BioResearch and complete blood counts were performed using a Hemavet hematology system.

NADH Fluorescence Lifetime Imaging Microscopy (FLIM). Lifetime images were acquired using a Zeiss 780 microscope coupled to a Ti:Sapphire laser system (Spectra-Physics Mai Tai). The excitation wavelength was 740 nm and a dichroic filter (690 nm) was used to separate the fluorescence signal from the laser light. A 63X 1.15 water immersion objective was used. Image acquisition settings were: image size of 256 x 256 pixels and scan speed of 25.21 µsec/pixel. The fluorescence was detected by a hybrid detector (HPM-100 Hamamatsu). Data was collected until 100 counts in the brightest pixel of the image were acquired. The FLIM system was calibrated during each imaging session by measuring the fluorescence decay of fluorescein with a single exponential of 4.04 nsec. Phasor transformation of FLIM images and analysis of the average lifetime in single cells were done as described previously (30,35,36). Data was processed by the SimFCS software developed at the Laboratory of Fluorescence Dynamics at UCI. The nucleus was excluded when determining the bound NADH fraction. Means +/- SEM are shown, n ≥ 45 cells from two independent experiments.

Coherent anti-Stokes Raman Spectroscopy (CARS). The CARS imaging system is described in detail in (61). Cells were fixed with 4% formaldehyde and imaged with a 60X water objective. The laser power on the sample was at 10 mW with 10 ms pixel dwell time. The lipid droplet area was estimated from CARS images using a customized Matlab program. Four components Otsu thresholding method was used to separate the lipid droplets, cell cytoplasm,

cell nucleus and the background. The lipid droplet area was defined as the number of pixels covered by lipid droplets over the number of pixels covered by cytoplasm.

PIKfyve in vitro kinase assay. FLAG-PIKfyve was expressed in HEK293T cells, purified with FLAG-beads, and eluted with FLAG peptides. PI3P and phosphatidylserine (C16) liposomes were generated by sonication in 2X lipid mixture buffer [40 mM Tris-HCl (pH 7.4), 200 mM NaCl, 1 mM EGTA] with or without FTY720. FLAG-PIKfyve and lipid mixtures were incubated with Mg^{2+}-ATP solution [6.5 mM HEPES (pH 7.3), 2.5 mM $MnCl_2$, 10 mM $MgCl_2$, 1 mM β-glycerophosphate, 0.1 mM ATP and [^{32}P]-γ-ATP] for 15 min at RT. The reaction was stopped by adding 4 M HCl, and phosphoinositides were extracted with methanol/chloroform (1:1). Phosphoinositides were spotted on silica thin-layer chromatography plates and separated with 2 M acetic acid/1-propanol (35:65). Membranes were dried, exposed to a Phospho Imager, and the counts from PI(3,5)P_2 spots quantified with ImageQuant.

Measurement of PI(3,5)P_2 by HPLC. HeLa cells were rinsed twice with PBS and incubated in for 48 h in inositol labeling medium (inositol-free DMEM containing 5 µg/ml transferrin, 5 µg/ml insulin, 10% dialyzed FCS, 20 mM HEPES, 2 mM L-glutamine), and 10 µCi/ml myo-[2-^{3}H]inositol. Cells were lysed with 4.5% perchloric acid, scraped, and centrifuged at 14,000 x g for 10 min at 4°C. Cell pellets were rinsed with 100 mM EDTA, centrifuged again, and re-suspended in 50 µl of water. To deacylate lipids, 1 ml methanol/40%methylamine/butanol (45.7% methanol, 10.7% methylamine, 11.4% butanol) were added and then the mixture was transferred to a glass vial and incubated at 55°C for 1 h. After cooling to room temperature, samples were vacuum dried and re-suspended in 0.5 ml water. Lipids were extracted twice with an equal volume of butanol/ethyl ether/ethyl formate (20:4:1). The aqueous phase was vacuum dried and re-suspended in 75 µl water and 50 µl of each sample was analyzed by HPLC. PI(3,5)P_2 levels were expressed as a percentage of total phosphatidylinositol.

PP2A phosphatase activity. PP2A activity was measured using a PP2A immunoprecipitation phosphatase assay kit (EMD Millipore). Briefly, the catalytic subunit of PP2A was immunoprecipitated from FL5.12 cell lysates with 4 µg anti-PP2A, C subunit. After four washes, the activity of immunoprecipitated PP2A was assessed by dephosphorylation of the phosphopeptide according to the manufacturer's instructions in the presence or absence of C_2-ceramide, dihydro-C_2-ceramide, FTY720, SH-BC-893, or calyculinA.

Mass spectrometry quantification of SH-BC-893. As an internal standard, 75 ng FTY720 was added to 50 µl plasma or 50 µl of tumor homogenate (0.25 M sucrose, 25 mM KCl, 50 mM Tris HCl, 0.5 mM EDTA, pH 7.4; 1:9 wt:volume) combined 1:1 with acetonitrile. Proteins were precipitated and removed by centrifugation (10 min at 15,000 rpm) and the supernatant transferred to a fresh tube on ice containing 50 µl of acetonitrile + 0.2% acetic acid. After a second de-proteination with acetonitrile + 0.2% acetic acid, 20 µl of de-proteinated samples were analyzed by UPLC-MS/MS using a Waters Micromass Quattro Premier XE equipped with a C18 reversed phase column (Waters) with an acetonitrile + 0.2 % acetic acid gradient elution. The instrument was operated in positive ion mode. Ion transition channels for multiple reaction monitoring were 290 → 104 for SH-BC-893 with a dwell time of 200 msec. The cone voltage was 30V. Standard curves used for quantitation were linear from 50 – 1000 ng/ml with an R^2 of 0.98 or greater. Recovery of internal standard was $\geq$80%. Tumor concentrations were calculated assuming that 1 gm = 1 mL.

Statistical methods and data analysis. Significance was determined using a paired t-test for a single pairwise comparison. Tukey's method was utilized and adjusted p-values are reported where multiple comparisons were made. In tumor studies where data was not normally

distributed, a Mann-Whitney U test was used to compare treated mice with controls. *, $P < 0.05$; **, $P < 0.01$; ***, $P < 0.001$; n.s., not significant ($P > 0.05$). For lipid droplet area in CARS experiments, the mean values between the control and experiment groups were compared with a two-tailed ANOVA.

Study approval. Experiments conducted in mice were performed in accordance with the Institutional Animal Care and Use Committee of University of California, Irvine. PBMCs were obtained from the normal blood donor program run by the CTSA-supported Institute for Clinical and Translational Science at UCI under IRB protocols 2015-1883 (Edinger) and 2001-2058 (ICTS).

REFERENCES

1. McCracken AN, Edinger AL: Nutrient transporters: the Achilles' heel of anabolism. *Trends Endocrinol Metab* 2013, 24:200–8.

2. Garcia-Cao I, Song MS, Hobbs RM, Laurent G, Giorgi C, De Boer VCJ, Anastasiou D, Ito K, Sasaki AT, Rameh L, Carracedo A, Vander Heiden MG, Cantley LC, Pinton P, Haigis MC, Pandolfi PP: Systemic elevation of PTEN induces a tumor-suppressive metabolic state. *Cell* 2012, 149:49–62.

3. Shroff EH, Eberlin LS, Dang VM, Gouw AM, Gabay M, Adam SJ, Bellovin DI, Tran PT, Philbrick WM, Garcia-Ocana A, Casey SC, Li Y, Dang C V., Zare RN, Felsher DW: MYC oncogene overexpression drives renal cell carcinoma in a mouse model through glutamine metabolism. *Proc Natl Acad Sci* 2015, 112:6539–6544.

4. Ying H, Kimmelman AC, Lyssiotis C a., Hua S, Chu GC, Fletcher-Sananikone E, Locasale JW, Son J, Zhang H, Coloff JL, Yan H, Wang W, Chen S, Viale A, Zheng H, Paik JH, Lim C, Guimaraes AR, Martin ES, Chang J, Hezel AF, Perry SR, Hu J, Gan B, Xiao Y, Asara JM, Weissleder R, Wang YA, Chin L, Cantley LC, et al.: Oncogenic kras maintains pancreatic tumors through regulation of anabolic glucose metabolism. *Cell* 2012, 149:656–670.

5. Yue S, Li J, Lee SY, Lee HJ, Shao T, Song B, Cheng L, Masterson T a., Liu X, Ratliff TL, Cheng JX: Cholesteryl ester accumulation induced by PTEN loss and PI3K/AKT activation underlies human prostate cancer aggressiveness. *Cell Metab* 2014, 19:393–406.

6. Guillaumond F, Bidaut G, Ouaissi M, Servais S, Gouirand V: Cholesterol uptake disruption, in association with chemotherapy, is a promising combined metabolic therapy for pancreatic adenocarcinoma. *Proc Natl Acad Sci U S A* 2015, 112:2473–2478.

7. Edinger AL, Thompson CB: Akt maintains cell size and survival by increasing mTOR-dependent nutrient uptake. *Mol Biol Cell* 2002, 13:2276–2288.

8. Palm W, Park Y, Wright K, Pavlova NN, Tuveson DA, Thompson CB: The Utilization of Extracellular Proteins as Nutrients Is Suppressed by mTORC1. *Cell* 2015, 162:1–12.

9. Commisso C, Davidson SM, Soydaner-Azeloglu RG, Parker SJ, Kamphorst JJ, Hackett S, Grabocka E, Nofal M, Drebin JA, Thompson CB, Rabinowitz JD, Metallo CM, Vander Heiden MG, Bar-Sagi D: Macropinocytosis of protein is an amino acid supply route in Ras-transformed cells. *Nature* 2013, 497:633–7.

10. Pieters R, Hunger SP, Boos J, Rizzari C, Silverman L, Baruchel A, Goekbuget N, Schrappe M, Pui CH: L-asparaginase treatment in acute lymphoblastic leukemia. *Cancer* 2011, 117:238–249.

11. Feun LG, Kuo MT, Savaraj N: Arginine deprivation in cancer therapy. *Curr Opin Clin Nutr Metab Care* 2015, 18:78–82.

12. Jain M, Nilsson R, Sharma S, Madhusudhan N, Kitami T, Souza AL, Kafri R, Kirschner MW, Clish CB, Mootha VK: Metabolite Profiling Identifies a Key Role for Glycine in Rapid Cancer Cell Proliferation. *Science (80-)* 2012, 336(May):1040–1044.

13. Maddocks ODK, Berkers CR, Mason SM, Zheng L, Blyth K, Gottlieb E, Vousden KH: Serine starvation induces stress and p53-dependent metabolic remodelling in cancer cells. *Nature* 2013, 493:542–6.

14. McGranahan N, Swanton C: Perspective Biological and Therapeutic Impact of Intratumor

Heterogeneity in Cancer Evolution. *Cancer Cell* 2015, 27:15–26.

15. Patel AP, Tirosh I, Trombetta JJ, Shalek AK, Gillespie SM, Wakimoto H, Cahill DP, Nahed B V, Curry WT, Martuza RL, Louis DN, Rozenblatt-Rosen O, Suvà ML, Regev A, Bernstein BE: Single-cell RNA-seq highlights intratumoral heterogeneity in primary glioblastoma. *Science* 2014, 344:1396–401.

16. Garraway LA, Jänne PA: Circumventing cancer drug resistance in the era of personalized medicine. *Cancer Discov* 2012, 2:214–226.

17. Selwan EM, Finicle BT, Kim SM, Edinger AL: Attacking the supply wagons to starve cancer cells to death. *FEBS Lett* 2016, 590:885–907.

18. Guenther GG, Peralta ER, Rosales KR, Wong SY, Siskind LJ, Edinger AL: Ceramide starves cells to death by downregulating nutrient transporter proteins. *Proc Natl Acad Sci U S A* 2008, 105:17402–7.

19. Welsch C a., Roth LW a, Goetschy JF, Movva NR: Genetic, biochemical, and transcriptional responses of Saccharomyces cerevisiae to the novel immunomodulator FTY720 largely mimic those of the natural sphingolipid phytosphingosine. *J Biol Chem* 2004, 279:36720–36731.

20. Romero Rosales K, Singh G, Wu K, Chen J, Janes MR, Lilly MB, Peralta ER, Siskind LJ, Bennett MJ, Fruman D a, Edinger AL: Sphingolipid-based drugs selectively kill cancer cells by down-regulating nutrient transporter proteins. *Biochem J* 2011, 439:299–311.

21. Edinger AL: Starvation in the midst of plenty: making sense of ceramide-induced autophagy by analysing nutrient transporter expression. *Biochem Soc Trans* 2009, 37(Pt 1):253–258.

22. Camm J, Hla T, Bakshi R, Brinkmann V: Cardiac and vascular effects of fingolimod: Mechanistic basis and clinical implications. *Am Heart J* 2014, 168:632–644.

23. White E: Exploiting the bad eating habits of Ras-driven cancers. *Genes Dev* 2013, 27:2065–2071.

24. Neviani P, Santhanam R, Oaks JJ, Eiring AM, Notari M, Blaser BW, Liu S, Trotta R, Muthusamy N, Gambacorti-passerini C, Druker BJ, Cortes J, Marcucci G, Chen C, Verrills NM, Roy DC, Caligiuri MA, Bloomfield CD, Byrd JC, Perrotti D: FTY720 , a new alternative for treating blast crisis chronic myelogenous leukemia and Philadelphia chromosome – positive acute lymphocytic leukemia. *J Clin Invest* 2007, 117:2408–2421.

25. Azuma H, Takahara S, Horie S, Muto S, Otsuki Y, Katsuoka Y: Induction of apoptosis in human bladder cancer cells in vitro and in vivo caused by FTY720 treatment. *J Urol* 2003, 169:2372–7.

26. Azuma H, Takahara S, Ichimaru N, Wang JD, Itoh Y, Otsuki Y, Morimoto J, Fukui R, Hoshiga M, Ishihara T, Nonomura N, Suzuki S, Okuyama A, Katsuoka Y: Marked prevention of tumor growth and metastasis by a novel immunosuppressive agent, FTY720, in mouse breast cancer models. *Cancer Res* 2002, 62:1410–1419.

27. Chen B, Roy SG, McMonigle RJ, Keebaugh A, McCracken AN, Selwan E, Fransson R, Fallegger D, Huwiler A, Kleinman MT, Edinger AL, Hanessian S: Azacyclic FTY720 Analogues That Limit Nutrient Transporter Expression but Lack S1P Receptor Activity and Negative Chronotropic Effects Offer a Novel and Effective Strategy to Kill Cancer Cells in Vivo. *ACS Chem Biol* 2016, 11:409–14.

28. Kono M, Tucker AE, Tran J, Bergner JB, Turner EM, Proia RL: Sphingosine-1-phosphate

receptor 1 reporter mice reveal receptor activation sites in vivo. *J Clin Invest* 2014, 124:2076–2086.

29. Birsoy K, Possemato R, Lorbeer FK, Bayraktar EC, Thiru P, Yucel B, Wang T, Chen WW, Clish CB, Sabatini DM: Metabolic determinants of cancer cell sensitivity to glucose limitation and biguanides. *Nature* 2014, 508:108–12.

30. Digman M a, Caiolfa VR, Zamai M, Gratton E: The phasor approach to fluorescence lifetime imaging analysis. *Biophys J* 2008, 94:L14–L16.

31. Bird DK, Yan L, Vrotsos KM, Eliceiri KW, Vaughan EM, Keely PJ, White JG, Ramanujam N: Metabolic mapping of MCF10A human breast cells via multiphoton fluorescence lifetime imaging of the coenzyme NADH. *Cancer Res* 2005, 65:8766–73.

32. Stringari C, Cinquin A, Cinquin O, Digman MA, Donovan PJ, Gratton E: Phasor approach to fl uorescence lifetime microscopy distinguishes different metabolic states of germ cells in a live tissue. *Proc Natl Acad Sci USA* 2011, 108:13582–13587.

33. Stringari C, Wang H, Geyfman M, Crosignani V, Kumar V, Takahashi JS, Andersen B, Gratton E: In Vivo Single-Cell Detection of Metabolic Oscillations in Stem Cells. *Cell Rep* 2015, 10:1–7.

34. Stringari C, Nourse JL, Flanagan L a., Gratton E: Phasor Fluorescence Lifetime Microscopy of Free and Protein-Bound NADH Reveals Neural Stem Cell Differentiation Potential. *PLoS One* 2012, 7.

35. Pate KT, Stringari C, Sprowl-Tanio S, Wang K, TeSlaa T, Hoverter NP, McQuade MM, Garner C, Digman M a, Teitell M a, Edwards R a, Gratton E, Waterman ML: Wnt signaling directs a metabolic program of glycolysis and angiogenesis in colon cancer. *EMBO J* 2014, 33:1454–73.

36. Stringari C, Edwards R a, Pate KT, Waterman ML, Donovan PJ, Gratton E: Metabolic trajectory of cellular differentiation in small intestine by Phasor Fluorescence Lifetime Microscopy of NADH. *Sci Rep* 2012, 2:568.

37. Bauer DE, Harris MH, Plas DR, Lum JJ, Hammerman PS, Rathmell JC, Riley JL, Thompson CB: Cytokine stimulation of aerobic glycolysis in hematopoietic cells exceeds proliferative demand. *FASEB J* 2004, 18:1303–1305.

38. Gault CR, Eblen ST, Neumann CA, Hannun YA, Obeid LM: Oncogenic K-Ras regulates bioactive sphingolipids in a sphingosine kinase 1-dependent manner. *J Biol Chem* 2012, 287:31794–31803.

39. McCartney AJ, Zhang Y, Weisman LS: Phosphatidylinositol 3,5-bisphosphate: Low abundance, high significance. *BioEssays* 2014, 36:52–64.

40. Jefferies HBJ, Cooke FT, Jat P, Boucheron C, Koizumi T, Hayakawa M, Kaizawa H, Ohishi T, Workman P, Waterfield MD, Parker PJ: A selective PIKfyve inhibitor blocks PtdIns(3,5)P(2) production and disrupts endomembrane transport and retroviral budding. *EMBO Rep* 2008, 9:164–70.

41. Rutherford AC, Traer C, Wassmer T, Pattni K, Bujny M V, Carlton JG, Stenmark H, Cullen PJ: The mammalian phosphatidylinositol 3-phosphate 5-kinase (PIKfyve) regulates endosome-to-TGN retrograde transport. *J Cell Sci* 2006, 119(Pt 19):3944–57.

42. Zhang Y, McCartney AJ, Zolov SN, Ferguson CJ, Meisler MH, Sutton M a, Weisman LS:

Modulation of synaptic function by VAC14, a protein that regulates the phosphoinositides PI(3,5)P2 and PI(5)P. *EMBO J* 2012, 31:3442–3456.

43. Dong X, Shen D, Wang X, Dawson T, Li X, Zhang Q, Cheng X, Zhang Y, Weisman LS, Delling M, Xu H: PI(3,5)P(2) controls membrane trafficking by direct activation of mucolipin Ca(2+) release channels in the endolysosome. *Nat Commun* 2010, 1:38.

44. Li X, Wang X, Zhang X, Zhao M, Tsang WL, Zhang Y, Yau RGW, Weisman LS, Xu H: Genetically encoded fluorescent probe to visualize intracellular phosphatidylinositol 3,5-bisphosphate localization and dynamics. *Proc Natl Acad Sci U S A* 2013, 110:21165–70.

45. Chalfant CE, Kishikawa K, Mumby MC, Kamibayashi C, Bielawska A, Hannun YA: Long Chain Ceramides Activate Protein Phosphatase-1 and Protein Phosphatase-2A. 1999, 274:1–5.

46. Chalfant CE, Szulc Z, Roddy P, Bielawska A, Hannun Y a: The structural requirements for ceramide activation of serine-threonine protein phosphatases. *J Lipid Res* 2004, 45:496–506.

47. Ogretmen B, Hannun Y a: Biologically active sphingolipids in cancer pathogenesis and treatment. *Nat Rev Cancer* 2004, 4:604–616.

48. Wang W, Gao Q, Yang M, Zhang X, Yu L, Lawas M, Li X, Bryant-Genevier M, Southall NT, Marugan J, Ferrer M, Xu H: Up-regulation of lysosomal TRPML1 channels is essential for lysosomal adaptation to nutrient starvation. *Proc Natl Acad Sci* 2015, 112:E1373–81.

49. Vicinanza M, Korolchuk VI, Ashkenazi A, Puri C, Menzies FM, Clarke JH, Rubinsztein DC: PI(5)P Regulates Autophagosome Biogenesis. *Mol Cell* 2015, 57:219–234.

50. Zolov SN, Bridges D, Zhang Y, Lee W-W, Riehle E, Verma R, Lenk GM, Converso-Baran K, Weide T, Albin RL, Saltiel a. R, Meisler MH, Russell MW, Weisman LS: In vivo, Pikfyve generates PI(3,5)P2, which serves as both a signaling lipid and the major precursor for PI5P. *Proc Natl Acad Sci* 2012, 109:17472–17477.

51. Kerr MC, Wang JTH, Castro N a, Hamilton N a, Town L, Brown DL, Meunier F a, Brown NF, Stow JL, Teasdale RD: Inhibition of the PtdIns(5) kinase PIKfyve disrupts intracellular replication of Salmonella. *EMBO J* 2010, 29:1331–1347.

52. Wu X, Daniels G, Lee P, Monaco ME: Lipid metabolism in prostate cancer. *Am J Clin Exp Urol* 2014, 2:111–20.

53. Schwarzenböck S, Souvatzoglou M, Krause BJ: Choline PET and PET/CT in Primary Diagnosis and Staging of Prostate Cancer. *Theranostics* 2012, 2:318–330.

54. Chen Z, Trotman LC, Shaffer D, Lin H-K, Dotan ZA, Niki M, Koutcher JA, Scher HI, Ludwig T, Gerald W, Cordon-Cardo C, Pandolfi PP: Crucial role of p53-dependent cellular senescence in suppression of Pten-deficient tumorigenesis. *Nature* 2005, 436:725–730.

55. Lee C, Raffaghello L, Brandhorst S, Safdie FM, Bianchi G, Martin-Montalvo A, Pistoia V, Wei M, Hwang S, Merlino A, Emionite L, de Cabo R, Longo VD: Fasting Cycles Retard Growth of Tumors and Sensitize a Range of Cancer Cell Types to Chemotherapy. *Sci Transl Med* 2012, 4:124ra27.

56. Kalaany NY, Sabatini DM: Tumours with PI3K activation are resistant to dietary restriction. *Nature* 2009, 458:725–731.

57. Argilés JM, Busquets S, Stemmler B, López-Soriano FJ: Cancer cachexia: understanding the molecular basis. *Nat Rev Cancer* 2014, 14:754–762.

58. Schwartz S, Wongvipat J, Trigwell CB, Hancox U, Carver BS, Rodrik-Outmezguine V, Will M, Yellen P, de Stanchina E, Baselga J, Scher HI, Barry ST, Sawyers CL, Chandarlapaty S, Rosen N: Feedback Suppression of PI3Kα Signaling in PTEN-Mutated Tumors Is Relieved by Selective Inhibition of PI3Kβ. *Cancer Cell* 2015, 27:109–122.

59. Cai X, Xu Y, Cheung AK, Tomlinson RC, Alcázar-Román A, Murphy L, Billich A, Zhang B, Feng Y, Klumpp M, Rondeau JM, Fazal AN, Wilson CJ, Myer V, Joberty G, Bouwmeester T, Labow M a., Finan PM, Porter J a., Ploegh HL, Baird D, De Camilli P, Tallarico J a., Huang Q: PIKfyve, a class III PI Kinase, is the target of the small molecular IL-12/IL-23 inhibitor apilimod and a player in toll-like receptor signaling. *Chem Biol* 2013, 20:912–921.

60. Er EE, Mendoza MC, Mackey AM, Rameh LE, Blenis J: AKT facilitates EGFR trafficking and degradation by phosphorylating and activating PIKfyve. *Sci Signal* 2013, 6:ra45.

CHAPTER 2

Prostate cancer cells convert cell corpses into biomass via macropinocytosis

Seong M. Kim[1,*], Archna Ravi[1,*], Tricia T. Nguyen[1,*], Peter Kubiniok[2], Brendan Finicle[1], Jue Hou[3], Leonel Malacrida[4], Sarah Barr[1], Jane Robertson[1], Dong Gao[5], Yu Chen[5], Michelle Digman[4], Eric O. Potma[3], Bruce J. Tromberg[3], Pierre Thibault[2], and Aimee L. Edinger[1]

[1]Department of Developmental and Cell Biology, University of California Irvine, Irvine CA 92697

[2]Department of Chemistry, Université de Montréal, Quebec, Canada H3C 3J7

[3]Department of Biomedical Engineering, University of California Irvine, Irvine CA 92697

[4]Laboratory for Fluorescence Dynamics, University of California Irvine, Irvine CA 92697

[5]Human Oncology and Pathogenesis Program, Memorial Sloan Kettering Cancer Center, New York, NY 10065

[*] Equal contribution

ABSTRACT

All cancer cells import nutrients using surface transporters and receptors, but tumor cells with activating mutations in Ras also acquire exogenous amino acids via macropinocytosis. Here we report that prostate cancer cells deficient in the PI(3,4,5)P_3 3'-phosphatase PTEN also exhibit constitutive macropinocytosis that promotes survival and proliferation in low-nutrient environments. AMPK activation was necessary and sufficient for macropinocytosis in PTEN-deficient, but not PTEN-replete, cells. While albumin supplementation restored amino acid-dependent mTORC1 activity in nutrient-restricted PTEN-deficient prostate cancer cells, albumin was also taken up independent of macropinocytosis. In contrast, prostate cancer cells internalized necrotic cell debris solely via macropinocytosis. Macropinocytosed cellular corpses were converted into protein and lipid biomass, supporting prostate cancer proliferation in nutrient-deficient medium. Constitutive macropinocytosis was observed when patient-derived prostate cancer samples were maintained in organoid culture systems or as subcutaneous xenografts. Autochthonous tumors in mice lacking PTEN and p53 in the prostate also exhibited macropinocytosis in situ. As inhibiting macropinocytosis with EIPA profoundly inhibited prostate tumor growth, macropinocytosis could be a viable target for anti-metabolic therapies in a broader array of cancers than previously thought. Moreover, the catabolism of necrotic cell corpses to support tumor cell division suggests a novel explanation for the negative correlation between tumor necrosis and prognosis in multiple solid tumor classes characterized by mutations that stimulate macropinocytosis.

INTRODUCTION

Cancer cells up-regulate nutrient acquisition pathways in order to fuel oncogene-driven anabolism and proliferation (1–3). LDL and transferrin receptors and transporters for glucose and amino acids are all expressed on tumor cells, and high expression levels of these nutrient import proteins is uniformly a negative prognostic indicator associated with aggressive and metastatic disease (1,2). However, as tumors grow, their abnormal vasculature results in the development of extracellular nutrient limitation rendering these nutrient import pathways unable to meet nutrient demand, eventually leading to tumor necrosis(4). Recent studies have shown that macropinocytosis, a process by which cells non-specifically engulf extracellular materials via plasma membrane ruffling, allows nutrient-limited cancer cells to convert extracellular proteins such as albumin into amino acids to support survival and proliferation in poorly perfused areas (5–7). To date, macropinocytosis has only been reported in cancer cells with activating mutations in Ras. However, signaling through the epidermal growth factor receptor (EGFR) drives transient macropinocytosis in vitro (8); whether oncogenic forms of the EGFR or related receptor tyrosine kinases support constitutive macropinocytosis has not been assessed. Similarly, while Ras-driven macropinocytosis depends on PI 3-kinase activation (5,9,10), whether activation of the PI 3-kinase pathway through alternative mechanisms is sufficient to stimulate macropinocytosis has not been studied in cancer cells.

$PI(3,4,5)P_3$ produced by type I PI 3-kinases accumulates at sites of macropinosome formation where it recruits pleckstrin homology domain-containing Rac1 guanosine nucleotide exchange factors (GEFs) (11). Subsequent Rac1 activation induces the actin remodeling and membrane ruffling necessary to form macropinosomes. Both $PI(3,4,5)P_3$ and Rac1-GTP are essential for the initiation of macropinocytosis, and inhibition of either pathway ablates macropinosome formation (5,11,12). The PI 3-kinase inhibitors wortmannin and LY29400 inhibit macropinocytosis, but are non-specific and disrupt all $PI(3,4,5)P_3$-dependent phenotypes(11). A

more selective and commonly used macropinocytosis inhibitor is 5-(N-ethyl-N-isopropyl) amiloride (EIPA). EIPA inhibits Rac1 activation indirectly by reducing the submembranous pH (13). At present, no lipids or proteins have been identified that function solely in macropinocytosis and only selective, rather than specific, inhibitors are available.

The lipid phosphatase PTEN opposes PI 3-kinase pathway signaling by converting $PI(3,4,5)P_3$ to $PI(4,5)P_2$ (14). PTEN is the most frequently deleted tumor suppressor gene in prostate cancer, but is also commonly lost or mutated in breast, lung, and endometrial cancer and in glioblastoma (15–26). Monoallelic PTEN deletion occurs in up to 60% of localized prostate cancers and complete loss of PTEN is commonly associated with increased risk of metastasis and the development of lethal, castration resistant disease (26,27). Given the critical role for PI 3-kinase activation in macropinocytosis, we evaluated whether PI 3-kinase pathway activation downstream of PTEN loss could allow prostate cancer cells to withstand nutrient deprivation by stimulating macropinocytosis. Here we report that PTEN-deficient prostate cancer cells exhibit constitutive macropinocytosis and demonstrate that necrotic cell debris present in late stage and aggressive tumors can fuel the survival and proliferation of nutrient-deprived prostate cancer cells following uptake via macropinocytosis.

RESULTS

PTEN loss promotes macropinocytosis under nutrient limiting conditions. Oncogenic mutations constitutively drive anabolism and limit metabolic flexibility under nutrient stress (28). Nevertheless, tumor cells with activating mutations in Ras are resistant to amino acid deprivation. Since Ras activation drives macropinocytosis, these tumor cells can proliferate despite amino acid depletion because macropinocytosed proteins are converted into amino acids in the lysosome and then exported to the cytoplasm (6,7). Consistent with the critical role of PI 3-kinase activation for macropinocytosis downstream from Ras (5,11), PTEN null murine embryonic fibroblasts (PTEN KO MEFs) exhibited striking resistance to amino acid and glucose withdrawal compared to PTEN-replete (wild type,WT) MEFs (Figure 1A). To directly test whether PTEN deletion is sufficient to stimulate macropinocytosis, the uptake of fluorescently labeled 70 kD dextran was measured in PTEN wild type (WT) and KO MEFs in the presence or absence of the selective macropinocytosis inhibitor, EIPA. Intriguingly, neither PTEN WT nor PTEN KO MEFs took up dextran in complete medium. However, combined amino acid and glucose deprivation dramatically enhanced dextran uptake selectively in PTEN KO MEFs (Figure 1B). Dextran uptake was EIPA-sensitive confirming its internalization via macropinocytosis. Inhibiting PI 3-kinase in PTEN KO MEFs with a combination of the PI 3-kinase alpha and beta inhibitors BYL719 and AZD8186 blocked macropinocytosis in low nutrient conditions (Supplemental Figure 1A). Conversely, acutely inhibiting PTEN with Bpv(pic) stimulated macropinocytosis in PTEN WT MEFs when cells were placed under nutrient stress (Supplemental Figure 1B). These results indicate that PI 3-kinase pathway activation resulting from PTEN loss is sufficient to promote macropinocytosis selectively under nutrient-limiting conditions.

Ras-driven macropinocytosis confers on MEFs the ability to survive and even proliferate under nutrient limiting conditions (6,7). To determine whether macropinocytosis was responsible for

the enhanced survival of PTEN KO MEFs upon nutrient restriction (Figure 1A), the sensitivity of PTEN KO MEFs to EIPA in complete and low-nutrient medium was measured. EIPA was not toxic to MEFs in complete medium; however, blocking macropinocytosis with EIPA fully reversed the survival advantage of PTEN KO MEFs in low nutrients (Figure 1B,C). Albumin, the most abundant protein in blood plasma (29–31), can supply amino acids to macropinocytic K-RasG12D-expressing cells maintained in amino acid-deficient medium (6,7). Fatty acid-free bovine serum albumin (BSA) also promoted proliferation in amino acid- and glucose-deprived PTEN KO MEFs (Figure 1D). As the addition of 2% BSA to nutrient-deprived PTEN WT MEF cultures also enhanced proliferation in the absence of detectable macropinocytosis (Figure 1B and D), receptor-mediated BSA endocytosis likely contributes to BSA uptake in these MEFs (30,31). Taken together, these studies demonstrate that PI 3-kinase pathway activation upon PTEN deletion drives macropinocytosis that fuels survival and proliferation in nutrient-deficient medium.

AMPK activation is necessary for the induction of macropinocytosis in PTEN-deficient cells. Previous studies concluded that PTEN knockdown did not confer a survival or proliferative advantage on leucine-deprived MEFs (7). A key difference between this report and the experiments shown in Figure 1 is that here PTEN KO MEFs were subjected to combined glucose and amino acid limitation with the intention of more accurately mimicking the generalized nutrient stress expected in poorly perfused tumor tissues. As reported previously for knockdown cells (7), PTEN KO MEFs lacked proliferative advantage when deprived only of amino acids (Figure 2A). Intriguingly, PTEN KO MEFs proliferated more when both glucose and amino acids were withdrawn than when only amino acids were depleted (Figure 2A). Cells sense and respond to nutrient stress through several signaling pathways (32). While mTORC1 activity is regulated by amino acid levels (32), AMPK is activated by the increase in AMP and ADP levels that accompanies glucose deprivation (33). Given that glucose deprivation

stimulated proliferation in amino acid-deficient medium (Figure 2A) and prior observations that AMPK is essential for the macropinocytosis-dependent entry of Ebola and vaccinia viruses (34,35), we hypothesized that AMPK activation by glucose restriction is necessary to stimulate macropinocytosis in PTEN-deficient cells. Consistent with this model, amino acid deprivation alone failed to stimulate macropinocytosis in PTEN KO MEFs, while glucose depletion in the presence of amino acids robustly stimulated macropinocytosis to a similar degree as combined glucose and amino acid deprivation (Figure 2B). To directly test the importance of AMPK activation, the effect of the allosteric AMPK activator, A769662, on macropinocytosis was evaluated. A769622 stimulated macropinocytosis in complete medium selectively in PTEN KO MEFs demonstrating that both AMPK activation and PI 3-kinase pathway activation are necessary for macropinocytosis induction in MEFs (Figure 2C). Consistent with this, A769622 could also substitute for glucose deprivation in driving PTEN KO MEF proliferation in amino acid-deficient medium (Figure 2A). Conversely, the selective AMPK inhibitor Compound C inhibited macropinocytosis in PTEN KO MEFs in low nutrients (Figure 2C). Because Compound C also affects other targets (36), a genetic approach was also employed. MEFs lacking both AMPK catalytic subunits (37) failed to exhibit macropinocytosis in low nutrients following CRISPR/Cas9-mediated PTEN deletion although robust dextran uptake was observed following CRISPR deletion of PTEN from matched AMPK WT MEFs (Figure 2D and Supplemental Figure 1C). Together, these results suggest that AMPK activation, rather than mTORC1 inactivation, provides the stimulus for macropinocytosis in PTEN-deficient cells in low nutrient medium. Consistent with this model, the mTORC1 inhibitor rapamycin failed to induce macropinocytosis (Supplemental Figure 1D). In nutrient stressed PTEN KO MEFs, rapamycin did not enhance macropinocytosis or macropinosome-lysosome fusion (Supplemental Figure 1D). In summary, these results demonstrate that nutrient stress stimulates macropinocytosis in PTEN-deficient cells by activating AMPK and that AMPK activation stimulates proliferation rather than inducing quiescence and catabolism under nutrient-limiting conditions.

PTEN-deficient prostate cancer cells exhibit constitutive macropinocytosis. At diagnosis, the majority of prostate tumors exhibit PTEN deficiency or mutation, and complete loss of PTEN is closely linked to the castration resistance and metastasis that render prostate cancer a lethal disease (26,38). K-Ras-driven macropinocytosis promotes the growth of pancreatic tumors (6,7), and thus macropinocytosis may supply PTEN-deficient prostate cancers with fuel for biosynthesis and growth. For initial in vitro studies, human prostate cancer cells with PTEN deletion (PC3, LNCaP) or mutation (DU145) were utilized as well as mouse prostate cancer epithelial (mPCE) cells derived from *PTEN*$^{flox/flox}$*;tp53*$^{flox/flox}$*;PB-Cre4* mice, an established model for castration-resistant prostate cancer (CRPC) (39). These PTEN-deficient prostate cancer cell lines uniformly exhibited robust, EIPA-sensitive dextran uptake in complete medium (Figure 3A). In contrast, the immortalized but non-transformed PTEN-replete prostate epithelial cell line RWPE-1 did not exhibit macropinocytosis (Figure 3B). Macropinocytosis was not enhanced in prostate cancer cells lines by nutrient deprivation or exposure to A769622 (Figure 3A and Supplemental Figure 1E). Consistent with the observation that PTEN loss is necessary for AMPK activation to induce macropinocytosis (Figure 2C), RWPE-1 cells did not take up dextran in low nutrient medium (Figure 3B). These results suggest that prostate epithelial cells are not macropinocytic cells, and that macropinocytosis is a cancer-associated phenotype that stems from the loss of PTEN function. Confirming that macropinocytosis in prostate cancer cells depends on PTEN inactivation, reconstituting prostate cancer cells with PTEN blocked dextran uptake (Figure 3C). AMPK activation was also necessary for macropinocytosis in prostate cancer cells. Compound C blocked macropinocytosis as did expression of a dominant-negative AMPK mutant (Figure 3C,D). In summary, both PTEN inactivation and AMPK activation are necessary to induce macropinocytosis in prostate cancer cell lines.

Macropinocytosis supports prostate cancer cell survival and growth in low nutrients. Macropinocytosis allows pancreatic cancer cells with activating mutations in Ras to grow in

nutrient-limiting conditions (6,7). To assess whether macropinocytosis affords a similar advantage to PTEN-deficient prostate cancer cells, cell survival in low-nutrient or complete medium was monitored in the presence or absence of two agents that block macropinocytosis, EIPA or the allosteric Rac1 inhibitor, EHT1864 (40) (Figure 4A and Supplemental Figure 2A). Consistent with their high macropinocytic levels (Figure 3A), mPCE, PC3, and DU145 prostate cancer cells were resistant to death induced by nutrient deprivation similar to PTEN KO MEFs (Figures 1A and 4A). This survival advantage depended on macropinocytosis. Both EIPA and EHT-1864 dramatically reduced prostate cancer cell survival selectively in low nutrient medium (Figure 4A). The observation that EIPA and EHT-1864 are relatively non-toxic in complete medium demonstrates that, while macropinocytosis likely provides fuel for biosynthesis under standard culture conditions, it is only essential for survival upon nutrient deprivation.

Albumin is the most abundant serum protein and accumulates in tumors making it a physiologic fuel for macropinocytosis assays (29,31). In cells with activated Ras, supplementation of the medium with BSA is necessary to fully demonstrate the contribution macropinocytosis makes to proliferation in amino acid-deficient medium. Addition of 2% BSA to low nutrient medium increased proliferation in mPCE, PC3 and DU145 cells as expected (Figure 4B). However, at concentrations that completely blocked dextran uptake, EIPA only partially reduced BSA uptake in prostate cancer cells (Figure 4C). Macropinocytosis-independent uptake of BSA in prostate cancer cells is consistent with the observation that the proliferation of non-macropinocytic PTEN WT MEFs was stimulated by BSA (Figure 1D). Scavenger receptors that promote BSA uptake via receptor-mediated endocytosis are expressed on the surface of many tumor cells (29,31,41). The efficient uptake of BSA through macropinocytosis-independent mechanisms precludes the use of BSA to demonstrate that proteins taken up via macropinocytosis contribute to prostate cancer cell biomass and support proliferation. We therefore sought to define a specific,

physiologically relevant macropinocytic cargo that was taken up in a fully EIPA-sensitive manner.

As tumors grow, tortuous and poorly formed vasculature leads to the development of necrotic regions where oxygen and nutrient delivery are inadequate to meet tumor cell demand (4). Tumor necrosis is commonly present in aggressive, high-grade tumors, including prostate cancers, and correlates with negative patient outcomes and with resistance to radiation and chemotherapy (42,43). Given that macropinosomes range from 0.2 to 5 μM in diameter (11), we reasoned that necrotic cell debris may be small enough to enter cells via macropinocytosis. If so, cellular corpses could be a rich source of both proteins and lipids that could fuel growth in macropinocytic prostate cancer cells. Live or apoptotic cells would like be too large to enter prostate cancer cells via macropinocytosis, although secondary necrosis may produce fragments of apoptotic cells small enough to be incorporated into macropinosomes.

To determine whether cellular corpses could enter prostate cancer cells via macropinocytosis, murine hematopoetic FL5.12 cells were labeled with the fluorescent dye carboxyfluorescein succinimidyl ester (CFSE) and then killed using several different protocols. FL5.12 cells were ideal for these studies because purely apoptotic death is rapidly induced upon withdrawal of the cytokine IL-3 (44). The use of growth factor withdrawal to induce apoptosis avoids the need to remove a cytotoxic drug before supplying the corpses to prostate cancer cells in macropinocytosis assays. Because FL5.12 cells grown in high concentrations of IL-3 are highly anabolic (doubling time 12 h), a necrotic cell preparation is readily prepared by restricting cells for nutrients and IL-3 simultaneously. Apoptotic cells can be recognized by the exposure of phosphatidyl serine on the exofacial leaflet of the plasma membrane providing a binding site for Annexin V (45). As shown in Figure 5A, FL5.12 cells subjected to IL-3 withdrawal are intact, CFSE-positive, exhibit apoptotic morphology, and are universally Annexin V-positive. In

contrast, FL5.12 cells subjected to IL-3 withdrawal and nutrient stress die necrotically and fragment but retain CFSE-positivity. As predicted based on the size of cells or corpses, both mPCE and DU145 cells engulfed necrotic cellular corpses but not apoptotic or live FL5.12 cells (Figure 5B). Importantly, uptake of necrotic corpses by prostate cancer cells was completely EIPA-dependent indicating that it occurs via macropinocytosis. The selective uptake of necrotic corpses by prostate cancer cells clearly differentiates the macropinocytic uptake of cell corpses from efferocytosis (phagocytosis of apoptotic cells) (46) or oncosis (engulfment of a viable cell by cancer cells) (47) and is consistent with the non-specific nature of macropinocytosis.

Whether necrotic debris take up via macropinocytosis could drive prostate cancer cell proliferation in low nutrient medium was next assessed. Because macropinocytosis in prostate cancer cells did not depend on glucose depletion (Figure 3A), only amino acids were withdrawn to allow maximal macropinocytosis-driven proliferation. Even in the absence of necrotic cell debris, mPCE, PC3, and DU145 cells all survived amino acid deprivation as cell numbers did not drop below baseline (Figure 5C). However, DU145 and PC3 cells failed to proliferate under these culture conditions and mPCE proliferation was dramatically reduced (cell numbers in parallel mPCE cultures in complete medium increase >70-fold in the same time frame). The addition of cellular corpses to nutrient-deprived prostate cancer cells significantly stimulated proliferation in all three cell lines (Figure 5C). Consistent with its ability to block macropinocytosis (Figure 3C), PTEN reconstitution eliminated the ability of necrotic debris to drive proliferation in low nutrients (Figure 5D). These results demonstrate that PTEN-deficient prostate cancer cells can use macropinocytosis to convert necrotic cellular corpses into biomass and/or fuel to support proliferation.

Cell corpses consumed by macropinocytosis are used to build biomass. In cancer cells with activating mutations in Ras, proteins taken up by macropinocytosis are broken down into

amino acids, restoring mTORC1 signaling following amino acid deprivation (7). Prostate cancer cells were also able to use macropinocytosis to produce amino acids that restore mTORC1 signaling under amino acid limitation (Figure 6A). As expected, shifting mPCE cells to amino acid-deficient medium reduced phosphorylation of p70S6 kinase at Thr389, an mTORC1-dependent phosphorylation site (48) (Figure 6A). Over time, mTORC1 signaling was partially restored by macropinocytosis as the recovery of Thr389 phosphorylation was prevented by EIPA. These results suggest that macropinosome degradation produces amino acids that can fuel protein synthesis in nutrient-restricted prostate cancer cells.

To directly test whether necrotic debris consumed via macropinocytosis is broken down into amino acids that are used to build biomass, we developed a novel isotopic labeling strategy to follow the amino acids present in necrotic cell proteins into the prostate cancer cell proteome. FL5.12 cells were grown in $^{13}C_6/^{15}N_4$ lysine- and arginine-containing stable isotope labeling with amino acids in cell culture (SILAC) medium for more than 10 generations (Figure 6B) (49); complete labeling was confirmed by MS. Heavy-labelled FL5.12 cells were then killed and the necrotic debris fed to prostate cancer cells maintained in either complete or low-nutrient culture medium containing unlabeled amino acids and standard fetal bovine serum. Using this strategy, a population of newly synthesized, partially labeled proteins will be produced by prostate cancer cells if heavy amino acids from the necrotic debris and unlabeled amino acids from the culture medium are used for protein synthesis (Figure 6B). These proteins can be detected by digesting proteins with the LysC protease that cuts only after lysine rather than after both lysine and arginine as does trypsin. LysC digestion will generate peptides that contain both lysine and arginine and could therefore be partially labeled. Newly synthesized proteins containing labeled amino acids obtained via macropinocytosis can also be distinguished as heavy-labeled, human specific peptides. Both methods for calculating the contribution of macropinocytosed heavy-labeled cell corpses to prostate cancer cell biomass produced similar results. In amino acid

deficient medium, at least 11-12% of proteins and as much as 52-62% of prostate cancer cell protein biomass was derived from macropinocytosed cell corpses (Figure 6C). In complete medium where extracellular amino acids were much more abundant, between 1.5% and 12-15% of the protein biomass was derived from macropinocytosed cell corpses. This isotopic labeling experiment conclusively demonstrates that macropinocytosed cellular corpses contribute to prostate cancer biomass and established that the fraction of the prostate cancer proteome that is derived from macropinocytosed material is increased under low-nutrient conditions.

Cellular corpses are rich sources of other building blocks in addition to proteins. In particular, lipids and cholesterol are key drivers of prostate cancer growth (50,51). Thus, the membrane component of necrotic debris could also contribute to lipid pools in nutrient-stressed macropinocytic prostate cancer cells. Fatty acids and cholesterol are stored in lipid droplets, and depletion of these lipid pools suppresses prostate cancer proliferation (50–52). Lysosomal degradation of lipid droplets increases in response to amino acid or glucose depletion as triglycerides in these droplets are utilized to fuel mitochondrial metabolism (52–54). Using label-free Coherent Anti-stokes Raman Spectroscopy (CARS) (50,55), lipid droplet content declined significantly in glucose- and amino acid-restricted prostate cancer cells as expected (Figure 6D). Supplying nutrient-limited prostate cancer cells with necrotic cell debris completely restored lipid droplet content. As EIPA did not interfere with LDL uptake (Supplemental Figure 2B), the decrease in lipid accumulation upon EIPA addition stemmed from the block in the macropinocytic uptake of necrotic cell debris. The EIPA-sensitive restoration of lipid stores by supplementation with necrotic cell corpses suggests that prostate cancer cells can utilize macropinocytosis to acquire lipids as well as proteins.

Prostate cancer cells exhibit macropinocytosis under physiologic conditions. Culturing primary tumor cells in 3D matrices in the presence of cytokines and growth factors recapitulates physiological growth conditions better than 2D cell culture systems and can alter the metabolic profile and phenotype of cancer cells (56–58). Moreover, non-transformed primary cells that cannot be grown under standard 2D culture conditions can be propagated as organoids in 3D systems (59,60). To assess whether prostate epithelial cells perform macropinocytosis under more physiologic conditions, we evaluated dextran uptake in prostate organoids derived from wild type C57BL/6 mice and from *PTEN*$^{flox/flox}$*;tp53*$^{flox/flox}$*;PB-Cre4* mice that develop autochthonous prostate tumors. PTEN-deficient prostate cancer organoids but not PTEN-replete normal prostate epithelial organoids exhibited EIPA-sensitive macropinocytosis in standard 3D culture medium (Figure 7A). Primary, metastatic tumor cells from CRPC patients can also be propagated in 3D culture where they form tumor organoids that exhibit histological features that mimic the original patient tumor (61). One such patient sample deficient in both PTEN and p53, MSK-PCa1, also exhibited constitutive macropinocytosis in 3D culture (Figure 7B). Patient-derived prostate cancer xenografts (PDX) were also evaluated *in situ*. Subcutaneous PTEN and p53 deficient PDX tumors (Jackson Laboratory PDX model TM00298) also exhibited EIPA-sensitive dextran uptake following intratumoral injection of dextran (Figure 7C). Similarly, autochthonous tumors in *Pten* $^{flox/flox}$*;tp53*$^{flox/flox}$*;PB-Cre4* (pDKO) mice exhibited robust macropinocytosis of intravenously delivered 70 kD FITC-Ficoll; uptake was again EIPA-sensitive (Figure 7D). Thus, PTEN-deficient prostate cancer cells exhibit robust macropinocytosis under physiologic conditions.

To evaluate whether prostate tumors rely on macropinocytosis for growth, C57BL/6 mice bearing subcutaneous prostate cancer isografts were treated with subcutaneous injections of vehicle (1% DMSO in PBS) or 7.5 mg/kg EIPA every other day for 4 wk. Administration of EIPA inhibited mPCE isograft growth consistent with a role for macropinocytosis in driving prostate

tumor growth in vivo (Figure 7E, ongoing). While all prostate tumor cells evaluated exhibited macropinocytosis, published studies indicate that the growth of a non-macropinocytic pancreatic cancer cell line is not affected by EIPA (6). Taken together, these results in cell lines, organoid cultures, and mouse models support the conclusion that prostate cancers use macropinocytosis to acquire extracellular nutrients to fuel growth and proliferation both *in vitro* and *in vivo*.

DISCUSSION

This study demonstrated that PI3K pathway activated by PTEN mutation or deletion in the context of AMPK activation allows prostate cancer cells to consume extracellular materials by macropinocytosis to build protein and lipid biomass needed for proliferation (Figure 8). The importance of macropinocytosis as a nutrient acquisition strategy and its ability to fuel tumor cell growth in low-nutrient conditions is established for Ras-driven cancers (6,7). While Ras induces macropinosome formation downstream of PI 3-kinase, whether PI 3-kinase pathway activation in PTEN-deficient tumor cells would be sufficient to drive macropinocytosis remained untested. Our observation that macropinocytosis is constitutive in PTEN-deficient prostate cancer cells growing in 2D, as organoids, patient-derived xenografts, or as autochthonous tumors demonstrates that macropinocytosis can drive growth in tumor classes not generally associated with Ras mutations. In addition to prostate cancers, glioblastomas and lung, breast, and endometrial cancers often carry inactivating mutations or deletions in *PTEN* (15–26). Indeed, the majority of human tumors will have either an activating mutation in *Ras* or an inactivating mutation in *PTEN* (62–64). Thus, the studies reported here dramatically extend the potential applicability of metabolic therapies targeting macropinocytosis beyond the scope previously appreciated.

The observation that PTEN knockdown is not sufficient to stimulate macropinocytosis in amino acid-deprived MEFs (7) is readily explained by our finding that AMPK activation is essential for macropinocytosis in PTEN-deficient cells (Figure 2, 3, and Supplemental Figure 1). The critical role of AMPK in macropinocytosis is perhaps not surprising given published studies demonstrating that AMPK activation is essential for the entry of viruses such as Ebola and vaccinia that induce macropinocytosis to gain access to target cells (34,35). Interestingly, AMPK also promotes phagocytosis and efferocytosis in macrophages and neutrophils (65) suggesting that phosphorylation of an AMPK substrate is important for membrane remodeling

events that are shared between these processes. While a direct molecular connection between AMPK and Rac1 has not yet been established, multiple studies indicate that AMPK activity promotes Rac1 activation (65,66). Alternatively, AMPK regulates the localization of PI 3-kinase to the plasma membrane in neurons (67) and thus may stimulate macropinocytosis upstream of Rac1 through effects on PI 3-kinase trafficking. Uncovering the molecular mechanism by which AMPK regulates Rac1-driven macropinosome formation could identify elusive highly selective regulators of macropinocytosis. Given that all currently available macropinocytosis inhibitors also affect other processes, characterization of the pathway by which AMPK regulates macropinocytosis could identify genetic strategies to clarify the role of macropinocytosis in tumor growth in vivo or help to identify chemical macropinocytosis inhibitors with fewer off-target effects.

As macropinocytosis is constitutive but AMPK dependent in prostate cancer cells, metabolic stress associated with bearing multiple oncogenic mutations likely leads to AMPK activation in the absence of nutrient deprivation (68). However, the observation that AMPK activators stimulate macropinocytosis under some conditions (Figure 2C) raises the possibility that AMPK activators currently in clinical trials such as metformin and phenformin could actually confer a survival advantage on tumor cells in poorly perfused tumor regions. While AMPK activators such as metformin or AICAR can have anti-neoplastic activity in animal models (69,70), AMPK activation also promotes tumor survival by helping cells manage metabolic stresses, such as hypoxia and nutrient deprivation (68,70–72). In this role, AMPK is widely viewed as an enforcer of quiescence, triggering proliferative arrest and inducing catabolic processes such as autophagy which suppressing anabolic pathways that consume ATP (73). The observation that AMPK activation dramatically increases proliferation in nutrient-deprived PTEN-deficient MEFs (Figure 2A) runs counter to this prevailing view. AMPK activation also increases colorectal cancer cell proliferation exclusively in the absence of glucose (74) and has a tumor-promoting

role in myeloid leukemia (75). This concept of AMPK as a tumor promoter is similar to the finding that rapamycin can promote Ras-mutant tumor cell proliferation near the tumor core by promoting fusion of macropinosomes and lysosomes (7). Fusion between macropinosomes and lysosomes appeared to be quite efficient in PTEN-deficient prostate cancer cells (Figures 1B and Supplemental Figure 1D) suggesting that there may be differences in how these two oncogenic mutations affect lysosomal function. In summary, these work reported here suggest that more selective inhibitors of AMPK should be developed and tested for anti-neoplastic activity in established tumors with particular attention to tumors that exhibit necrosis.

Macropinocytosis inhibition may be most valuable in combination with other therapeutics. Macropinocytosis provides a bypass system that could rescue tumor cells not just from extracellular nutrient limitation, but also from metabolic therapies. While autophagy provides nutrients from internal sources and therefore does not allow cells to build biomass, macropinocytosis affords access to exogenous nutrients permitting tumor cell growth under nutrient stress. Thus, inhibiting macropinocytosis may have a greater impact on tumor growth than autophagy inhibition. As several studies have suggested that chloroquine limits tumor growth in an autophagy-independent manner (76–78), it is possible that a fraction of the tumor suppressive actions of this lysosomal degradation inhibitor stem from its ability to block macropinosome degradation. Whether a tumor cell is located near a region of necrosis, an abundant source of proteins and lipids for a macropinocytic tumor cell, may also contribute to the heterogenous response of tumors to therapy. The ability of macropinocytosis to sensitize tumor cells to other therapies has yet to be evaluated.

Histologic detection of tumor necrosis is a negative prognostic indicator that is correlated with recurrence and metastatic disease in multiple solid tumors, including prostate cancer (79–81) (82). Our observations that necrotic cell corpses are a rich source of proteins and lipids capable

of driving tumor cell growth (Figure 5C and 6) may partially explain this correlation. While our study was confined to PTEN-deficient prostate cancer cells, it is very likely that Ras-driven macropinocytosis also facilitates the conversion of necrotic cell debris to biomass and fuel for proliferation; necrosis is present in >60% of pancreatic cancers and correlates closely with a poor prognosis (81). A non-mutually exclusive mechanism by which necrosis may enhance tumor growth is its ability to induce immune cells to release cytokines that stimulate nearby tumor cells to proliferate (83). It is possible that these necrotic corpses simultaneously serve as a key fuel source for the cytokine-driven growth of macropinocytic tumor cells. As the correlation between inflammatory markers and necrosis is imperfect (42), in some tumors necrosis may promote cancer cell anabolism primarily by providing metabolic substrates rather than by stimulating a pro-tumorigenic immune response. A deeper understanding of the importance of macropinocytic consumption of cell corpses in vivo awaits the development of more specific chemical and genetic tools, but the studies reported here establish a new link between cancer metabolism and the tumor microenvironment.

Castration-resistant prostate cancer is an invariably lethal disease despite the introduction of new agents such as enzalutamide and abiraterone acetate; chemotherapy with docetaxel also affords little clinical benefit and carries significant toxicity concerns (84,85). Our results with EIPA (Figure 7E) suggest that inhibiting macropinocytosis could provide a new metabolic strategy for inhibiting CRPC growth. Macropinocytosis inhibition may also work synergistically with inhibitors of androgen signaling. Androgen deprivation therapy kills tumor cells, but leads to the emergence of castration-resistant disease. As CRPC is frequently PTEN-deficient, CRPC cells may survive in part off the corpses of their deceased, androgen-dependent brethren. Similarly, cell death resulting from chemotherapy or radiation therapy may actually increase the nutrient pool available to the surviving tumor cells. The dependence of prostate tumor cells on macropinocytosis may also partially explain the effectiveness of the synthetic sphingolipid SH-

BC-893 in prostate cancer models (28). SH-BC-893 does not block macropinosome formation but rather blocks their degradation by preventing macropinosome fusion with lysosomes. It is interesting to consider the possibility that blocking macropinosome degradation rather than macropinosome formation may kill macropinocytic cancers by inducing a form of cell death labeled methuosis characterized by the massive accumulation of macropinosomes (86). In the interim, agents with multifaceted effects such as EIPA and SH-BC-893 can be employed to inhibit macropinocytosis induction or completion.

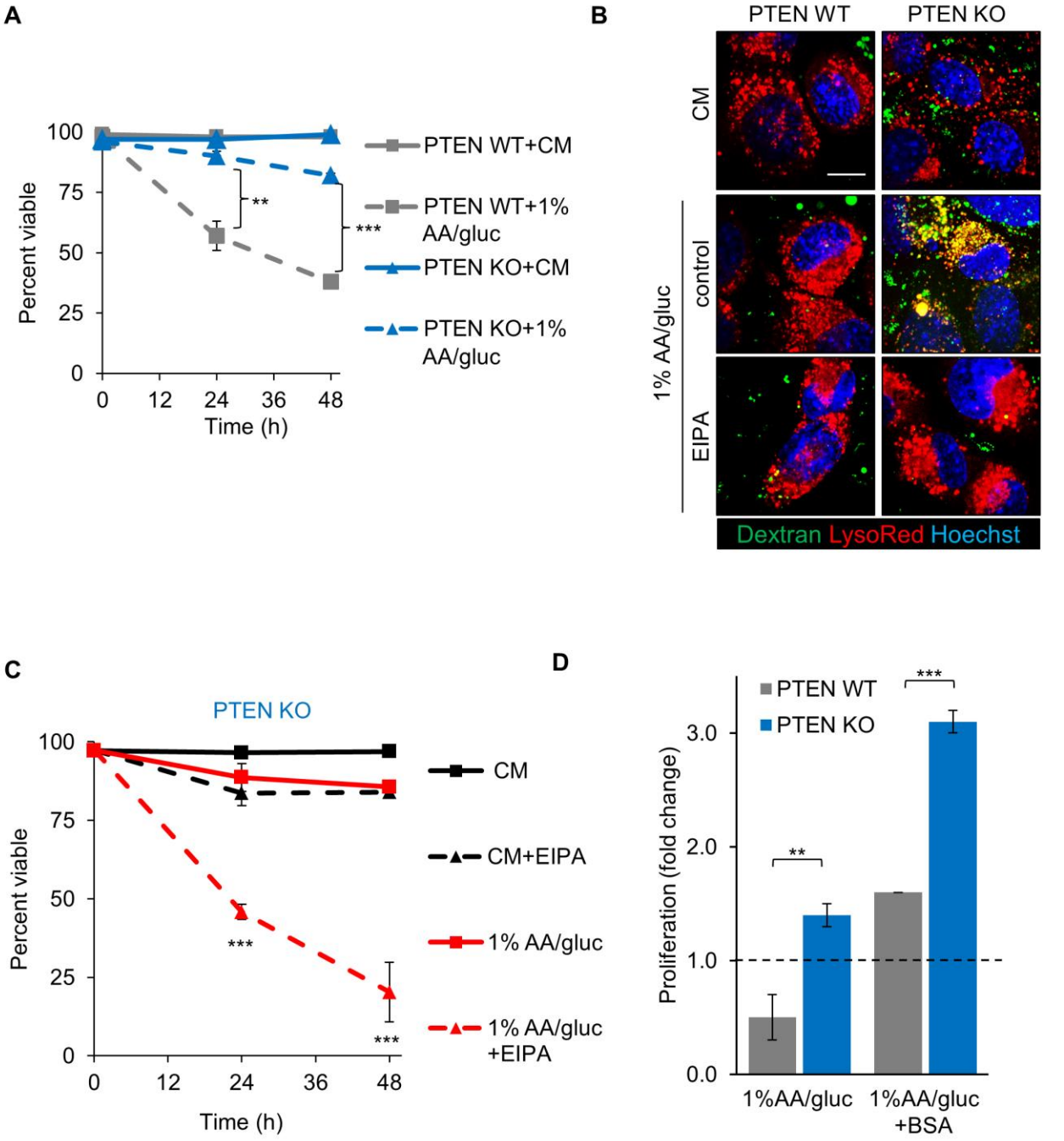

Figure 1: PTEN loss promotes growth and survival in nutrient-limiting conditions by increasing macropinocytosis. **A**) Viability of $p53^{+/+}PTEN^{+/+}$ (PTEN WT) or $p53^{-/-}PTEN^{-/-}$ (PTEN KO) MEFs incubated in complete medium (CM) or media with 1% amino acid and glucose (1% AA/gluc). **B**) After 16 h in in CM or 1%AA/gluc, PTEN WT or PTEN KO MEFs were treated with 50 μM EIPA for 2 h and then incubated with Oregon Green dextran, Lysotracker Red, and Hoechst dye for 30 min. **C**) Viability of PTEN KO MEFs in CM or 1%AA/gluc +/- EIPA. Statistics comparing 1%AA/gluc to 1% AA/gluc+EIPA. **D**) Fold change in live cell count of PTEN WT or KO MEFs after 72 h in 1%AA/gluc +/- 2% BSA. Scale bar, 20 μm.

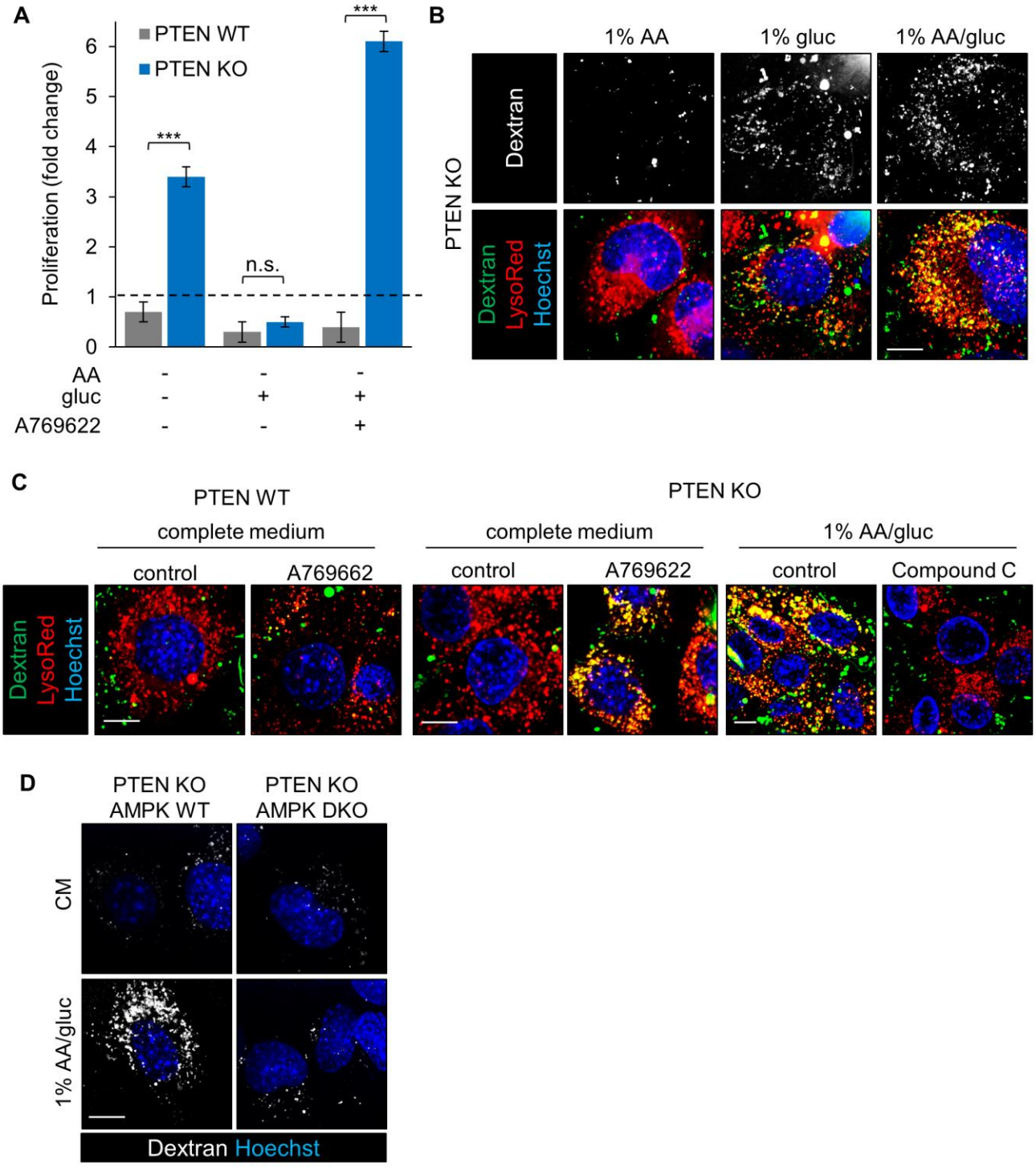

Figure 2: AMPK activation is necessary for induction of macropinocytosis by nutrient stress in PTEN-deficient cells. **A**) Fold change in live cell count of PTEN WT or KO MEFs after 72 h in 1% amino acid and glucose media or in 1% amino acid but glucose replete media with or without A769622. **B**) Dextran uptake of PTEN KO MEFs after 16 h in 1%AA/gluc, 1% AA or 1% gluc media. **C**) Dextran uptake of PTEN WT or KO MEFs in CM +/- A769622 or PTEN KO MEFs in 1% AA/gluc +/- Compound C. **D**) Dextran uptake in AMPK WT or DKO MEFs with PTEN deletion by CRISPR/Cas9 after 16 h incubation in 1% AA/gluc. Scale bar, 20 μm.

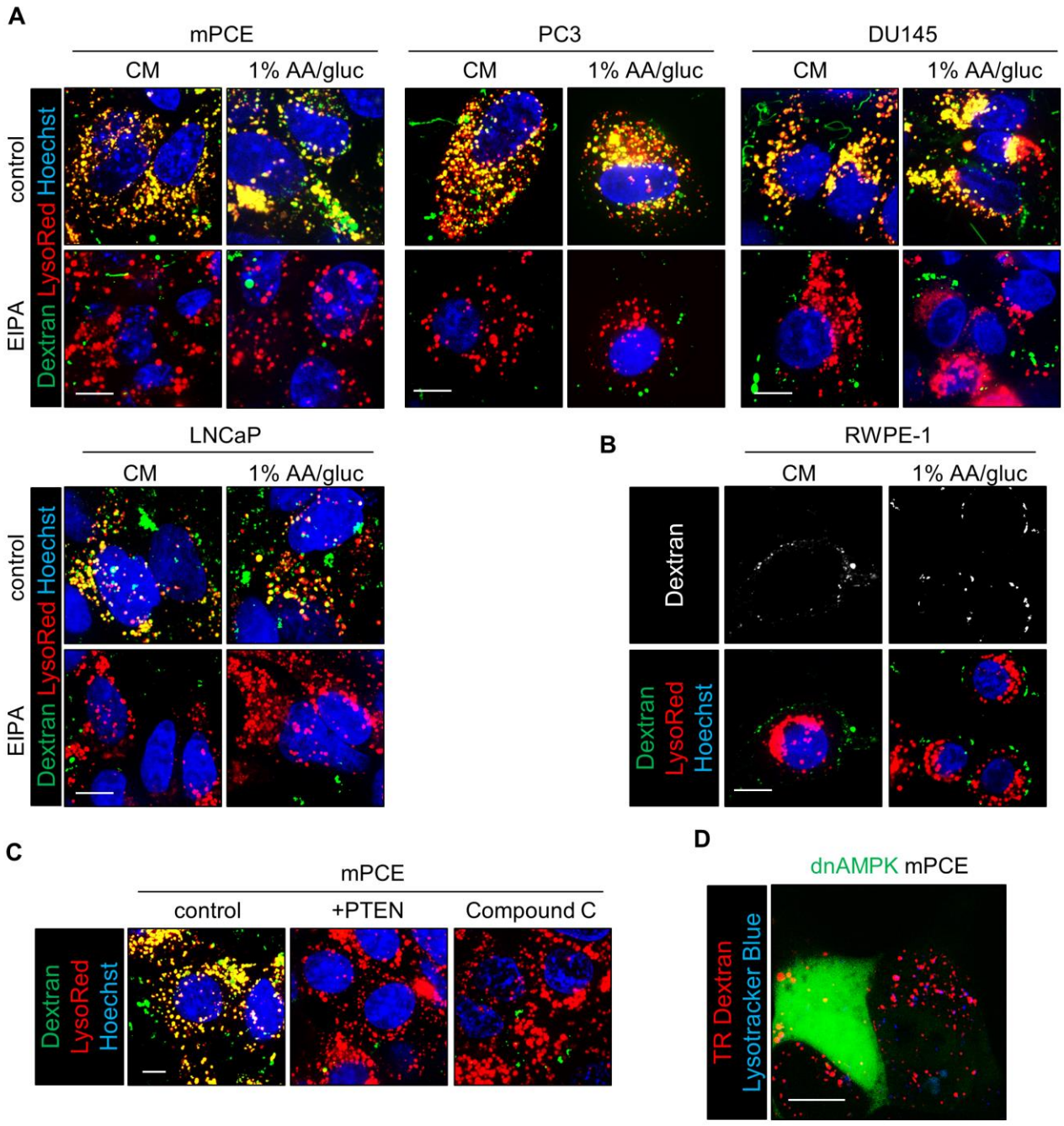

Figure 3: PTEN-deficient prostate cancer cells exhibit constitutive macropinocytosis. **A**) Dextran uptake in mPCE, PC3, DU145, or LNCaP prostate cells after 16 h in complete medium (CM) or 1% AA/gluc +/-EIPA. **B**) Dextran uptake in non-transformed human prostate epithelial RWPE-1 after 16 h in 1% AA/gluc. **C**) Dextran uptake in complete medium in mPCE cells with or without PTEN reconstitution or +/- Compound C. **D**) Dextran uptake in mPCE cells expressing dominant negative AMPK (dnAMPK). Scale bar, 20 μm.

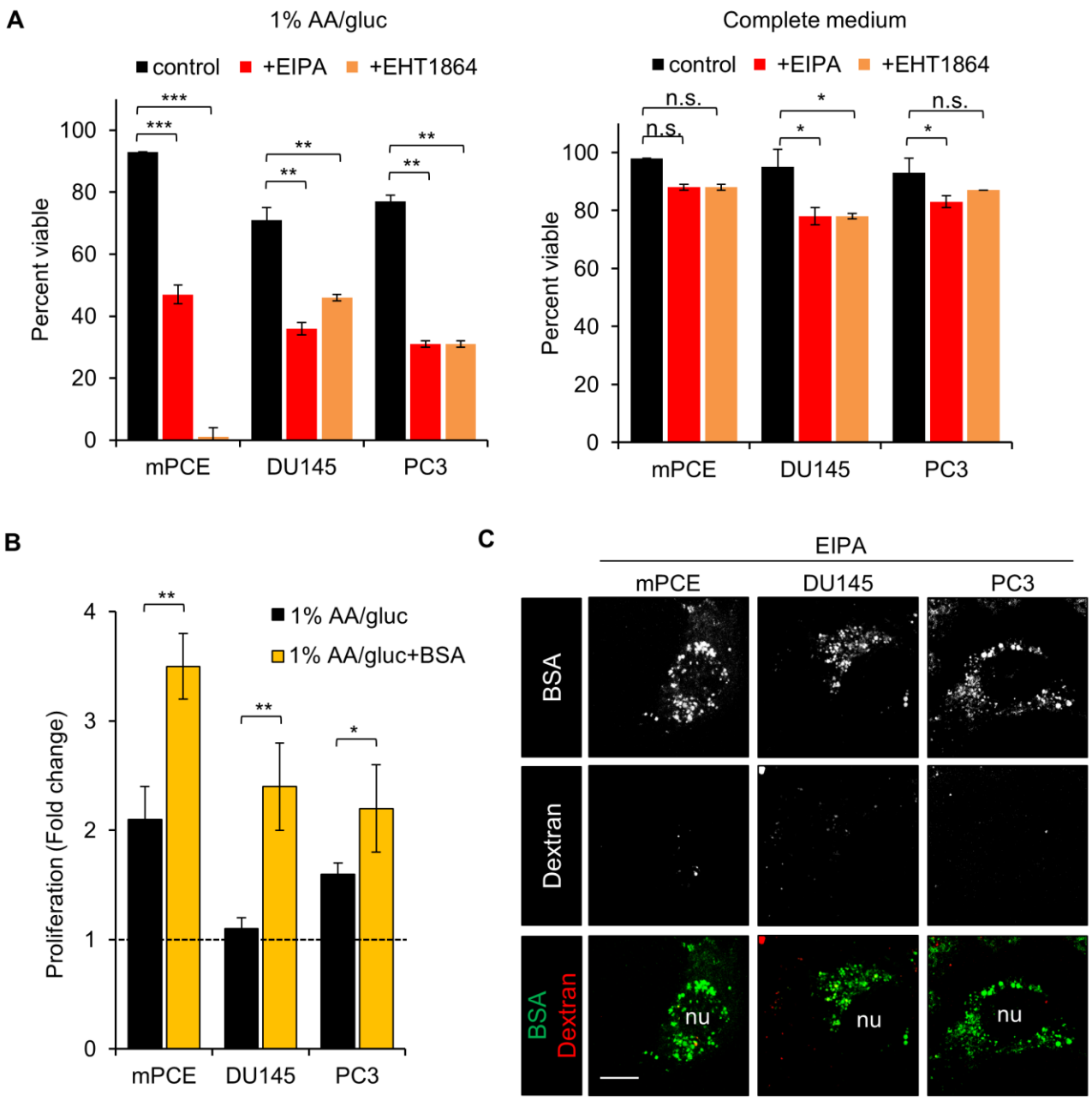

Figure 4: Prostate cancer cell survival and growth in low nutrients is supported by macropinocytosis. **A**) 48 h viability of mPCE, DU145, or PC3 cells in CM or 1% AA/gluc +/- EIPA (25 μM for mPCE and 50 μM for DU145 and PC3) or 50 μM Rac1 inhibitor EHT1864. **C**) DQ-BSA or Texas-Red dextran uptake in mPCE, DU145, or PC3 cells in the presence of 50 μM EIPA. Scale bar, 20 μm.

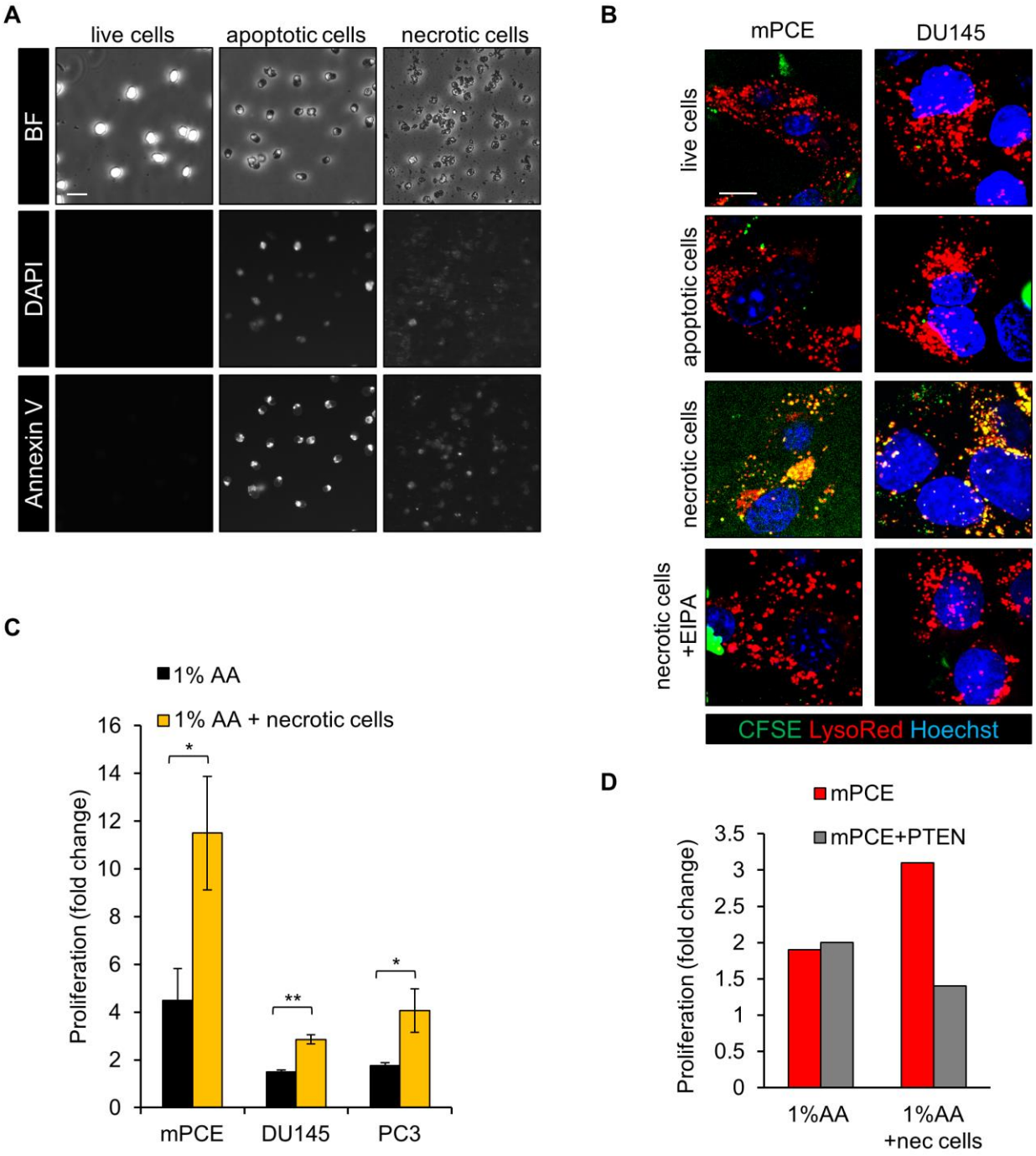

Figure 5: PTEN-deficient prostate cancer cells can consume dead cells by macropinocytosis to fuel growth. **A**) CFSE-labelled FL5.12 cells were killed by IL3 withdrawal for 24 h (apoptotic cells) or 72 h (necrotic cells) and stained as indicated. **B**) Fold change in live cell count of mPCE, DU145, or PC3 cells after 72 h in 1% AA/gluc +/- 2% BSA. **C**) 1 million live FL5.12 cells, apoptotic cells, or necrotic cells were pelleted and fed to mPCE or DU145 for 30 min and imaged. **C**) Fold change in live cell count of mPCE, DU145, or PC3 after 72 h in 1% AA +/- necrotic cells. **D**) Fold change in live cell count of mPCE cells with or without PTEN reconstitution after 72 h in 1% AA +/- necrotic cells. n=1, more replicates are ongoing. Scale bar, 20 μm.

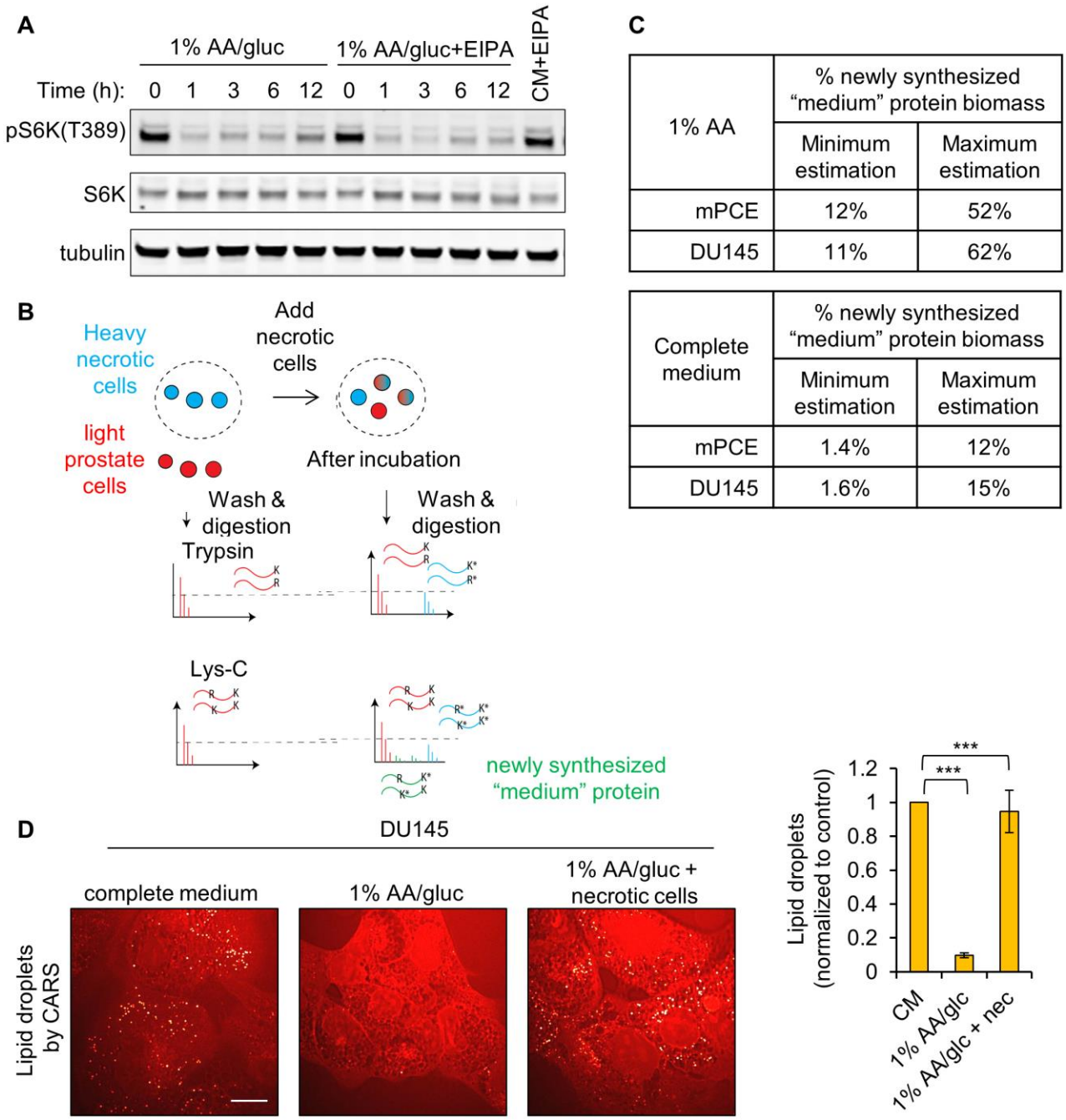

1% AA	% newly synthesized "medium" protein biomass	
	Minimum estimation	Maximum estimation
mPCE	12%	52%
DU145	11%	62%

Complete medium	% newly synthesized "medium" protein biomass	
	Minimum estimation	Maximum estimation
mPCE	1.4%	12%
DU145	1.6%	15%

Figure 6: Necrotic debris consumed by macropinocytosis are used to build biomass. **A**) Lysates from mPCE cells cultured in 1% AA/gluc media +/-EIPA for indicated time points were probed for phospho-S6K. **B**) Experimental design for stable isotope labeling by amino acids in cell culture (SILAC). FL5.12 cells labeled with heavy Arg and Lys ($^{13}C_6/^{15}N_4$) were fed to prostate cancer cells with unlabeled (light) amino acids. Proteins synthesized by prostate cancer cells using heavy FL5.12 cell debris taken up through macropinocytosis will have both heavy and light amino acids (medium). After 4-6 doublings, prostate cancer cells were washed and harvested. Prostate cancer cell lysates were digested with Trypsin or Lys-C and subjected to mass spectrometry. **C**) Percent of newly synthesized protein biomass that have mixture of heavy and light peptides (medium). **D**) DU145 cells were culture in 1% AA/gluc +/- 5 million necrotic debris for 24 h and fixed with 4% PFA. Lipid droplets were imaged by Coherent anti-Stokes Raman Spectroscopy (CARS). Quantification on the right. Scale bar, 20 μm.

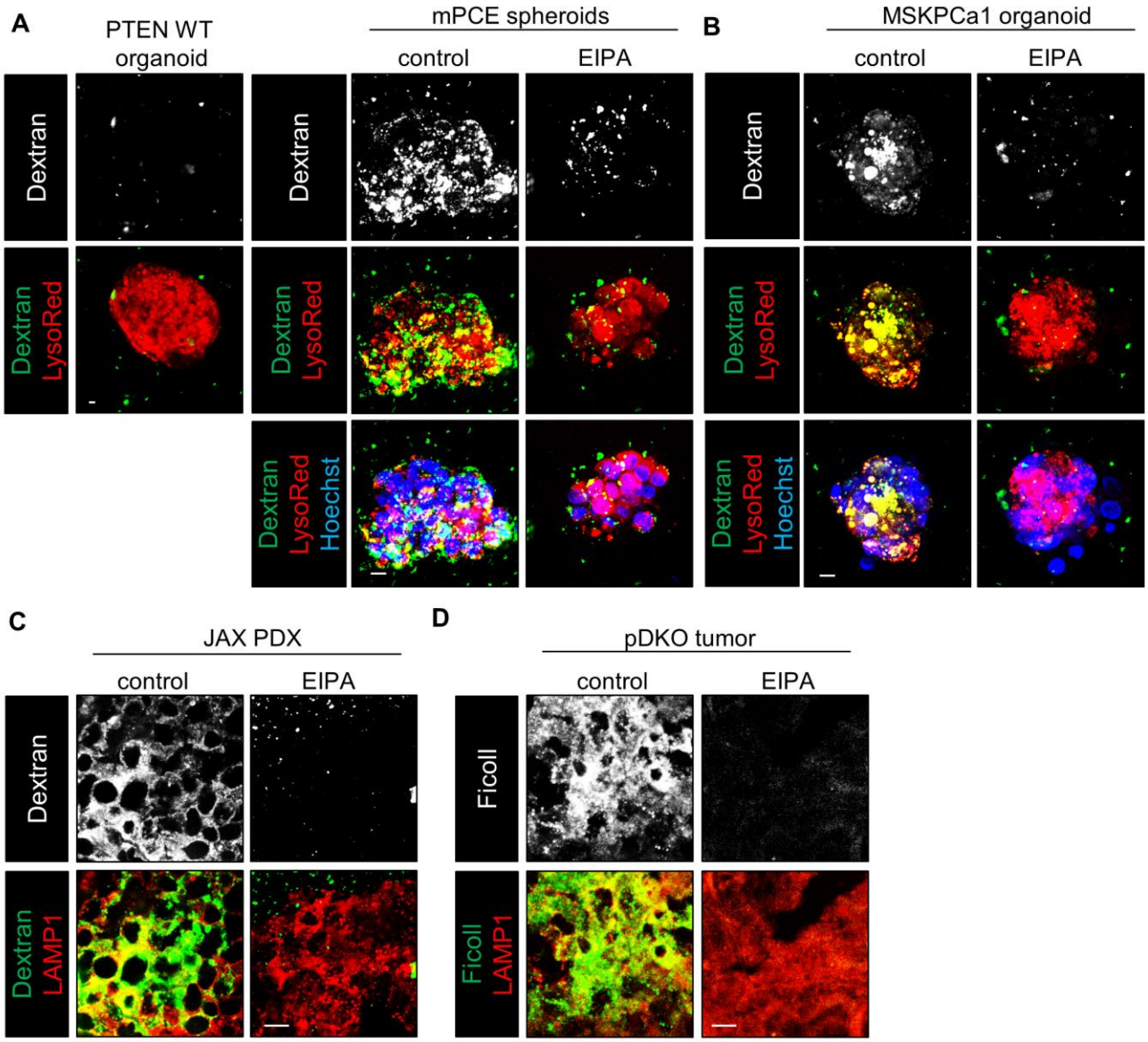

Figure 7: Prostate cancer cells grown in 3D and *in vivo* do macropinocytosis. A-B) Dextran uptake in 3D organoids generated from PTEN WT prostate epithelial cells or mPCE cells (**A**) or MSK-PCa1, human prostate cancer organoids derived from metastatic CRPC (**B**). **C**) Dextran was intratumorally injected into p53-/-; PTEN-/- CRPC PDX (TM00298 from Jackson Laboratory (JAX)) with or without 10 mg/kg EIPA treatment. **D**) Ficoll uptake in autochthonous tumors in *Pten*$^{flox/flox}$;*tp53*$^{flox/flox}$;*PB-Cre4* (pDKO) mice with or without 10mg/kg EIPA treatment. **E**) Tumor volume of mPCE isografts in C57BL/6 mice subcutaneously injected with vehicle or 7.5 mg/kg EIPA. This *in vivo* study is currently ongoing. Scale bar, 20 μm.

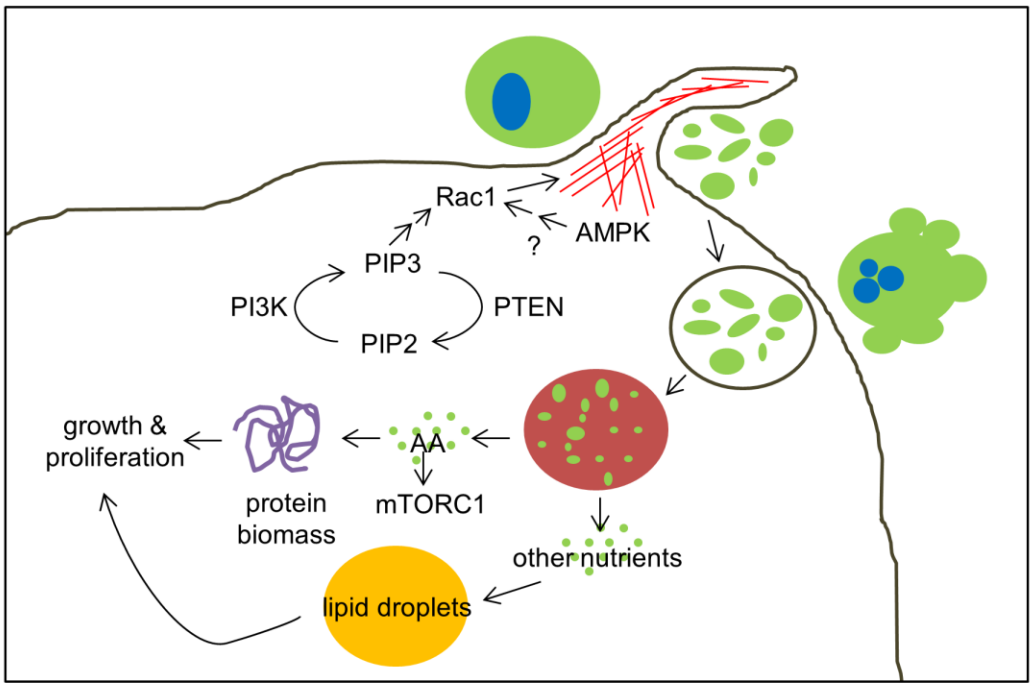

Figure 8: Prostate cancers consume necrotic debris to build biomass and proliferate. PTEN mutant or deficient prostate cancer cells have AMPK-dependent constitutive macropinocytosis that allows them to eat extracellular debris from necrotic cells. Macropinosomes containing these debris fuse with lysosomes and are degraded into amino acids which activate mTORC1 and are incorporated into protein biomass. Other nutrients from macropinosomes are used to increase lipid droplets. Macropinocytosis-derived nutrients build biomass and fuel proliferation.

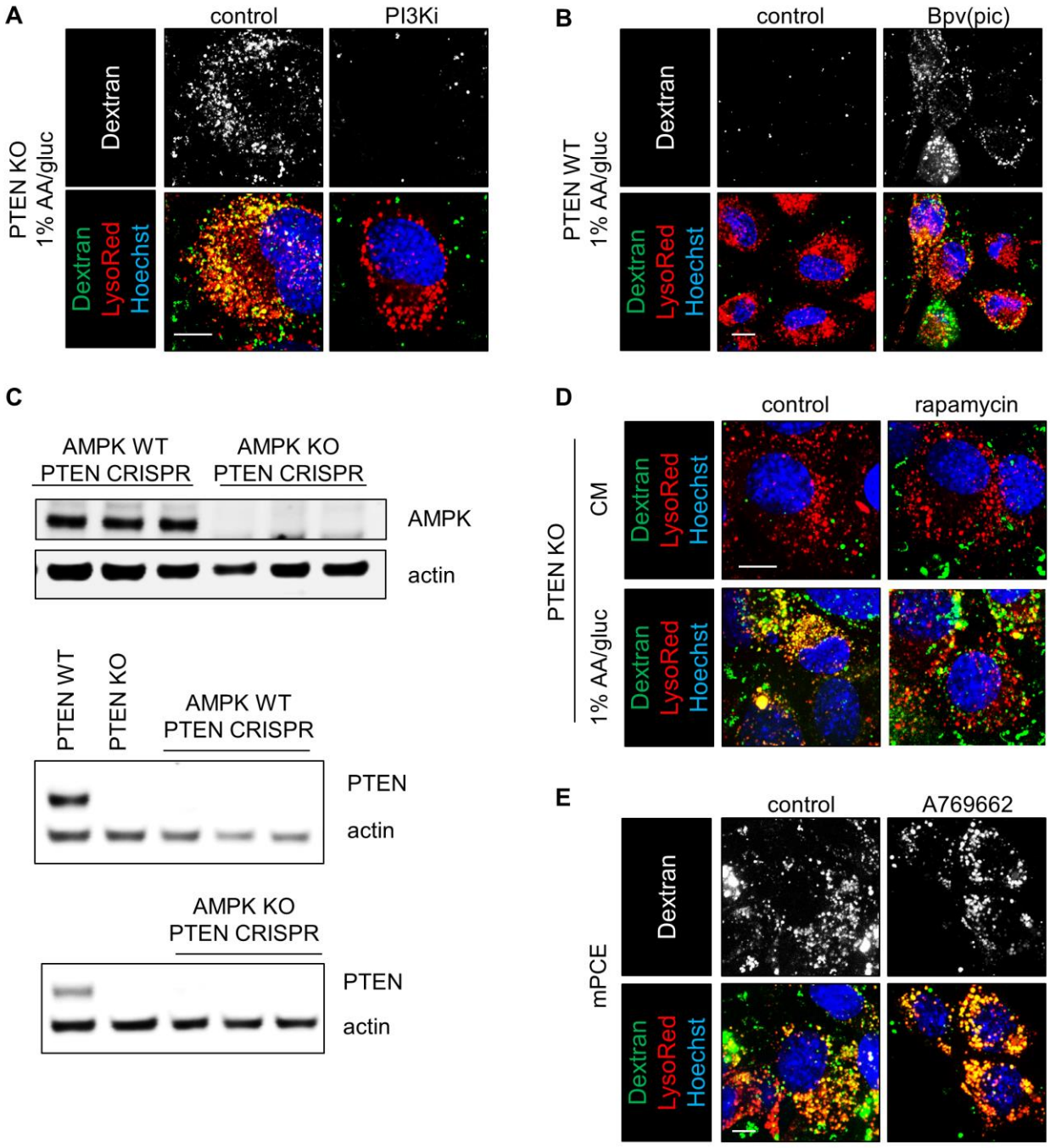

Supplemental Figure 1: PTEN-deficient cells have AMPK-dependent macropinocytosis. A-B) Dextran uptake in PTEN KO MEFs in 1% AA/gluc +/- 2h incubation of PI3K inhibitors BYL719 (2.5 μM) and AZD8186 (250 nM) (**A**); PTEN WT MEFs in 1% AA/gluc +/- 15 min incubation of 10 μM PTEN inhibitor Bpv(pic) (**B**). **C**) Western blot of AMPK WT and DKO MEFs following CRISPR/Cas9-mediated PTEN deletion. **D**) PTEN KO MEFs in CM or 1% AA/gluc +/- 2h incubation of 20 μM rapamycin. **E**) mPCE cells in CM +/- 2h incubation of 100 μM A769622.

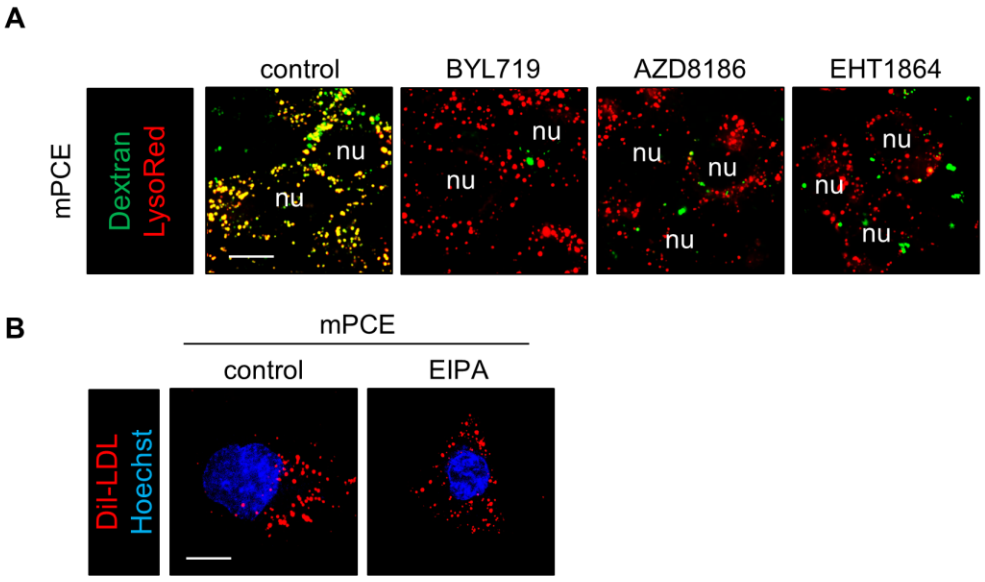

Supplemental Figure 2: Macropinocytosis support prostate cancer proliferation in low nutrients. **A**) Dextran uptake in mPCE cells in CM +/- +/- 2h incubation of 2.5 μM BYL719, 250 nM AZD8186, or 50 μM EHT8164. **B**) mPCE cells were incubated in media with 5% charcoal-stripped media, treated with 50 μM EIPA for 2 h then incubated with DiI-LDL for 1 h.

MATERIALS AND METHODS

Cell culture. mPCE cells generated from $p53^{-/-}$ $PTEN^{-/-}$ mouse prostate tissue were maintained in DMEM with 10% FBS, 25 µg/ml bovine pituitary extract, 5 µg/ml bovine insulin and 6 ng/ml recombinant human epidermal growth factor. FL5.12 cells were maintained in RPMI 1640 medium supplemented with 10% fetal calf serum (FCS), 10 mM HEPES, 55 µM 2-mercaptoethanol, antibiotics, 2 mM L-glutamine, and 500 pg/ml rIL-3. Necrotic debris of FL5.12 cells were generated by placing them in FL5.12 media without IL-3 for 72 h. DU145 and MEF cells were cultured in DMEM with 4.5 g/L glucose and L-glutamine. PC3 cells were cultured in Ham's F12K media. RWPE-1 and LNCaP cells were cultured in RPMI media (ATTC). All media were supplemented with 10% FCS and antibiotics. Cell viability was measured by vital dye exclusion using either propidium iodide or DAPI at 1 µg/ml.

Light Microscopy. Confocal microscopy was performed on a Nikon Eclipse Ti spinning disk confocal microscope. Macropinocytosis was measured after 16 h incubation in 1% amino acids and glucose media and then treatment with macropinocytosis inhibitor 5-(N-ethyl-N-isopropyl) amiloride (EIPA, 50-75 µM) for 1 h. Oregon Green dextran (Life Technologies, cat# D7173) (1 mg/mL) and Lysotracker Red (Life Technologies, cat# L-7525) (1:2,000 dilution) were added for 30 min and live cells were evaluated on the spinning disc confocal microscope. For Dil-LDL uptake, mPCE and DU145 cells were incubated in media with 10% charcoal-stripped serum for 24 h then incubated with 20 µg/ml Dil-LDL (Life Technologies, cat# L3482) +/- EIPA for 2 h. mPCE isograft and JAX PDX tumors were intratumorally injected with 2 mg Oregon Green dextran dissolved in 1% Evan's Blue Dye 1 h after vehicle or 10 mg/kg Intraperitoneal EIPA injection. $p53^{-/-}$; $PTEN^{-/-}$ PDKO prostate tumors were intravenously injected with 250 mg/kg FITC-Ficoll dissolved in 1% Evan's Blue Dye 1 h after vehicle or 10 mg/kg Intraperitoneal EIPA injection. Tumors were excised after 0.5-1 h and sections that were blue from Evan's Blue Dye were frozen in OCT cryomold. Cryosectioned tumor slices were fixed in 4% paraformaldehyde

and probed for LAMP1 (Cell Signaling, cat # 9091P). Tumor samples were processed by the Pathology Research Services Core Facility at UC Irvine.

***In vivo* studies.** Experiments conducted in mice were performed in accordance with the Institutional Animal Care and Use Committee of University of California, Irvine following a power analysis conducted in consultation with the Biostatistics Shared Resource of Chao Family Comprehensive Cancer Center at UCI. Prostate isografts were produced by injecting 5 million mPCE cells subcutaneously in the flank of male 6-8 wk old C57BL/6 mice. Once tumors reached 100 mm^3, 7.5 mg/kg EIPA was administered by subcutaneous injection. Tumor volume was calculated using the formula, volume (mm^3) = length [mm] x (width [mm])^2 x 0.52; To generate pDKO mice on the C57BL6 background, *Pten^{flox}* mice (stock No. 0045597) and *p53^{flox}* mice (stock No. 008462) were obtained from the Jackson Laboratory and *PB-Cre4* mice (strain #01XF5) were obtained from the NCI-Frederick Mouse Repository. Age-matched cohorts of pDKO males were generated by *in vitro* fertilization executed with the assistance of the Transgenic Mouse Facility at UC Irvine. C57BL/6 mice bearing CRPC PDX TM00298 were purchased from the Jackson Laboratory.

Stable isotope labeling with amino acids in cell culture (SILAC). FL5.12 cells were incubated in SILAC media containing “heavy” 13C- or 15N-labeled arginine and lysine for XX days. FL5.12 cells were killed by IL-3 withdrawal and debris from 100 million FL5.12 cells were pelleted and fed to prostate cancer cells. After 4-6 doublings, prostate cells were washed and harvested lysates were digested with Trypsin or Lys-C. Relative abundance of heavy, light, and medium labelled peptides were identified by mass spectrometry. Median values of distributions were used to calculate minimum and maximum estimation of newly synthesized medium-labelled protein biomass.

Coherent anti-Stokes Raman Spectroscopy (CARS). The CARS imaging system is described in detail in (cite). Cells were fixed with 4% formaldehyde and imaged with a 60X water objective. The laser power on the sample was at 10 mW with 10 ms pixel dwell time. The lipid droplet area was estimated from CARS images using a customized Matlab program. Four components Otsu thresholding method was used to separate the lipid droplets, cell cytoplasm, cell nucleus and the background. The lipid droplet area was defined as the number of pixels covered by lipid droplets over the number of pixels covered by cytoplasm.

Statistical methods and data analysis. Significance was determined using a paired t-test to compare experimental groups to controls as indicated. *, $P < 0.05$; **, $P < 0.01$; ***, $P < 0.001$; n.s., not significant ($P > 0.05$). For lipid droplet area in CARS experiments, the mean values between the control and experiment groups were compared with a two-tailed ANOVA.

REFERENCES

1. McCracken AN, Edinger AL: Nutrient transporters: the Achilles' heel of anabolism. *Trends Endocrinol Metab* 2013, 24:200–8.

2. Selwan EM, Finicle BT, Kim SM, Edinger AL: Attacking the supply wagons to starve cancer cells to death. *FEBS Lett* 2016, 590:885–907.

3. Ward PS, Thompson CB: Metabolic Reprogramming: A Cancer Hallmark Even Warburg Did Not Anticipate. *Cancer Cell* 2012, 21:297–308.

4. Weis SM, Cheresh DA: Tumor angiogenesis: molecular pathways and therapeutic targets. *Nat Med* 2011, 17:1359–1370.

5. Lim JP, Gleeson PA: Macropinocytosis : an endocytic pathway for internalising large gulps. *Immunol Cell Biol* 2011, 89:836–843.

6. Commisso C, Davidson SM, Soydaner-Azeloglu RG, Parker SJ, Kamphorst JJ, Hackett S, Grabocka E, Nofal M, Drebin JA, Thompson CB, Rabinowitz JD, Metallo CM, Vander Heiden MG, Bar-Sagi D: Macropinocytosis of protein is an amino acid supply route in Ras-transformed cells. *Nature* 2013, 497:633–7.

7. Palm W, Park Y, Wright K, Pavlova NN, Tuveson DA, Thompson CB: The Utilization of Extracellular Proteins as Nutrients Is Suppressed by mTORC1. *Cell* 2015, 162:1–12.

8. Nakase I, Kobayashi NB, Takatani-nakase T: Active macropinocytosis induction by stimulation of epidermal growth factor receptor and oncogenic Ras expression potentiates cellular uptake efficacy of exosomes. *Sci Rep* 2015, 5:10300.

9. Basquin C, Sauvonnet N: Phosphoinositide 3-kinase at the crossroad between endocytosis and signaling of cytokine receptors. *Commun Integr Biol* 2013, 6:1–4.

10. Kerr MC, Teasdale RD: Defining Macropinocytosis. *Traffic* 2009, 10:364–371.

11. Swanson J a: Shaping cups into phagosomes and macropinosomes. *Nat Rev Mol Cell Biol* 2008, 9:639–649.

12. Wu CYC, Carpenter ES, Takeuchi KK, Halbrook CJ, Peverley L V., Bien H, Hall JC, Delgiorno KE, Pal D, Song Y, Shi C, Lin RZ, Crawford HC: PI3K regulation of RAC1 is required for KRAS-induced pancreatic tumorigenesis in mice. *Gastroenterology* 2014, 147:1405–1416.e7.

13. Koivusalo M, Welch C, Hayashi H, Scott CC, Kim M, Alexander T, Touret N, Hahn KM, Grinstein S: Amiloride inhibits macropinocytosis by lowering submembranous pH and preventing Rac1 and Cdc42 signaling. *J Cell Biol* 2010, 188:547–563.

14. Fruman D a, Rommel C: PI3K and cancer: lessons, challenges and opportunities. *Nat Rev Drug Discov* 2014, 13:140–56.

15. Zhang L, Zhang S, Yao J, Lowery FJ, Zhang Q, Huang W, Li P, Li M, Wang X, Zhang C, Wang H, Ellis K, Cheerathodi M, Mccarty JH, Palmieri D, Saunus J, Lakhani S, Huang S, Sahin

AA, Aldape KD, Steeg PS, Yu D: microRNA primes brain metastasis outgrowth. *Nature* 2015, 527:100–104.

16. Zhang H-Y, Liang F, Jia Z-L, Song S-T, Jiang Z-F: PTEN mutation , methylation and expression in breast cancer patients. *Oncol Lett* 2013, 6:161–168.

17. Kechagioglou P, Papi RM, Provatopoulou X, Zografos G, Kyriakidis DA, Gounaris A: Tumor Suppressor PTEN in Breast Cancer : Heterozygosity , Mutations and Protein Expression. *Anticancer Res* 2014, 34:1387–1400.

18. Soria J, Lee H, Lee JI, Wang L, Issa J, Kemp BL, Liu DD, Kurie JM, Mao L, Khuri FR: Lack of PTEN Expression in Non-Small Cell Lung Cancer Could Be Related to Promoter Methylation 1. *Clin Cancer Res* 2002, 8(May):1178–1184.

19. Noro R, Gemma A, Miyanaga A, Kosaihira S, Minegishi Y: PTEN inactivation in lung cancer cells and the effect of its recovery on treatment with epidermal growth factor receptor tyrosine kinase inhibitors. *Int J Oncol* 2007, 31:1157–1163.

20. Djordjevic B, Hennessy BT, Li J, Barkoh BA, Luthra R, Mills GB, Broaddus RR: Clinical assessment of PTEN loss in endometrial carcinoma : immunohistochemistry outperforms gene sequencing. *Mod Pathol* 2012, 25:699–708.

21. Yang Y, Shao N, Luo G, Li LU, Zheng LU, Nilsson-ehle P, Xu N: Mutations of PTEN Gene in Gliomas Correlate to Tumor Differentiation and Short-term Survival Rate. *Anticancer Res* 2010, 30:981–985.

22. Endersby R, Baker SJ: PTEN signaling in brain: neuropathology and tumorigenesis. *Oncogene* 2008, 27:5416–5430.

23. Wang SI, Puc J, Li J, Bruce JN, Cairns P, Sidransky D, Parsons R: Somatic Mutations of PTEN in Glioblastoma Multiforme. *Cancer Res* 1997, 57:4183–4186.

24. Jiao J, Wang S, Qiao R, Vivanco I, Watson P a., Sawyers CL, Wu H: Murine cell lines derived from Pten null prostate cancer show the critical role of PTEN in hormone refractory prostate cancer development. *Cancer Res* 2007, 67:6083–6091.

25. Dillon LM, Miller TW: Therapeutic targeting of cancers with loss of PTEN function. *Curr Drug Targets* 2014, 15:65–79.

26. Phin S, Moore MW, Cotter PD: Genomic Rearrangements of PTEN in Prostate Cancer. *Front Oncol* 2013, 3(September):240.

27. Shen M, Abate-Shen C: Molecular genetics of prostate cancer: new prospects for old challenges. *Genes Dev* 2010, 24:1967–2000.

28. Kim SM, Roy SGR, Chen B, Nguyen T, McMonigle RJ, McCracken AN, Zhang Y, Kofuji S, Hou J, Selwan E, Finicle BT, Nguyen T, Ravi A, Ramirez MU, Wiher T, Guenther GG, Kono M, Sasaki AT, Weisman LS, Potma EO, Tromberg BJ, Edwards RA, Hanessian S, Edinger AL: Targeting cancer metabolism by simultaneously disrupting parallel nutrient access pathways. *J Clin Invest* 2016.

29. Merlot AM, Kalinowski DS, Richardson DR: Unraveling the mysteries of serum albumin-more than just a serum protein. *Front Physiol* 2014, 5:1–7.

30. Frei E: Albumin binding ligands and albumin conjugate uptake by cancer cells. *Diabetol Metab Syndr* 2011, 3:11.

31. Bern M, Sand KMK, Nilsen J, Sandlie I, Andersen JT: The role of albumin receptors in regulation of albumin homeostasis: Implications for drug delivery. *J Control Release* 2015, 211:144–162.

32. Efeyan A, Comb WC, Sabatini DM: Nutrient-sensing mechanisms and pathways. *Nature* 2015, 517:302–310.

33. Hardie DG, Ross FA, Hawley SA: F O C U S O N m e ta o l l R b E is AMPK : a nutrient and energy sensor that maintains energy homeostasis. *Nat Publ Gr* 2012, 13:251–262.

34. Moser TS, Jones RG, Thompson CB, Coyne CB, Cherry S: A kinome RNAi screen identified AMPK as promoting poxvirus entry through the control of actin dynamics. *PLoS Pathog* 2010, 6.

35. Kondratowicz AS, Hunt CL, Davey R a, Cherry S, Maury WJ: AMP-activated protein kinase is required for the macropinocytic internalization of ebolavirus. *J Virol* 2013, 87:746–55.

36. Bain J, Plater L, Elliott M, Shpiro N, Hastie CJ, Mclauchlan H, Klevernic I, Arthur JSC, Alessi DR, Cohen P: The selectivity of protein kinase inhibitors : a further update. *Biochem J* 2007, 408:297–315.

37. Viollet B, Athea Y, Mounier R, Guigas B, Zarrinpashneh E, Lantier L, Hebrard S, Devin-leclerc J, Foretz M, Andreelli F, Ventura-clapier R, Bertrand L: AMPK: Lessons from transgenic and knockout animals. *Front Biosci* 2009, 14:19–44.

38. Wang S, Gao J, Lei Q, Rozengurt N, Pritchard C, Jiao J, Thomas G V., Li G, Roy-Burman P, Nelson PS, Liu X, Wu H: Prostate-specific deletion of the murine Pten tumor suppressor gene leads to metastatic prostate cancer. *Cancer Cell* 2003, 4:209–221.

39. Chen Z, Trotman LC, Shaffer D, Lin H, Zohar A, Niki M, Koutcher JA, Scher HI, Ludwig T, Cordon-cardo C, Pandolfi PP: Crucial role of p53-dependent cellular senescence in suppression of Pten-deficient tumorigenesis. *Nature* 2007, 436:725–730.

40. Shutes A, Onesto C, Picard V, Leblond B, Schweighoffer F, Der CJ: Specificity and Mechanism of Action of EHT 1864, a Novel Small Molecule Inhibitor of Rac Family Small GTPases *. *J Biol Chem* 2007, 282:35666–35678.

41. Merlot AM, Kalinowski DS, Richardson DR: Unraveling the mysteries of serum albumin — more than just a serum protein. *Front Physiol* 2014, 5:1–7.

42. Sharma V, Kerr SH, Kawar Z, Kerr DJ: Challenges of cancer control in developing countries: current status and future perspective Vanita. *Futur Oncol* 2011, 7:1213–1222.

43. Humphrey PA: Gleason grading and prognostic factors in carcinoma of the prostate. *Mod Pathol* 2004, 17:292–306.

44. Bauer DE, Harris MH, Plas DR, Lum JJ, Hammerman PS, Rathmell JC, Riley JL, Thompson CB: Cytokine stimulation of aerobic glycolysis in hematopoietic cells exceeds proliferative demand. *FASEB J* 2004, 18:1303–1305.

45. Arandjelovic S, Ravichandran KS: Phagocytosis of apoptotic cells in homeostasis. *Nat Immunol* 2015, 16:907–917.

46. Green DR, Oguin TH, Martinez J: The clearance of dying cells: table for two. *Cell Death Differ* 2016, 23:1–12.

47. Overholtzer M, Mailleux AA, Mouneimne G, Normand G, Schnitt SJ, King RW, Cibas ES, Brugge JS: A Nonapoptotic Cell Death Process, Entosis, that Occurs by Cell-in-Cell Invasion. *Cell* 2007, 131:966–979.

48. Blenis J: Molecular mechanisms of mTOR- mediated translational control. *Mol Cell Biol* 2009, 10:307–318.

49. Ong SE, Mann M: A practical recipe for stable isotope labeling by amino acids in cell culture (SILAC). *Nat Protoc* 2006, 1:2650–2660.

50. Yue S, Li J, Lee SY, Lee HJ, Shao T, Song B, Cheng L, Masterson T a., Liu X, Ratliff TL, Cheng JX: Cholesteryl ester accumulation induced by PTEN loss and PI3K/AKT activation underlies human prostate cancer aggressiveness. *Cell Metab* 2014, 19:393–406.

51. Wu X, Daniels G, Lee P, Monaco ME: Lipid metabolism in prostate cancer. *Am J Clin Exp Urol* 2014, 2:111–20.

52. Kaini RR, Sillerud LO, Zhaorigetu S, Hu CA: Autophagy Regulates Lipolysis and Cell Survival Through Lipid Droplet Degradation in Androgen-Sensitive Prostate Cancer Cells. *Prostate* 2012, 72:1412–1422.

53. Rambold AS, Cohen S, Lippincott-schwartz J: Fatty acid trafficking in starved cells: regulation by lipid droplet lipolysis, autophagy and mitochondrial fusion dynamics Angelika. *Dev Cell* 2015, 32:678–692.

54. Liu K, Czaja MJ: Regulation of lipid stores and metabolism by lipophagy. *Cell Death Differ* 2013, 20:3–11.

55. El-Diasty F: Coherent anti-Stokes Raman scattering: Spectroscopy and microscopy. *Vib Spectrosc* 2011, 55:1–37.

56. Birgersdotter A, Sandberg R, Ernberg I: Gene expression perturbation in vitro — A growing case for three-dimensional (3D) culture systems. *Semin Cancer Biol* 2005, 15:405–412.

57. Edmondson R, Broglie JJ, Adcock AF, Yang L: Three-Dimensional Cell Culture Systems and Their Applications in Drug Discovery and Cell-Based Biosensors. *Assay Drug Dev Technol* 2014, 12:207–218.

58. Takai A, Fako V, Dang H, Forgues M, Yu Z, Budhu A: Three-dimensional Organotypic Culture Models of Human Hepatocellular Carcinoma. *Nat Publ Gr* 2016(February):1–11.

59. Schlaermann P, Toelle B, Berger H, Schmidt SC, Glanemann M, Ordemann J, Bartfeld S, Mollenkopf HJ, Meyer TF: A novel human gastric primary cell culture system for modelling Helicobacter pylori infection in vitro. *Gut* 2014, 0:1–12.

60. Sharbati J, Hanisch C, Pieper R, Einspanier R, Sharbati S: Small molecule and RNAi induced phenotype transition of expanded and primary colonic epithelial cells. *Nat Publ Gr* 2015:1–11.

61. Gao D, Vela I, Sboner A, Iaquinta PJ, Karthaus WR, Gopalan A, Dowling C, Wanjala JN, Undvall EA, Arora VK, Wongvipat J, Kossai M, Ramazanoglu S, Barboza LP, Di W, Cao Z, Zhang QF, Sirota I, Ran L, Macdonald TY, Beltran H, Mosquera J, Touijer KA, Scardino PT, Laudone VP, Curtis KR, Rathkopf DE, Morris MJ, Danila DC, Slovin SF, et al.: Organoid Cultures Derived from Patients with Advanced Prostate Cancer. *Cell* 2014, 159:176–187.

62. Yuan TL, Cantley LC: PI3K pathway alterations in cancer: variations on a theme. *Oncogene* 2008, 27:5497–510.

63. Downward J: Targeting RAS signalling pathways in cancer therapy. *Nat Rev Cancer* 2003, 3:11–22.

64. Keniry M, Parsons R: The role of PTEN signaling perturbations in cancer and in targeted therapy. *Oncogene* 2008, 27:5477–5485.

65. Bae HB, Zmijewski JW, Deshane JS, Tadie JM, Chaplin DD, Takashima S, Abraham E: AMP-activated protein kinase enhances the phagocytic ability of macrophages and neutrophils. *Faseb J* 2011, 25:4358–4368.

66. Xing J, Wang Q, Coughlan K, Viollet B, Moriasi C, Zou M: Inhibition of AMP-Activated Protein Kinase Accentuates Lipopolysaccharide-Induced Lung Endothelial Barrier Dysfunction and Lung Injury in Vivo. *Am J Pathol* 2013, 182:1021–1030.

67. Bodzin JL, Saltiel AR, Gurnell M, Kalkhoven E, Helming L, Gordon S, Shinkai K, Mohrs K, Locksley RM, Wakil AE, Killeen N, Locksley RM, Mohrs M, Rooijen N Van, Locksley RM, Hogan SP: AMP-Activated Protein Kinase Regulates Neuronal Polarization by Interfering with PI 3-Kinase Localization. *Science (80-)* 2011, 332:247–251.

68. Kuhajda FP: AMP-activated protein kinase and human cancer : cancer metabolism revisited. *Int J Obes* 2008, 32:36–41.

69. Vander Heiden MG: Targeting cancer metabolism: a therapeutic window opens. *Nat Rev Drug Discov* 2011, 10:671–684.

70. Zadra G, Batista JL, Loda M: Dissecting the Dual Role of AMPK in Cancer: From Experimental to Human Studies. *Mol Cancer Res* 2015, 13:1059–72.

71. Chhipa RR, Wu Y, Mohler JL, Ip C: Survival advantage of AMPK activation to androgen-independent prostate cancer cells during energy stress. *Cell Signal* 2010, 22:1554–1561.

72. Jeon S-M, Chandel NS, Hay N, Jeon SM, Chandel NS HN: AMPK regulates NADPH homeostasis to promote tumour cell survival during energy stress. *Nature* 2012, 485:661–665.

73. Hardie DG, Schaffer BE, Brunet A: Review AMPK : An Energy-Sensing Pathway with Multiple Inputs and Outputs. *Trends Cell Biol* 2016, 26:190–201.

74. Vincent EE, Coelho PP, Blagih J, Griss T, Viollet B, Jones RG: Differential effects of AMPK agonists on cell growth and metabolism. *Oncogene* 2014, 34:3627–3639.

75. Saito Y, Chapple RH, Lin A, Kitano A, Saito Y, Chapple RH, Lin A, Kitano A, Nakada D: Article AMPK Protects Leukemia-Initiating Cells in Myeloid Leukemias from Metabolic Stress in the Bone Article AMPK Protects Leukemia-Initiating Cells in Myeloid Leukemias from Metabolic Stress in the Bone Marrow. *Stem Cell* 2015, 17:585–596.

76. Maes H, Kuchnio A, Peric A, Moens S, Nys K, Bock K De, Quaegebeur A, Schoors S, Georgiadou M, Wouters J, Vinckier S, Radtke F, Boulanger C, Vankelecom H, Garmyn M, Annaert W, Agostinis P: Tumor Vessel Normalization by Chloroquine Independent of Autophagy. *Cancer Cell* 2014, 26:190–206.

77. Maes H, Kuchnio A, Carmeliet P, Agostinis P, Maes H, Kuchnio A, Carmeliet P, Agostinis P, Maes H, Kuchnio A, Agostinis P, Maes H, Kuchnio A, Carmeliet P, Agostinis P: Chloroquine anticancer activity is mediated by autophagy-independent effects on the tumor vasculature Chloroquine anticancer activity is mediated by autophagy-independent effects on the tumor vasculature. *Mol Cell Oncol* 2016, 3:e970097.

78. Maycotte P, Aryal S, Cummings CT, Thorburn J, Morgan MJ, Thorburn A: Chloroquine sensitizes breast cancer cells to chemotherapy independent of autophagy. *Autophagy* 2012, 8:200–212.

79. Pichler M, Hutterer GC, Chromecki TF, Jesche J, Kampel-Kettner K, Rehak P, Pummer K, Zigeuner R: Histologic tumor necrosis is an independent prognostic indicator for clear cell and papillary renal cell carcinoma. *Am J Clin Pathol* 2012, 137:283–289.

80. Lee SE, Hong SK, Han BK, Yu JH, Han JH, Jeong SJ, Byun SS, Park YH, Choe G: Prognostic significance of tumor necrosis in primary transitional cell carcinoma of upper urinary tract. *Jpn J Clin Oncol* 2007, 37:49–55.

81. Hiraoka N, Ino Y, Sekine S, Tsuda H, Shimada K, Kosuge T, Zavada J, Yoshida M, Yamada K, Koyama T, Kanai Y: Tumour necrosis is a postoperative prognostic marker for pancreatic cancer patients with a high interobserver reproducibility in histological evaluation. *Br J Cancer* 2010, 103:1057–1065.

82. Gkogkou C, Frangia K, Saif MW, Trigidou R, Syrigos K: Necrosis and apoptotic index as prognostic factors in non-small cell lung carcinoma: a review. *Springerplus* 2014, 3:1–5.

83. Kuraishy A, Karin M, Grivennikov SI: Review Tumor Promotion via Injury- and Death-Induced Inflammation. *Immunity* 2011, 35:467–477.

84. Nussbaum N, George DJ, Abernethy AP, Dolan CM, Oestreicher N, Flanders S, Dorff TB: Patient experience in the treatment of metastatic castration-resistant prostate cancer : state of the science. *Prostate Cancer Prostatic Dis* 2016, 19:111–121.

85. Hotte SJ, Saad F: Current management of castrate-resistant prostate cancer. *Curr Oncol* 2010, 17(SUPPL. 2):72–79.

86. Overmeyer JH, Kaul A, Johnson EE, Maltese W a: Active ras triggers death in glioblastoma cells through hyperstimulation of macropinocytosis. *Mol Cancer Res* 2008, 6:965–977.

DISCUSSION

Sphingolipid compounds are broadly effective because they target a cancer phenotype not an oncogene.

Enzymes that play crucial roles in metabolic reprogramming are tractable drug targets, but tumor heterogeneity may limit the effectiveness of these therapies. Enzymatic inhibitors may enrich pre-existing cancer cells that rely on a different anabolic pathway or cause cancer cells to up-regulate alternative, compensatory pathways (1,2). Making nutrients scarce to anabolic enzymes could circumvent these resistance mechanisms. The sphingolipid-based compound SH-BC-893 effectively limits access to multiple nutrients simultaneously by down-regulating surface nutrient transporters and LDL-receptors and by blocking lysosomal degradation of macropinosomes and autophagosomes (Chapter 1 Figure 9). Regardless of which particular oncogenic mutation is present, all cancer cells need glucose and amino acids to build biomass for proliferation. SH-BC-893's ability to simultaneously block multiple nutrient acquisition pathways therefore blocks cancer anabolism in many different cancer classes.

Because SH-BC-893 targets a cancer phenotype—nutrient addiction—rather than a specific oncoprotein, it is effective against a broad range of cancer types (3). Both fast growing and glycolytic Ras-driven tumors, as well as slower growing prostate tumors lacking functional PTEN or p53, are sensitive to SH-BC-893 (Chapter 1 Figures 2G-I and 8I,J). The broad activity of SH-BC-893 may limit the development of resistance in individual, heterogeneous tumors. In addition, reducing nutrient uptake may maintain cancer cells in a more differentiated state as evidenced by increased organization and growth arrest in 3D-cultured breast cancer cells upon glucose restriction and the delayed tumor progression in SH-BC-893-treated pDKO mice (Chapter 1 Figure 8I-J and Supplemental Figure 9) (4). Limiting access to nutrients may help target even the cancer cells that have stemcell-like properties (5,6). The metabolic state of cancer stem cells (CSC) is very complex; while quiescent CSCs rely heavily on oxidative

phosphorylation, proliferative CSCs can also upregulate glycolysis (7). Simultaneously blocking both glycolysis and mitochondrial respiration would be necessary to effectively eliminate CSCs. SH-BC-893's ability to block multiple nutrient acquisition pathways may be able to limit proliferative CSCs. Populations of quiescent CSCs that already have high levels of mitochondrial respiration may be sensitive to SH-BC-893 because they are unable to further increase oxidative phosphorylation. It will be important to clarify whether any tumor subsets or genetic markers correlate with innate resistance to SH-BC-893 and to identify potential mechanisms for acquired resistance.

As the SH-BC-893-induced block in nutrient acquisition pathways required PP2A activation (Chapter 1, Figure 5), loss of PP2A may be one of the mechanisms by which cancer cells acquire resistance to SH-BC-893. Cancers cells may inactivate PP2A through mutation or deletion of scaffold (A) and regulatory (B) subunits which would disrupt PP2A holoenzyme formation and function (8,9). PP2A may also be inactivated at the catalytic subunit (C) by the phosphorylation and/or methylation of the C-terminal tail or through increased expression of endogenous PP2A inhibitors. However, since PP2A, together with PP1, is responsible for the majority of serine/threonine dephosphorylation, cells may not be able to survive with complete loss of PP2A activity (9). Indeed, chemical PP2A inhibitors are quite toxic and most of the PP2A mutations found in clinical specimens generally involve only a single allele and reduce rather than eliminate activity (8). SH-BC-893's parent compound FTY720 was shown to be effective even in cell lines with reduced expression of A subunits of PP2A by down-regulating PP2A inhibitor SET, up-regulating A subunits of PP2A and de-phosphorylating PP2A C subunits (9).

Therefore, it is more likely that the acquired resistance to SH-BC-893 would arise from pathways downstream of PP2A. An example of this would be a gain-of-function in PIKfyve complex that prevents its recruitment to the MVB in a PP2A-sensitive manner (Chapter 1 Figure

4B) or loss of function mutations in the enzymes that degrade $PI(3,5)P_2$ (10,11). PIKfyve is activated by Akt-dependent phosphorylation of Ser318 (12). Consistent with the observation that PIKfyve kinase activity was not altered (Chapter 1 Figure 4A), the ability of an antibody recognizing phosphorylated Akt substrates to detect immunoprecipitated PIKfyve was not affected by SH-BC-893 (data not shown), and Akt inhibitors did not induce vacuolation (data not shown). AMPK has also been reported to phosphorylate PIKfyve (13); the AMPK inhibitor compound c also did not trigger vacuolation (data not shown). The phosphorylation site regulating PIKfyve localization could be in PIKfyve, another member of the complex, or in a protein outside of the complex that modulates PIKfyve membrane association. Over-expression of Vac14 reduced SH-BC-893-induced vacuolation and conferred partial resistance to SH-BC-893 (Chapter 1 Figure 7). We speculate that Vac14 over-expression likely restores some PIKfyve complex to the multivesicular membranes near its effector protein TRPML1.

Compensatory upregulation of metabolic pathways not inhibited by SH-BC-893 may also confer resistance. Since SH-BC-893 limits but does not completely blocks all nutrient acquisition, normal cells resist SH-BC-893-induced nutrient stress by increasing oxidative phosphorylation to more efficiently generate ATP. Fatty acid oxidation may also be providing substrates needed to increase oxidative phosphorylation in normal cells as fatty acids can likely enter cells without a transporter (14,15). If this is the case, cancer cells that can increase fatty oxidation may be able to adapt to SH-BC-893-induced nutrient stress and become resistant. Identifying biomarkers that correlate with sensitivity and resistance to SH-BC-893 will be an important goal if SH-BC-893 advances to clinical trials.

Sphingolipid-based therapies are effective and selective.

Ras is a difficult drug target (16). Directly targeting Ras by inhibiting its processing or localization or reducing its expression by antisense oligonucleotides has not been very successful in clinical trials (17). Small molecule inhibitors of kinases downstream of Ras such as MEK and ERK are more promising but have shown little clinical benefit as single agents (18). SH-BC-893 blocks all Ras-driven fuel acquisition pathways: membrane transporters, macropinocytosis, and autophagy (19) (Chapter 1 Figure 9). Ras activation was sufficient to sensitize MEFs to SH-BC-893, consistent with the model that Ras-driven cells rely heavily on these nutrient access pathways (Chapter 1 Figures 2D,E). SH-BC-893 may improve therapeutic efficacy of inhibitors of Ras signaling pathway such as the FDA-approved MEK inhibitor trametinib. However, it would be important to consider that inhibiting growth signals may make cells more resistant to SH-BC-893 by slowing down anabolic processes and thereby decreasing bioenergetic demand. Careful analysis of the metabolic state of cancers would be necessary to develop potential combination therapy involving SH-BC-893. SH-BC-893 is also effective against PTEN-deficient prostate cancer cells that are metabolically distinct from Ras-driven cancer cells (Chapter 1 Figures 8I,J). This may be because SH-BC-893 also reduces LDL uptake that fuels prostate tumor proliferation. Interestingly, compounds that slow proliferation and anabolism do not protect cancer cells from SH-BC-893. Rather mTORC1 inhibitor rapamycin protects normal cells and sensitizes cancer cells to SH-BC-893 (data not shown). These results suggest that a carefully designed combination therapy may be able to decrease toxicity and increase efficacy of sphingolipid-based therapies.

Importantly, at doses that inhibit tumor growth, SH-BC-893 had minimal toxicity to normally proliferating cells as evidenced by normal organ function, hematopoiesis and intestinal crypt histology (Chapter 1 Supplemental Figure 8E, Supplemental Table 1 and 2). This suggests that SH-BC-893 would have an acceptable therapeutic index. Non-transformed cells are likely to experience less metabolic stress and have more metabolic flexibility to adapt to nutrient stress

as they lack oncogenic mutations that drive anabolism and decrease autophagic capacity. Consistent with this hypothesis, expression of KRASG12D or loss of PTEN prevented MEFs from increasing oxidative phosphorylation in an adaptive response to SH-BC-893 (Chapter 1 Figure 2D and Supplemental Figure 2A). Water-soluble and orally bioavailable sphingolipid drugs like SH-BC-893 could provide a new approach to safely target the metabolic changes that drive tumor growth and progression independent of a tumor's mutational landscape. Although optimization of pharmacological properties, formulation, dose, and schedule of administration is warranted, SH-BC-893's effectiveness and selectivity against broad range of tumor classes in these preclinical studies makes it a promising anti-cancer therapy.

SH-BC-893 has potential to be used as a calorie restriction mimetic to reduce obesity. Although the overall health of the mice that were treated with SH-BC-893 was not compromised, these mice did not gain as much weight as vehicle-treated animals (Chapter 1 Supplemental Figure 8D). Since SH-BC-893 simultaneously blocks multiple nutrient acquisition pathways but is not toxic to normal cells, it is possible SH-BC-893 could be used as a calorie restriction mimetic. Treatment of SH-BC-893 is probably more similar to intermittent rather than continuous calorie restriction as SH-BC-893 levels peak and trough off. Intermittent fasting is shown to be beneficial to patient undergoing chemotherapy and may reduce risk of chronic degenerative and inflammatory diseases (20–22). More extensive examination of normally proliferating cells *in vivo* would be required, but lowering doses and reducing the frequency of treatment may be helpful in reducing toxicity. In yeast, the transcriptional response to starvation, phytosphingosine, and FTY720 treatment are very similar (23). Investigating the long-term effect of SH-BC-893 treatment on insulin and insulin-like growth factor (IGF) will elucidate further whether SH-BC-893 can be used as a safe way to mimic calorie restriction or intermittent fasting.

Prostate cancers can use macropinocytosis to fuel growth even in nutrient-replete conditions.

The ability of Ras-driven pancreatic cancer cells to use macropinocytosis is well characterized in the literature (24,25). Ras activates PI 3-kinase whose activity at the plasma membrane is required for macropinocytic membrane ruffling, and PI 3-kinase inhibitors block macropinocytosis (26). Given these findings and the various cancer classes that have PI 3-kinase mutations or PTEN loss, it is surprising that macropinocytosis has not been detected in cells other than Ras-driven cancer cells. We have demonstrated that PTEN-null prostate cancer cells have constitutively high levels of macropinocytosis and that nutrients taken in by macropinocytosis are used to build protein and lipid biomass needed for proliferation (Chapter 2 Figures 6 and 7).

Previous studies on Ras-driven pancreatic cancer cells showed that these cells take up albumin via macropinocytosis in amino acid-depleted conditions (24,25). However, whether nutrient acquisition via macropinocytosis contributes to building biomass in nutrient-rich environments was unclear. We have demonstrated that PTEN-deficient cancers rely on macropinocytosis even in nutrient-replete conditions (Chapter 2 Figures 3A and 6C) albeit to a lesser degree. This suggests that inhibiting macropinocytosis would be effective against both starving and non-starving tumors.

The difference in the stimulation and regulation of macropinocytosis in Ras-driven prostate cancers and PTEN-deficient prostate requires further investigation. The Rac1 inhibitor EHT-1864 inhibited the macropinocytic uptake of dextran in PTEN-deficient cells (Chapter 2 Supplemental Figure 1F). This suggests that, like Ras activation, PTEN loss activates Rac1. Since loss of PTEN phosphatase function leads to increased PI3K/AKT/mTOR signaling pathway activity, it is likely that PTEN loss activates Rac1 through the same signaling cascade activated by Ras. PTEN also has both phosphatase-independent roles such as promoting

chromosome stability and DNA repair (27). However, as PTEN phosphatase inhibitor induces and PI3K inhibitors block macropinocytosis (Chapter 2 Supplemental Figure 1A,B), it is unlikely that phosphatase-independent functions of PTEN play a role in stimulating macropinocytosis.

AMPK activity contributes to macropinocytic uptake of nutrients.

Tumor cells exhibit “non-oncogene addictions” or dependence on genes and pathways that do not undergo mutations or genomic alterations but are essential to support the oncogenic phenotype of cancer cells (28). AMPK inhibits anabolic metabolism and is generally considered a tumor suppressor. However, AMPK is a key enzyme that helps cells cope with cellular stress such as starvation and hypoxia. In order to survive and proliferate successfully, cancer cells need to deal with these stress factors. Our findings suggest prostate cancer cells rely on AMPK activity for macropinocytosis. This suggests that AMPK may represent a non-oncogene addiction in some cancer cells.

PTEN-deficient MEFs increase macropinocytic uptake when AMPK is activated either by glucose deprivation or by treatment with an AMPK activator (Chapter 2 Figures 1B and 2C). Prostate cancer cells likely have constitutively high AMPK activity that allows them to have high levels of macropinocytosis even in full nutrient conditions (Chapter 2 Figure 3A). These findings are consistent with previous studies that have implicated AMPK to be regulating phagocytosis and macropinocytosis. For instance, the ability of neutrophils or macrophages to ingest bacteria is increased by AMPK activation (29). Macrophages from diabetic mice have low AMPK activity and macropinocytosis, and activation of AMPK with leptin or 5-aminoimidazole-4-carboxamide-1-β-riboside (AICAR) increased macropinocytosis in these cells (30). Mouse embryonic fibroblasts lacking the AMPKα1 and AMPKα2 catalytic subunits have decreased macropinocytic uptake of viral particles (31,32). Our findings have elucidated that AMPK activation is

necessary but not sufficient to stimulate macropinocytosis. Thus, it should be considered that therapies that increase AMPK activity may enhance macropinocytosis in tumor cells and protect them from metabolic therapies or nutrient stress.

How AMPK contributes to inducing macropinocytosis in PTEN-deficient cells is an important question that merits future investigation. Our lab's preliminary data shows that activating AMPK is sufficient to induce Rac1 activation at the plasma membrane of PTEN KO MEFs and increase membrane ruffling (data not shown). Additional evidence links AMPK and Rac1. For instance, AMPK inhibition blocks retinoic acid (RA)-induced Rac1 activation and phosphorylation of its downstream target, p21-activated kinase (PAK) (33). Since Rac1 is a small GTPase, AMPK activation may be indirectly increasing Rac1 activity by promoting Rac1 guanine nucleotide exchange factor (GEF) activity or inhibiting Rac1 GTPase-activating protein (GAP) activity. Similar to AMPK-induced rapid translocation of GLUT4 to the plasma membrane, it is also possible that AMPK may be promoting Rac1 localization to the plasma membrane (34). AMPK activation may also be increasing Rac1 localization to lipid in plasma membrane which has been shown to increase local Rac1-GTP levels (35). It is also feasible that AMPK and Rac1 may be direct interactors as suggested by the large-scale affinity purification-mass spectrometry study using AMPK-α1 and -β1 subunits (36). Elucidating how AMPK regulates Rac1 activity will contribute to deeper understanding of the link between membrane biology and cellular metabolic state.

Necrotic cells may be a nutrient source for surrounding proliferating cancer cells.

As tumors enlarge, cells that are not sufficiently perfused will inevitably undergo cell death due to oxygen and nutrient deprivation (37). As cells near the periphery that are closer to blood vessels continue to proliferate around dying cells, a necrotic center develops (38). Cellular

debris and cytokines released from immune cells attracted to the necrotic center may provide nutrients and survival signals to the surrounding proliferating tumor cells. We have demonstrated in this study that PTEN-deficient prostate cancer cells can take up necrotic debris via macropinocytosis and build biomass to support growth and proliferation (Chapter 2 Figure 5-7). As many types of solid tumors can exhibit, it would be important to investigate what other types of cancers can also use macropinocytosis to consume necrotic debris to grow and proliferate. Clearance of dead cells by cancer cells is an exciting and novel finding and highlights that necrotic centers may have a previously unappreciated role as a nutrient source for cancer cells. Like cancer-associated fibroblasts, dying or dead tumor cells must be considered a crucial part of the tumor supporting microenvironment (39). This also brings out the concern that after suboptimal treatment, some cancer cells that escape therapy may survive by feeding off surrounding dead cells. In such cases, combining macropinocytosis inhibitors with chemotherapy or other targeted therapy could be useful. However, inhibitors that selectively block macropinocytosis are not currently available. We have shown that the sphingolipid-derived compound SH-BC-893 inhibits macropinosomes from fusing with lysosomes and thereby blocks macropinocytic nutrient acquisition (Chapter 1 Figure 6G). SH-BC-893 would block cancer cells' ability to use necrotic debris as a nutrient source and simultaneously inhibit other nutrient acquisition pathways as well. In conclusion, studies in this dissertation have uncovered prostate cancers' reliance on macropinocytosis and elucidated the mechanism by which the synthetic sphingolipid compound SH-BC-893 targets the nutrient addiction of prostate and other cancers.

REFERENCES

1. McGranahan N, Swanton C: Perspective Biological and Therapeutic Impact of Intratumor Heterogeneity in Cancer Evolution. *Cancer Cell* 2015, 27:15–26.

2. Patel AP, Tirosh I, Trombetta JJ, Shalek AK, Gillespie SM, Wakimoto H, Cahill DP, Nahed B V, Curry WT, Martuza RL, Louis DN, Rozenblatt-Rosen O, Suvà ML, Regev A, Bernstein BE: Single-cell RNA-seq highlights intratumoral heterogeneity in primary glioblastoma. *Science* 2014, 344:1396–401.

3. Chen B, Roy SG, McMonigle RJ, Keebaugh A, McCracken AN, Selwan E, Fransson R, Fallegger D, Huwiler A, Kleinman MT, Edinger AL, Hanessian S: Azacyclic FTY720 Analogues That Limit Nutrient Transporter Expression but Lack S1P Receptor Activity and Negative Chronotropic Effects Offer a Novel and Effective Strategy to Kill Cancer Cells in Vivo. *ACS Chem Biol* 2016, 11:409–14.

4. Onodera Y, Nam J, Bissell MJ: Increased sugar uptake promotes oncogenesis via EPAC / RAP1 and O-GlcNAc pathways. *J Clin Invest* 2014, 124:367–384.

5. Visvader JE, Lindeman GJ: Cancer stem cells in solid tumours: accumulating evidence and unresolved questions. *Nat Rev Cancer* 2008, 8:755–768.

6. Kreso A, Dick JE: Evolution of the Cancer Stem Cell Model. *Stem Cell* 2014, 14:275–291.

7. Peiris-pagès M, Martinez-outschoorn UE, Pestell RG, Sotgia F, Lisanti MP, Warburg O: Cancer stem cell metabolism. *Breast Cancer Res* 2016, 18:1–10.

8. Sangodkar J, Farrington CC, Mcclinch K, Galsky MD, David B: All roads lead to PP2A : exploiting the therapeutic potential of this phosphatase. *FEBS J* 2016, 283:1004–1024.

9. Kiely M, Kiely PA: PP2A: The Wolf in Sheep's Clothing. *Cancers (Basel)* 2015, 7:648–669.

10. McCartney AJ, Zhang Y, Weisman LS: Phosphatidylinositol 3,5-bisphosphate: Low abundance, high significance. *BioEssays* 2014, 36:52–64.

11. Ho CY, Alghamdi T a, Botelho RJ: Phosphatidylinositol-3,5-bisphosphate: no longer the poor PIP2. *Traffic* 2012, 13:1–8.

12. Er EE, Mendoza MC, Mackey AM, Rameh LE, Blenis J: AKT facilitates EGFR trafficking and degradation by phosphorylating and activating PIKfyve. *Sci Signal* 2013, 6:ra45.

13. Liu Y, Lai Y-C, Hill E V, Tyteca D, Carpentier S, Ingvaldsen A, Vertommen D, Lantier L, Foretz M, Dequiedt F, Courtoy PJ, Erneux C, Viollet B, Shepherd PR, Tavaré JM, Jensen J, Rider MH: Phosphatidylinositol 3-phosphate 5-kinase (PIKfyve) is an AMPK target participating in contraction-stimulated glucose uptake in skeletal muscle. *Biochem J* 2013, 455:195–206.

14. Hamilton JA, Johnson RA, Corkey B, Kamp F: The Diffusion Mechanism in Model and Biological Membranes. *J Mol Neurosci* 2001, 16:99–108.

15. Mcarthur MJ, Atshaves BP, Frolov A, Foxworth WD, Kier AB, Schroeder F: Cellular uptake and intracellular trafficking of long chain fatty acids. *J Lipid Res* 1999, 40:1371–1383.

16. Mattingly RR: Activated Ras as a Therapeutic Target: Constraints on Directly Targeting Ras Isoforms and Wild-Type versus Mutated Proteins. *ISRN Oncol* 2013, 2013:536529.

17. Downward J: Targeting RAS signalling pathways in cancer therapy. *Nat Rev Cancer* 2003, 3:11–22.

18. Gysin S, Salt M, Young A, McCormick F: Therapeutic strategies for targeting ras proteins. *Genes Cancer* 2011, 2:359–372.

19. White E: Exploiting the bad eating habits of Ras-driven cancers. *Genes Dev* 2013, 27:2065–2071.

20. Michalsen A, Li C: Fasting Therapy for Treating and Preventing Disease –. *Forsch Komplementmed* 2013, 20:444–453.

21. Harvie MN, Howell T: Could Intermittent Energy Restriction and Intermittent Fasting Reduce Rates of Cancer in Obese , Overweight , and Normal-Weight Subjects ? A Summary of Evidence 1 , 2. *Adv Nutr* 2016, 7:690–705.

22. Simone BA, Champ CE, Rosenberg AL, Berger AC, Monti DA, Dicker AP, Simone NL: Selectively starving cancer cells through dietary manipulation: methods and clinical implications. *Futur Oncol* 2013, 9:959–976.

23. Welsch CA, Roth LWA, Franc J, Movva NR: Genetic , Biochemical , and Transcriptional Responses of Saccharomyces cerevisiae to the Novel Immunomodulator FTY720 Largely Mimic Those of the Natural Sphingolipid Phytosphingosine. *J Biol Chem* 2004, 279:36720–36731.

24. Commisso C, Davidson SM, Soydaner-Azeloglu RG, Parker SJ, Kamphorst JJ, Hackett S, Grabocka E, Nofal M, Drebin JA, Thompson CB, Rabinowitz JD, Metallo CM, Vander Heiden MG, Bar-Sagi D: Macropinocytosis of protein is an amino acid supply route in Ras-transformed cells. *Nature* 2013, 497:633–7.

25. Palm W, Park Y, Wright K, Pavlova NN, Tuveson DA, Thompson CB: The Utilization of Extracellular Proteins as Nutrients Is Suppressed by mTORC1. *Cell* 2015, 162:1–12.

26. Lim JP, Gleeson PA: Macropinocytosis : an endocytic pathway for internalising large gulps. *Immunol Cell Biol* 2011, 89:836–843.

27. Dillon LM, Miller TW: Therapeutic targeting of cancers with loss of PTEN function. *Curr Drug Targets* 2014, 15:65–79.

28. Luo J, Solimini NL, Elledge SJ: Principles of Cancer Therapy: Oncogene and Non-oncogene Addiction. *Cell* 2009, 136:823–837.

29. Bae HB, Zmijewski JW, Deshane JS, Tadie JM, Chaplin DD, Takashima S, Abraham E: AMP-activated protein kinase enhances the phagocytic ability of macrophages and neutrophils. *Faseb J* 2011, 25:4358–4368.

30. Guest CB, Chakour KS, Freund GG: Macropinocytosis is decreased in diabetic mouse macrophages and is regulated by AMPK. *BMC Immunol* 2008, 9:42.

31. Kondratowicz AS, Hunt CL, Davey R a, Cherry S, Maury WJ: AMP-activated protein kinase is required for the macropinocytic internalization of ebolavirus. *J Virol* 2013, 87:746–55.

32. Moser TS, Jones RG, Thompson CB, Coyne CB, Cherry S: A kinome RNAi screen identified AMPK as promoting poxvirus entry through the control of actin dynamics. *PLoS Pathog* 2010, 6.

33. Lee YM, Lee JO, Jung J, Kim JH, Park S, Park JM, Kim E, Suh P, Kim HS: Retinoic Acid Leads to Cytoskeletal Rearrangement through AMPK-Rac1 and Stimulates Glucose Uptake through AMPK-p38 MAPK in Skeletal Muscle Cells *. *J Biol Chem* 2008, 283:33969–33974.

34. Hardie DG: AMP-activated protein kinase — an energy sensor that regulates all aspects of cell function. *Genes Dev* 2011, 25:1895–1908.

35. Moissoglu K, Kiessling V, Wan C, Hoffman BD: Regulation of Rac1 translocation and activation by membrane domains and their boundaries. *J Cell Sci* 2014, 127:2565–2576.

36. Moon S, Han D, Kim Y, Jin J, Ho W: Interactome analysis of AMP-activated protein kinase (AMPK)- a 1 and - b 1 in INS-1 pancreatic beta-cells by affinity purification-mass spectrometry. *Sci Rep* 2014, 4:4376.

37. Weis SM, Cheresh DA: Tumor angiogenesis: molecular pathways and therapeutic targets. *Nat Med* 2011, 17:1359–1370.

38. Philipp S, Sosna J, Adam D: Cancer and necroptosis: friend or foe? *Cell Mol Life Sci* 2016, 73:1–11.

39. Madar S, Goldstein I, Rotter V: “Cancer associated fibroblasts” - more than meets the eye. *Trends Mol Med* 2013, 19:447–453.